



UNIVERSIDADE D  
COIMBRA



**Joana Moura Mateus**

**ADULT OLIGODENDROGENESIS IN A  
MOUSE MODEL OF MULTIPLE  
SCLEROSIS**

Dissertação de Mestrado em Biologia Celular e Molecular com especialização em Neurobiologia, orientada pela Professora Doutora Sara Xapelli (Instituto de Medicina Molecular João Lobo Antunes, Faculdade de Medicina da Universidade de Lisboa) e pelo Professor Doutor Carlos Bandeira Duarte (Departamento de Ciências da Vida, Faculdade de Ciências e Tecnologia, Universidade de Coimbra), apresentada ao Departamento de Ciências da Vida da Universidade de Coimbra.

**Setembro 2018**



The experimental work described in this thesis was performed at Instituto de Medicina Molecular João Lobo Antunes, Faculdade de Medicina, Universidade de Lisboa, under the supervision of Professor Sara Alves Xapelli.

O trabalho experimental descrito nesta tese foi realizado no Instituto de Medicina Molecular João Lobo Antunes, Faculdade de Medicina, Universidade de Lisboa, sob a orientação da Professora Sara Alves Xapelli.



“The most effective way to do it, is to do it.”

Amelia Earhart



## Agradecimentos

Em primeiro lugar gostaria de agradecer à Professora Ana Sebastião, pela oportunidade de conhecer o trabalho desenvolvido no seu laboratório, e pela disponibilidade de me aceitar no seu grupo para a realização deste projeto.

Um particular agradecimento à minha orientadora, a Professora Sara Xapelli. Por todo o apoio e ensinamentos transmitidos (para o laboratório e para a vida), pela disponibilidade, confiança, e paciência para me aturar quando a Ciência nos prega partidas. Um obrigada nunca será suficiente.

Aos Xapellis. Pela ajuda, por tudo. À Filipa Ribeiro, por ser a voz da calma e da razão no meio da tempestade, mas que ao mesmo tempo consegue encaixar os A<sub>2</sub>A numa piada. Ao Rui Rodrigues, o Chefinho, por tudo aquilo que traz para as pessoas à sua volta. Serei a tua *life planner* pelo pequeno preço de nos fazeres rir todos os dias no laboratório, pode ser? O teu 'Está tudo bem' vai ficar comigo p'rá vida. À Rita Soares, por toda a ajuda e por ser a minha companheira nos jantares na biblioteca. À Sara Paulo que, clichés à parte, me ensinou tudo o que sei. És uma chefe muito melhor que o Gru. Que encontremos sempre alegria nas viagens, na comida, nos gelados e chocolates. À Marta Gomes e ao Diogo Lourenço, os membros recém-chegados: o vosso entusiasmo encaixa aqui na perfeição, sejam sempre assim (mesmo que eu diga que já chega ;) ).

A todos os ASebs: muito obrigada por tudo. O espírito de entreajuda e camaradagem que existe neste laboratório ultrapassa todos os limites. Um obrigada especial ao Francisco Mouro, por toda a ajuda com as injeções intraperitoneais, com as sessões de handling e com os testes de comportamento, e à Leonor Rodrigues e à Catarina Almeida, pelo auxílio com os testes de ELISA. A todos aqueles que, numa dada altura, despenderam um pouco do seu tempo para me ajudar com um detalhe técnico, com um composto que andava perdido no laboratório, ou mesmo com o vosso espírito crítico característico que me faz sempre pensar que posso fazer mais e melhor. Vocês fazem com que seja um prazer vir para o laboratório todos os dias. Espero que saibam que por baixo deste OCD e perfeccionismo sou um coração mole... por chocolate, bebés e vocês. Obrigada.

Uma palavra de agradecimento também ao Professor Carlos Bandeira Duarte, por tudo aquilo que me ensinou durante o ano passado, naquele que foi o meu primeiro contacto com as neurociências.

Ao Doutor Ângelo Chora, por toda a ajuda e partilha de conhecimento para a indução do modelo de EAE.

Ao Daniel Costa, ao Filipe Delgado e à Iolanda Moreira, do biotério do iMM, pelo apoio em todos os procedimentos, injeções, cirurgias e respetivos *follow-ups*.

Ao António Temudo e à Ana Nascimento, do *Bioimaging*, pelo apoio no capítulo da microscopia.

À Ana Rita Pires, da Histologia, pela troca de ideias e por todo o trabalho desenvolvido.

A todos aqueles com quem partilhei uma bancada de laboratório, colegas e superiores, quer tenha sido em aulas, em rotações laboratoriais ou durante este ano. Mesmo que esse contacto tenha sido breve, acreditem que houve sempre algo a aprender.

Ao Miguel, à Belo e à Moreira, os amigos de Bioquímica, um obrigado pelos melhores anos da minha vida. Por estarem sempre aqui, mesmo quando estamos um em cada lado. Que sejamos assim até sermos velhinhos.

À Mariana, à Dina e à Xana, as minhas 'migas de Coimbra', obrigado por terem feito dessa a minha casa longe de casa o ano passado. Sei que vocês acham que eu não gostava de Coimbra, mas para mim foram vocês que fizeram a minha estadia nessa cidade. Obrigada pela amizade, pela paciência, pela companhia.

Aos que têm partilhado este caminho comigo, e também àqueles que o deixaram, entretanto. Os primeiros porque são o que adoça esta viagem, e me mostram que na verdade aquilo que é bom fica sempre connosco. Aos últimos, que me mostraram que só precisamos de ter connosco quem cá quer estar para sermos plenos.

Por último, à minha Família, em especial aos meus Pais e Avó: não pode ser expresso em palavras. Obrigada por me darem asas e tornarem tudo possível. Todo o apoio e carinho (e comida) foram indispensáveis para concretizar esta etapa. Sou a pessoa que sou por causa de vocês. À minha Madrinha e ao meu 'Senhorio', que me 'adotaram' em Lisboa: sem vocês não estaria onde estou hoje. Muito obrigada por tudo.

É com imenso orgulho e prazer que digo que todos vocês, direta ou indiretamente, moldaram o meu caminho na Ciência, assim como na Vida. Estou para sempre grata a todos.



## Table of Contents

Abbreviations .....	12
List of figures and tables.....	14
Abstract.....	16
Resumo.....	19
CHAPTER 1 – INTRODUCTION & AIMS .....	23
1. Multiple Sclerosis .....	25
1.1 Disease characteristics and role of oligodendrocytes .....	25
1.2 Research models .....	27
1.2.1 <i>In vitro</i> models.....	28
1.2.2 <i>In vivo</i> models .....	29
1.2.2.1 Autoimmune models .....	29
a. Experimental autoimmune encephalomyelitis (EAE) .....	29
b. Models of neuromyelitis optica (NMO).....	30
1.2.3 Viral models .....	30
a. Theiler’s Murine Encephalomyelitis Virus (TMEV) .....	30
1.2.4 Toxin-induced models .....	31
1.3 Cellular mechanisms behind inflammation in MS: brief considerations from the human and the mouse model.....	32
1.3.1 Role for TNF $\alpha$ , IL-1 $\beta$ and the Nuclear Factor kappa B (NF- $\kappa$ B) pathway .....	33
1.4 Therapeutic approaches.....	34
2. Oligodendrocytes .....	35
2.1 Differentiation of OPCs.....	35
2.2 Function of OLGs and synaptic communication.....	36
2.3 Plasticity and homeostasis of the oligodendrocytic population.....	37
3. Myelin.....	38
3.1 Myelination in development and adulthood: myelin structure and composition .....	38
3.2 Myelin damage and remyelination .....	41
3.2.1 Characteristics of remyelinated axons and role of remyelination .....	41
3.2.2 Steps for remyelination and factors controlling the process .....	41
4. Stem cell niches in the brain.....	43
4.1 From development to adulthood .....	43
4.1.1 Neurogenic niches during development.....	43
4.1.2 Neurogenic niches in the adult brain .....	44

4.1.2.1	Oligodendrocyte production from SVZ precursor cells .....	46
5.	Commitment to the oligodendrocytic lineage: intrinsic and extrinsic factors .....	46
5.1.1	Intrinsic factors .....	46
5.1.2	Extrinsic factors .....	47
CHAPTER 2 – MATERIALS & METHODS .....		51
1.	Ethics Statement .....	53
2.	Animals .....	53
3.	Timeline for experimental procedures.....	53
4.	EAE model induction .....	54
4.1	MOG emulsion preparation from scratch .....	54
4.2	EAE kit from Hooke Laboratories .....	55
4.3	Clinical scores .....	55
5.	BrdU administration.....	55
6.	Behaviour tests .....	56
6.1	Open field.....	56
6.2	Rotarod .....	57
6.3	Pole test .....	57
7.	Animal sacrifice .....	58
8.	Tissue processing .....	58
9.	Cellular and Molecular Analysis.....	59
9.1	Histological protocol .....	59
9.1.1	Luxol Fast Blue staining .....	59
9.2	Free-floating immunohistochemistry (IHC).....	59
9.2.1	Image acquisition and analysis.....	60
9.3	Western Blot (WB).....	61
9.4	Enzyme-Linked Immunosorbent Assay (ELISA) .....	62
10.	Statistical analysis .....	63
CHAPTER 3 - RESULTS.....		65
1.	Clinical scores .....	67
2.	Locomotor activity characterization of the EAE animal model.....	69
2.1	EAE IV animals show impaired OF performance on weeks 2 and 3 post-induction	69
2.2	EAE IV and IP animals show impaired rotarod performance on week 3 post – induction .....	71

2.3	EAE IV animals show impaired pole test performance in week 3 post-induction.....	72
3.	Cellular and molecular analysis .....	74
3.1	Demyelination in brain and spinal cord of EAE animals was not observed .....	74
3.2	Myelin proteins MBP and PLP seem to remain unaltered in EAE mice.....	75
3.3	MBP fluorescence levels in the corpus callosum do not change in EAE.....	76
3.4	SPF animals show significantly increased levels of TNF $\alpha$ inflammatory responses, combined with a tendency for increased levels of IL-1 $\beta$ .....	77
3.5	NF- $\kappa$ B pathway does not seem to be activated in the EAE mice.....	78
3.6	Oligodendroglial differentiation in the EAE brain from adult progenitors of the SVZ	79
3.6.1	Volume of the brain regions studied .....	79
3.6.2	Cellular survival.....	80
3.6.3	Oligodendroglial differentiation .....	80
3.6.4	Neuronal differentiation .....	82
CHAPTER 4 – DISCUSSION .....		83
CHAPTER 5 – CONCLUSIONS AND FUTURE PERSPECTIVES.....		91
CHAPTER 6 – BIBLIOGRAPHY .....		95

## **Abbreviations**

**BBB** Blood-brain barrier  
**BrdU** 5-bromo-2'deoxyuridine  
**BSA** Bovine serum albumin  
**CC** Corpus callosum  
**CFA** Complete Freund's adjuvant  
**CNS** Central Nervous System  
**CSF** Cerebrospinal fluid  
**CT** Cerebral cortex  
**CTRL** Control  
**DCX** Doublecortin  
**EAE** Experimental autoimmune encephalomyelitis  
**ECM** Extracellular matrix  
**EDTA** Ethylenediamine tetraacetic acid  
**ELISA** Enzyme-linked immunosorbent assay  
**FGF** Fibroblast growth factor  
**i.p.** Intraperitoneal  
**i.v.** Intravenous  
**IGF** Insulin – like growth factor  
**IL-1 $\beta$**  Interleucin - 1 $\beta$   
**IP** Mice administered i.p. (intraperitoneal) PTx  
**IV** Mice administered i.v. (intravenous) PTx  
**I $\kappa$ B $\alpha$**  Inhibitor protein of  $\kappa$ B family  
**MBP** Myelin basic protein  
**miRNA** microRNA  
**MMPs** Metalloproteinases  
**MS** Multiple Sclerosis  
**NF- $\kappa$ B** Nuclear factor kappa B  
**NMO** Neuromyelitis optica  
**NOR** Nodes of Ranvier  
**NSCs** Neural stem cells  
**OF** Open field  
**OLGs** Oligodendrocytes  
**OPCs** Oligodendrocyte precursor cells  
**p.i.** post – induction  
**PBS** Phosphate – buffered saline  
**PDGF** Platelet – derived growth factor

**PDGFR $\alpha$**  Platelet – derived growth factor receptor- $\alpha$   
**PLP** Proteolipid protein  
**PT** Pole test  
**PTx** Pertussis Toxin  
**RIPA** Radio immuno precipitation assay  
**RR** Rotarod  
**RT** Room temperature  
**SDS** Sodium dodecyl sulphate  
**SPF** Specific – pathogen free  
**ST** Striatum  
**SVZ** Subventricular zone  
**TBS – T** Tris buffered saline with Tween 20  
**TMEV** Theiler's Murine Encephalomyelitis Virus  
**TNFR** Tumour necrosis factor receptor  
**TNF $\alpha$**  Tumour necrosis factor –  $\alpha$   
**VAF** virus – antibody free

## List of figures and tables

Fig. 1 – Representation of the two hypotheses for the origin of MS. ....	26
Fig. 2 - Differences observed among myelin sheaths, axons, and inflammatory cells in Multiple Sclerosis.....	27
Fig. 3 - Available research models to study MS. ....	28
Fig. 4 – Molecular mechanism behind the EAE model.....	32
Fig. 5 - Roles of TNF $\alpha$ (A), IL-1 $\beta$ (B) and NF- $\kappa$ B (C) in EAE pathogenesis. ....	34
Fig. 6 - Oligodendrocyte lineage.....	36
Fig. 7 - Schematic model of the differentiation of a committed OPC into a mature myelinating oligodendrocyte.....	39
Fig. 8 - Phases of remyelination. ....	42
Fig. 9 - Adult NSCs in the SVZ and SGZ of the mammalian brain. ....	45
Fig. 10 – Timeline for <i>in vivo</i> experiments.....	53
Fig. 11 -Schematic representation of the open field arena. ....	57
Fig. 12 – Brain regions evaluated in IHC experiments. ....	61
Fig. 13 - Clinical scores registered as a measure of EAE phenotype progression for the different experimental groups. ....	68
Fig. 14 - Locomotor activity is impaired on EAE IV animals on weeks 2 and 3 after model induction, as assessed by the OF test. ....	70
Fig. 15 - Rotarod test results expose impairments for EAE IV and IP animals on week 3 after model induction. ....	71
Fig. 16 - Pole test performance on week 3 post-induction shows deficits for EAE IV mice in all criteria. ....	73
Fig. 17 - Myelin in EAE brain and spinal cord appears similar to controls. ....	74
Fig. 18 - Levels of myelin proteins MBP (A) and PLP (B) did not seem to change in EAE animals at 31 days p.i.....	75
Fig. 19 - MBP fluorescence in the CC is not altered by EAE.....	76
Fig. 20 - Inflammatory cytokines IL-1 $\beta$ (A) and TNF $\alpha$ (B) levels in EAE animals. ....	77
Fig. 21 - Levels of pNF $\kappa$ B (A) and plkB $\alpha$ (B) seem to remain unaltered in EAE mice 31 days p.i.....	78
Fig. 22 - Volume does not change in EAE animals in the different brain regions studied. ....	79

Fig. 23 - Cell survival is not altered between CTRL and EAE groups.....	80
Fig. 24 - NG2 <sup>+</sup> BrdU <sup>+</sup> cells are increased in the corpus callosum of EAE animals.....	81
Fig. 25 - Neuronal differentiation in the SVZ of control and EAE animals.....	82
Fig. 26 - Schematic summary of the main findings of this work.....	94
Table 1 – Compounds used for emulsion preparation for EAE model induction.....	54
Table 2 – Experimental groups of this project.....	55
Table 3 – Primary antibodies used to assess adult oligodendrogenesis. ....	60
Table 4 – Primary antibodies used for western blotting.....	62

## Abstract

Multiple Sclerosis (MS) is one of the most frequent disorders of the central nervous system (CNS), affecting young individuals, primarily women. MS is an inflammatory disease, characterized by demyelinating events, oligodendrocyte (OLGs) loss, and neuronal degeneration. These damages to the myelin sheath, responsible for axon insulation, impede the rapid and efficient transmission of the nervous impulse, resulting in movement and coordination deficits, with an impact in the quality of life of the patients, with a possible impairment in their autonomy. Experimental Autoimmune Encephalomyelitis (EAE) is the most common *in vivo* model to study MS, allowing the study of the relationship between inflammation and immunity. Albeit the cause for MS remains unknown, one of the proposed hypotheses relies in the neuronal degeneration due to the CNS chronic inflammation, by action of immune cells (CD4<sup>+</sup> and CD8<sup>+</sup> T cells and B cells, for example) and glial cells, which together release cytokines and mediators responsible for the observed pathology. The combination of immunologic and neurologic mechanisms depicted by EAE animals is similar to several features presented by MS patients, from inflammation, demyelination, axonal loss and gliosis. In the animal model, the administration of the peptide MOG<sub>35-55</sub> leads to the activation of specific CD4<sup>+</sup> T cells in the periphery. In addition, Pertussis toxin (PTx) compromises the blood-brain barrier (BBB), allowing the crossing of these immune cells into the CNS, where an inflammatory cascade is triggered with the release of several factors, such as tumour necrosis factor- $\alpha$  (TNF $\alpha$ ), interleucine-1 $\beta$  (IL-1 $\beta$ ), interferon- $\gamma$  (IFN $\gamma$ ) or activation of the nuclear factor kappa B (NF- $\kappa$ B) pathway, and the recruitment of macrophages, ultimately leading to myelin loss and neurodegeneration.

OLGs are the CNS cells responsible for myelin production. They go through distinct stages during their differentiation process, characterized by morphological changes, different marker expression and migratory capabilities, becoming functional and capable of producing myelin when they reach their maximum maturation state. For remyelination, replacement of myelin, to occur, OLG precursor cells (OPCs) have to be recruited. OPCs are present in the brain parenchyma or can be generated by neural stem cells (NSCs) present in the subventricular zone (SVZ), one of the germinal niches present in the adult mammalian brain. Under physiological conditions, NSCs in the SVZ give rise to interneurons, to replace the population present in the olfactory bulb. Nevertheless, upon demyelinating conditions, these NSCs can migrate to the lesioned areas, where they differentiate into OLGs that partially remyelinate these regions. Hence, the aim of this work was to characterize the commonly used animal model to study MS, the EAE. Both behaviour and cellular and molecular analysis were performed, and how the process of adult oligodendrogenesis unveils under these demyelinating conditions was assessed.



For this, C57BL/6 female 8 weeks-old mice were induced with EAE with a subcutaneous injection (s.c.) of the MOG<sub>35-55</sub> peptide (200 µg/mouse) emulsified in Complete Freund's adjuvant (CFA) and PTx (200 ng) was injected (intravenous (i.v.) or intraperitoneal (i.p.)) 2h after MOG injection and again 48 h later. The following day, mice received 7 i.p. injections with 2 hour-intervals of 5-bromo-2'-deoxyuridine (BrdU, 50 mg/kg) to label proliferating cells in order to study cell survival and differentiation from SVZ NSCs. Animals were scored daily for the onset and progression of the EAE model, and open field (OF), rotarod (RR) and pole test (PT) were performed two and three weeks after model induction, to assess motor impairment. Four weeks after EAE induction, animals were sacrificed and cellular and molecular characterization of the inflammatory EAE components, as well as of myelin protein levels and adult oligodendrogenesis was performed.

Regarding model induction, this process can be influenced by distinct factors, from the age and sex of the animals, to their diet, stress levels and housing conditions. Scores registered for the different experimental groups, in specific-pathogen free (SPF) or virus-antibody free (VAF) environment denoted, as previously described, the influence of the microbiome of the animals in EAE induction: distinct environments lead to different EAE induction patterns.

Behavioural results highlight motor impairment of the animals relative to the EAE clinical score. Regarding the cellular and molecular tests, no changes were seen for luxol fast blue tests assessing demyelination in EAE mice. Myelin basic protein (MBP) and proteolipid protein (PLP) levels remained identical between control and EAE groups. Importantly, levels of TNF $\alpha$  were significantly increased for animals housed in SPF conditions, accompanied by a tendency for increased IL-1 $\beta$  levels in these mice, while no alterations were seen for the NF- $\kappa$ B pathway. However, when the animals were sacrificed their clinical scores were already low, due to the endogenous remyelination process that had occurred, justifying the decreased inflammation and the levels of MBP and PLP identical to the control groups.

To study the process of oligodendrogenesis, cell survival (BrdU<sup>+</sup> cells) and differentiation (cells positive for NG2, a marker of OPCs, and BrdU, NG2<sup>+</sup>BrdU<sup>+</sup> cells) were assessed, in four brain regions of interest: SVZ, where the NSCs are located, and the corpus callosum (CC), cerebral cortex (CT) and striatum (ST), since these are the most affected regions in brain EAE. BrdU<sup>+</sup> cells resulted from cell replication after mice were injected with BrdU in the beginning of the protocol and that survived during our experimental protocol timeframe. A tendency for increased cell survival (number of BrdU<sup>+</sup> cells) can be observed in the SVZ, CC and CT. Importantly, an increase in NG2<sup>+</sup>BrdU<sup>+</sup> cells for EAE animals in the CC suggests that differentiation of SVZ NSCs into precursors of the oligodendroglial lineage occurred with migration to the CC.

In the future, an overall increase in sample size for all the tests performed, as well as sample collection at the time of EAE maximum score will allow for an accurate characterization

of the EAE model, its inflammatory cascade, and the mechanisms of new oligodendrocyte formation for the remyelination process. Therefore, this would confirm or dissipate the trends here observed, allowing for the establishment of adult oligodendrogenesis as a potential therapeutic target for MS therapy.

**Keywords** Experimental Autoimmune Encephalomyelitis; Multiple Sclerosis; Oligodendrogenesis; Subventricular Zone

## Resumo

A Esclerose Múltipla (EM) é uma das doenças mais comuns do sistema nervoso central (SNC), afetando jovens adultos e sendo mais frequente em mulheres. A EM é uma doença inflamatória, que resulta na desmielinização e perda de oligodendrócitos (OLGs), bem como na neurodegeneração. Estes danos na bainha de mielina, que fornece isolamento aos axónios, impedem a rápida e eficiente transmissão do impulso nervoso, provocando défices a nível motor e de coordenação, e resultando num declínio da qualidade de vida e possível perda de autonomia do paciente. O modelo mais utilizado para os estudos *in vivo* de EM é o modelo da Encefalite Autoimune Experimental (EAE). Este modelo permite o estudo da relação entre inflamação e imunidade. Apesar de não ser conhecida a natureza da EM, uma das hipóteses assenta na degeneração neuronal causada pela inflamação crónica do SNC, devido à ação, entre outros intervenientes, de células imunitárias (células T CD4<sup>+</sup> e CD8<sup>+</sup> e células B, por exemplo) e células gliais que, em conjunto, libertam citocinas e outros fatores responsáveis pela patologia observada. A combinação de mecanismos imunológicos e neurológicos apresentada por animais com EAE partilha características apresentadas por pacientes com EM, desde a inflamação, à desmielinização, perda axonal e gliose. No modelo animal, a administração do péptido MOG<sub>35-55</sub> conduz à ativação de células T CD4<sup>+</sup> específicas na periferia. Por sua vez, a toxina Pertussis (PTx) compromete a barreira hematoencefálica, permitindo a passagem destas células imunes para o SNC, onde é desencadeada uma cascata inflamatória com a libertação de diversos fatores e citocinas, como o Fator de Necrose Tumoral- $\alpha$  (TNF $\alpha$ ), a Interleucina-1 $\beta$  (IL-1 $\beta$ ), o Interferão- $\gamma$  (IFN $\gamma$ ) ou a ativação da via do Fator Nuclear kappa B (NF- $\kappa$ B), assim como o recrutamento de macrófagos levando, em última análise, à perda de mielina e neurodegeneração.

Os OLGs são as células do SNC responsáveis pela produção de mielina. Estas células atravessam diferentes estádios durante o seu processo de diferenciação, caracterizados por alterações morfológicas, expressão de diferentes marcadores e capacidades migratórias, tornando-se funcionais e capazes de produzir mielina quando atingem a sua máxima maturação. De modo a que ocorra o processo de remielinização, em que a bainha de mielina é repostada, são recrutadas células precursoras de OLGs (CPOs), que podem ter origem no parênquima cerebral, mas também na zona subventricular (ZSV), um dos nichos germinais presentes no cérebro de mamíferos adultos. Em condições fisiológicas, as células precursoras neurais (CPNs) presentes na ZSV dão maioritariamente origem a interneurónios, repondo a população dos mesmos que existe no bulbo olfativo. Contudo, em condições de desmielinização, estas células precursoras têm a capacidade de migrar para as regiões lesionadas, onde se diferenciam em OLGs que remielinizam parcialmente essas áreas. Deste modo, o objetivo deste trabalho incidia na caracterização do modelo de EAE, a nível

comportamental, mas também dos seus mecanismos celulares e moleculares, bem como na avaliação do processo de oligodendrogénese neste ambiente patológico.

Para tal, murganhos C57BL/6 fêmea com 8 semanas de idade foram induzidos com o modelo de EAE. No primeiro dia, os animais receberam uma injeção subcutânea (s.c.) do péptido MOG<sub>35-55</sub> (200 µg/murganho) emulsificado em adjuvante; seguida de uma injeção de PTx (200 ng) (intravenosa (i.v.) ou intraperitoneal (i.p)), 2 horas após a injeção de MOG e que foi repetida após 48 horas. No dia seguinte, os animais receberam 7 injeções i.p., com intervalos de 2 horas, de 5-bromo-2'-desoxiuridina (BrdU) (50 mg/kg), de forma a marcar células em proliferação para estudar a sobrevivência e diferenciação celulares a partir de células precursoras da ZSV. Foram registados os *scores* diários dos animais, de acordo com a progressão do modelo de EAE, e testes comportamentais como o teste do campo aberto (do inglês, *open field*) para avaliar a atividade locomotora, ou o *rotarod* e o *pole test*, para avaliar a coordenação e equilíbrio dos animais, foram realizados na 2<sup>a</sup> e 3<sup>a</sup> semanas após a indução do modelo. Quatro semanas depois da indução do modelo de EAE, os animais foram sacrificados e procedeu-se à caracterização celular e molecular dos componentes inflamatórios presentes em EAE, assim como dos níveis de proteínas de mielina e do processo de oligodendrogénese.

Relativamente à indução do modelo, esta pode ser afetada por diferentes fatores, desde a idade e sexo dos animais, à sua dieta, aos níveis de stress e às condições em que estão alojados. Os registos dos *scores* obtidos para os diferentes grupos experimentais, que estavam alojados em diferentes ambientes, na ausência de agentes patogénicos específicos (*specific-pathogen free* - SPF) ou num ambiente isento de vírus e anticorpos (*virus-antibody free* - VAF), demonstrou, tal como já tinha sido descrito na literatura, a influência do microbioma dos animais na indução de EAE: diferentes ambientes levam a padrões distintos de desenvolvimento de EAE.

Os resultados obtidos nos três testes comportamentais demonstraram, como esperado, que os défices na atividade locomotora e coordenação dos animais são proporcionais aos *scores* registados. A nível celular e molecular, não foram observadas alterações nos níveis de desmielinização em murganhos EAE, avaliados com a marcação histológica de luxol, quando comparados com os animais controlo. Os níveis das proteínas MBP e PLP, quantificados por western blot também permaneceram inalterados entre os grupos estudados. Porém, os níveis de TNF $\alpha$  estavam significativamente aumentados nos animais com EAE alojados em instalações SPF, enquanto que uma tendência para o aumento dos níveis de IL-1 $\beta$  também se observou para estes animais. Contudo, não foram observadas alterações para os níveis de NF- $\kappa$ B. No entanto, aquando do sacrifício, os animais já tinham regredido nos seus *scores*, pelo que o processo de remielinização endógena já tinha ocorrido, justificando assim o

decréscimo na inflamação e a presença de níveis de MBP e PLP idênticos aos dos animais controle.

Com o intuito de estudar o processo de oligodendrogénese, a sobrevivência (células positivas para BrdU, BrdU<sup>+</sup>) e diferenciação (células positivas para NG2, um marcador de precursores de OLGs e BrdU, NG2<sup>+</sup>BrdU<sup>+</sup>) celulares foram quantificadas, em quatro regiões de interesse, na ZSV, local onde se encontram as células precursoras, e no corpo caloso (CC), córtex cerebral (CT) e estriado (ES), algumas das regiões mais afetadas em EAE. As células BrdU<sup>+</sup> resultam dos processos de replicação celular após a administração de BrdU no início das experiências e que sobreviveram ao longo do protocolo experimental. Uma tendência para o aumento da sobrevivência celular (número de células BrdU<sup>+</sup>) foi observada para a SVZ, CC e CT. De forma relevante, foi observado um aumento no número de células NG2<sup>+</sup>BrdU<sup>+</sup> para os murganhos EAE no CC, o que sugere a ocorrência de diferenciação de precursores da ZSV em células da linhagem oligodendroglial, que terão migrado para o CC.

De futuro, o aumento do número de amostras para as experiências realizadas, bem como o sacrifício dos animais e recolha das amostras quando os animais apresentarem os défices motores máximos (maior *score*) irá permitir uma adequada caracterização do modelo de EAE, não só da sua componente inflamatória, mas também dos mecanismos de formação de novos OLGs para o processo de remielinização. Deste modo, será possível confirmar ou dissipar as tendências observadas neste trabalho, permitindo a formulação da hipótese da oligodendrogénese em adulto como potencial alvo terapêutico em EM.

**Palavras-Chave** Encefalite Autoimune Experimental; Esclerose Múltipla; Oligodendrogénese; Zona Subventricular



# **CHAPTER 1 – INTRODUCTION & AIMS**







# 1. Multiple Sclerosis

## 1.1 Disease characteristics and role of oligodendrocytes

Multiple sclerosis (MS) is one of the most common chronic neurological and demyelinating disorders characterized by several sites of demyelination<sup>1</sup>. These lesions in the myelin sheath surrounding axons lead to deficits in the transmission of information between neurons both in the brain and in the spinal cord, ultimately impairing movement and coordination of the patient<sup>2</sup>. It affects mainly young adults, and women are twice more likely than men to develop this neurological disorder. In Portugal between 20 – 60 individuals per 100,000 are affected by this condition<sup>3</sup>. Most MS patients (85%) portrait a relapsing-remitting form of this condition (RRMS), characterized by abrupt symptomatic episodes followed by recovery periods. This phenotype changes after 5 to 25 years, when the severity of the symptoms increases, and is designated as secondary progressive MS (SPMS). In cases where patients show merely a steady progression of the disease (10% of patients), without RRMS symptoms, this pathology is designated as primary progressive MS (PPMS)<sup>4</sup>. There are two major difficulties associated with this pathology: first, the disease course varies from patient to patient; and second, a patient can be already at an advanced stage of progression once it is diagnosed, since a major part of the process is clinically silent<sup>5</sup>.

Although the aetiology of MS remains to be found, several environmental and genetic risk factors might have a role in MS development. Vitamin D levels, smoking, age, diet, hormones and genetic susceptibility are some of the factors which might influence not only the propensity to develop MS, but also the disease course<sup>2,6</sup>. Moreover, infection has also been described to play a role in MS susceptibility, namely patients with high levels of Epstein-Barr virus (EBV) antibodies have been shown to have an increased risk for developing MS, and this increase is potentiated if EBV infection occurs at a later age, rather than during adolescence<sup>7-9</sup>.

Furthermore, two competing hypotheses for the origin of MS remain in discussion, depending if inflammation is considered the cause (the 'outside-in' theory of immune dysregulation) or the consequence (the 'inside-out' model in which CNS malfunction leads to the release of immune components) of neurodegeneration<sup>10-12</sup> (Fig. 1).

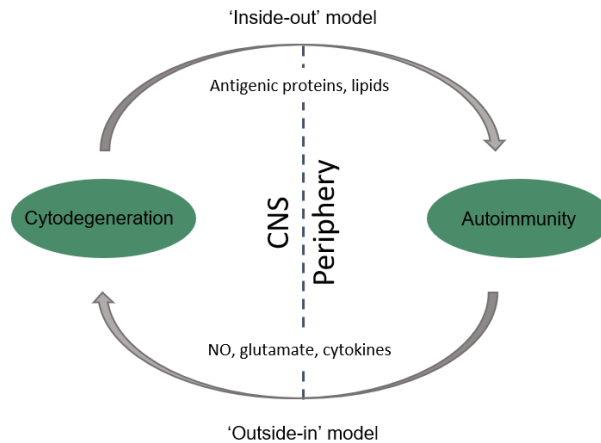


**Fig. 1 – Representation of the two hypotheses for the origin of MS.** The ‘outside-in’ model hypothesizes that dysregulated auto-reactive cells present in the periphery are able to cross the blood-brain barrier (BBB), and together with B cells and macrophages lead to CNS injury. In turn, the ‘inside-out’ theory states that initial dysfunction takes place in the CNS, possibly in oligodendrocytes and myelin, which results in the release of antigenic molecules that trigger an inflammatory response, further potentiating degeneration. Adapted from Nat Rev Neurosci 2012; 13:507–514.

In MS inflammation mediated by cytokines, proteolytic enzymes or free radicals, released by glial and immune cells promotes a microenvironment that damages the axons<sup>5,13</sup> (Fig. 2). Moreover, inflammation can also reduce the energy metabolism in demyelinated axons, for instance by interfering directly with mitochondria or with the blood supply, inducing degeneration<sup>5,14</sup>.

In the central nervous system (CNS) OLGs are the cells responsible for myelinating the axons, therefore these cells have a predominant role in MS. Oligodendrocyte precursor cells (OPCs) present in the brain parenchyma are capable of generating new OLGs under demyelinating conditions, demonstrating the rapid endogenous response to the pathophysiological alterations presented<sup>15</sup>. Also, it was shown by Picard – Riera *et al.* that in a mouse model of MS (Experimental Autoimmune Encephalomyelitis (EAE)), although cells from the adult subventricular zone (SVZ) generate neurons, astrocytes and OLGs that will migrate to the olfactory bulb (OB), they are also responsible for the repopulation of astrocytes and OLGs in the lesioned white matter. This means that under pathological situations, these progenitors are able to migrate and be recruited to lesioned areas, where they will differentiate<sup>16</sup>. Furthermore, a human post-mortem study developed by Nait-Oumesmar *et al.* showed increased cellular density and proliferation in the SVZ of MS patients<sup>1</sup>. All these studies highlight the importance of SVZ progenitor cells which, even in the adult brain, are able to proliferate and differentiate under specific conditions and cues, as a mechanism to increase oligodendrogenesis and attempt to recover from the damage<sup>17</sup>.

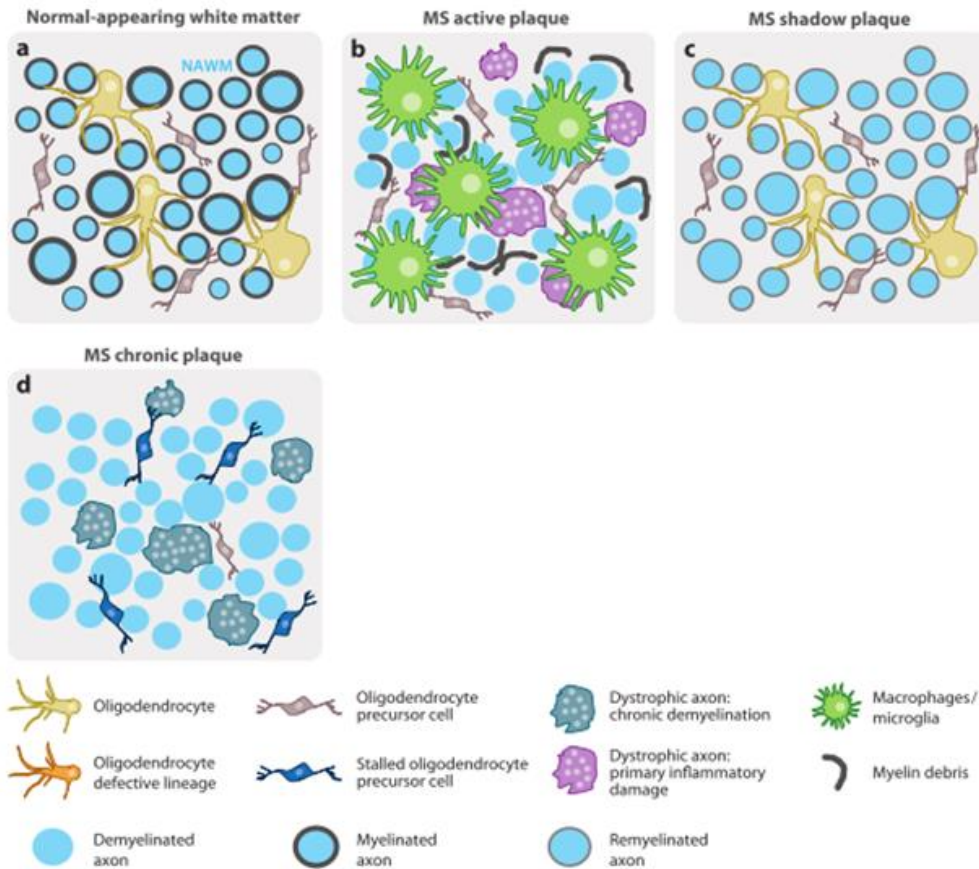


**Fig. 2 - Differences observed among myelin sheaths, axons, and inflammatory cells in Multiple Sclerosis.** Transverse sections through white matter axons (blue circles) of (a) normal-appearing white matter (NAWM), (b) acutely injured white matter (active plaque), (c) myelin regeneration in a shadow plaque, or (d) chronic demyelination (chronic plaque). (a) In MS, remyelinated axons have thinner myelin sheaths than normal undamaged axons. (b) Acute inflammation, with microglia and molecules such as cytokines produced by immune cells lead to axonal damage, and macrophages are responsible for clearing myelin debris. In areas where remyelination occurs (c), there is less axonal loss than when these demyelination events are chronic (d). Adapted from *Annu. Rev. Neurosci.* 2011. 34:21–43.

## 1.2 Research models

To study the pathological component of MS, the complexity of cellular interactions can be simplified using cell lines or primary cell cultures (of one type of cells or co-cultures with different cell types). Nevertheless, *in vivo* models are necessary to study the efficacy and safety of possible therapeutic compounds that can be for example discovered using cell cultures<sup>18</sup>(Fig. 3).

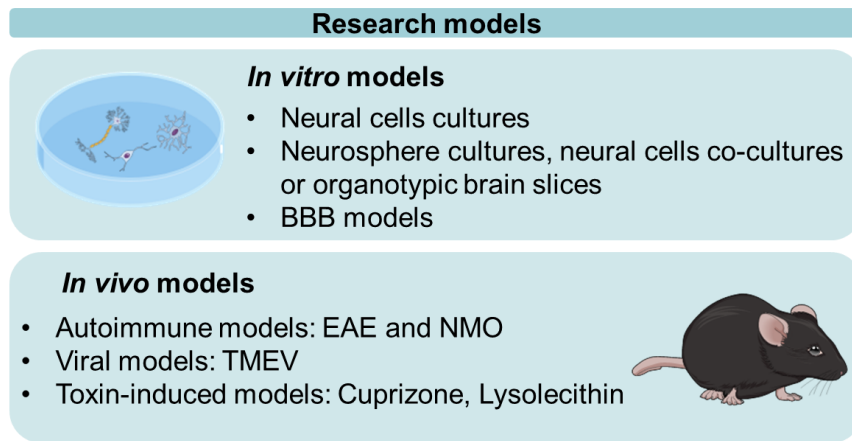


**Fig. 3 - Available research models to study MS.** *In vitro* models are commonly used to study the pathology of this disease. The models of cell lines or transformed cells include neural cell cultures (neurons, astrocytes, microglia, oligodendrocytes); neurospheres cultures, neural cells co-cultures or organotypic brain slices, to attempt at mimicking the cellular organization and communication that happens in the brain. Blood-brain barrier (BBB) models are also used since the impairment of this blood-brain interface is also a characteristic of MS. Regarding the *in vivo* models, they are useful to understand the link between CNS, neuroinflammation and demyelination. There are three main types of animal models: autoimmune, viral and toxin-induced. Two examples of autoimmune models are Experimental Autoimmune Encephalomyelitis (EAE), the most common, easily induced, and reproducible model; and Neuromyelitis Optica (NMO), a disease with a severe outcome and which is often misdiagnosed as MS. One example of virus-induced models is Theiler's Murine Encephalomyelitis Virus (TMEV). Finally, when considering the toxin-induced models, the Cuprizone models of de- and remyelination and the Lysolecithin model of focal demyelination are the most studied.

### 1.2.1 *In vitro* models

Regarding the *in vitro* models, several types of cell cultures are used, microglia, OLGs, neurons, and astrocytes, due to the fact that all these cell types can be involved and altered in MS. Therefore, these cultures are necessary essentially to study the role and behaviour of these cells under these specific conditions<sup>18</sup>.

Using pure primary cell cultures with only one type of cell raises the question of whether it represents what happens *in vivo*. So, due to the need of cells to communicate with different cell types and the fact that they can be influenced by the surrounding environment, neurospheres cultures (which can be composed of neurons or glial cells), neural cell co-cultures or organotypic brain slices are used in an attempt to mimic as closely as possible what happens in the brain<sup>18</sup>. Moreover, the blood-brain barrier (BBB), one of the interfaces between blood and the CNS<sup>19</sup>, has been shown to play an important role in MS, being impaired in MS patients and allowing the passage of immune cells, such as leukocytes, into the CNS<sup>18,20</sup>. Some examples of BBB models are cultures of endothelial cells since major BBB properties arise from the junctional complexes between the cerebral endothelial cells<sup>20</sup>. Moreover, more

elaborate BBB co-culture systems can also be used in an attempt to mimic the real BBB components: astrocyte foot processes (which communicate with blood vessels) and basement membranes and endothelial cells<sup>18</sup>. One advantage of BBB models is that they can also be created using computational methods (*in silico*) to study the permeability of this barrier to a certain molecule, based on its properties<sup>18</sup>.

### 1.2.2 *In vivo* models

Several animal models can be used to study MS. Nevertheless, there is not one universally accepted, due to the clinical, immunological and pathological complexity of this disease, that cannot be reproduced in its entirety using the current models<sup>21</sup>.

Animal models of MS are crucial to better understand the link between the CNS, neuroinflammation, demyelination and neuronal injury. There are three main types of models – autoimmune, viral, and toxin-induced. However, it is possible that different models can lead to different conclusions, that cannot all be directly extrapolated for the human condition<sup>22</sup>.

Another problem with these models is that the cause for MS is not truly known and differing from patient to patient, then the induction of demyelinating lesions through these processes is merely an attempt and may not recapitulate what happens in human patients.

#### 1.2.2.1 Autoimmune models

##### a. Experimental autoimmune encephalomyelitis (EAE)

The EAE is the most studied and used animal model, since it is a rapidly induced and reproducible model of autoimmunity, useful to study the relationship between neuroinflammation and immunity. Here, the autoimmune component is introduced through immunization with self-antigens derived from basic myelin protein. Freund's adjuvant and Pertussis toxin (PTx) are also administered in order to enhance humoral response and increase BBB permeability, respectively, similar to the symptoms portrayed by patients<sup>8,23</sup>. However other variants of the model can be obtained by mutant mice, that were genetically altered and do not need PTx or Freund's adjuvant<sup>22,24</sup>. Furthermore, three different approaches can be used for the induction of this model: active induction (aEAE), in which animals are immunized with myelin antigens in adjuvant; passive induction (pEAE), characterized by the transfer of activated myelin – specific T cells into naïve animals; and the spontaneous induction models (sEAE) which allow the study of autoimmune mechanisms without exogenous manipulation<sup>25,26</sup>. aEAE is the most frequently used method in mice, allowing for fast and robust results, modelling for the induction (T cell priming following immunization) and effector (migration of T cells into the CNS, followed by chemokine and cytokine production, macrophage activation and demyelination) stages of EAE<sup>25,27,28</sup>. The usual development of the

aEAE model throughout time consists in developing weakness around day 10 post-induction (p.i.) and maximum disability 10-14 days after immunization. Mice normally recover their strength 3 – 4 weeks after the induction of the model<sup>22</sup>. EAE manifestation (acute, chronic or relapsing – remitting course) can differ due to factors such as the mice strain, the immunogen, the use of PTx or the age and gender of the animals<sup>29,30</sup>.

#### b. Models of neuromyelitis optica (NMO)

NMO is often misdiagnosed as MS although its cause seems to be more defined than MS, as in human patients it is the result of an autoantibody. The animal models developed for this pathology consist in the administration of IgG from patients with NMO to the animals directly in the CNS or after EAE induction and BBB disruption<sup>22</sup>. Notwithstanding, NMO should be considered as a model for experimental studies since the outcome is very severe (spinal cord injury and visual loss). It would be important to find a distinctive marker for NMO, as it has been proposed by Lennon *et al.*, that identified an IgG autoantibody (NMO-IgG) in patients with NMO<sup>31</sup>.

### 1.2.3 Viral models

Several epidemiological studies have hypothesized that a viral infection conjugated with a specific genetic background might increase propensity to an immune attack to the CNS<sup>8,32</sup>.

#### a. Theiler's Murine Encephalomyelitis Virus (TMEV)

Viral infections of the CNS can induce demyelination in mice and the best studied are the picorna virus, for instance TMEV. After its intracerebral injection into a mouse's brain, there are two stages of the disease: first the infection predominantly affects neurons, and after there is the chronic phase, starting about 1 month after infection, and it is characterized by progressive disability, inflammation, demyelination and remyelination episodes and axonal damage<sup>22,33</sup>. It has several positive characteristics over EAE, such as the clinical manifestation similar to that of chronic MS patients; and the pathology is associated with the activation of the immune response, and not due to toxic effects related with the virus. Whereas EAE can be induced in other species such as primates or rodents, TMEV can only be induced in certain mouse strains, which are divided into two subgroups: one group consists of virulent strains that cause fatal encephalitis (strains GDVII and FA); whilst the other, by inducing acute polioencephalomyelitis, is less virulent and used as a MS model (strains DA and BeAn8386 (BeAn))<sup>8,34</sup>.

#### 1.2.4 Toxin-induced models

Toxin-induced demyelination is also a way to study MS. The advantage of these models is that they are not associated to inflammatory processes, being used merely to study the demyelination and remyelination mechanisms<sup>21</sup>.

##### a. Cuprizone model of de – and remyelination

This is the most common model of toxic demyelination used. Cuprizone (bis-cyclohexanone-oxaldihydrazone) is a copper chelating drug, which acts by causing oxidative damage, ultimately triggering apoptosis in OLGs and inducing demyelination<sup>8,21</sup>. When demyelination is complete, OPCs are recruited to form new OLGs to start the remyelination process<sup>8</sup>. This model can be applied to different species, not only several mouse strains, but also rats or guinea pigs<sup>21,35</sup>. In most cases, C57BL/6 mice are administered cuprizone for 4 weeks, inducing demyelination followed by rapid and extensive remyelination within weeks<sup>21,36</sup>. One of its main advantages is that the lesions are characteristic of the corpus callosum, and their time course is well established. Nevertheless, the process of spontaneous remyelination occurs very swiftly, which is an obstacle to study the process and apply it to remyelination therapies, because it does not mimic the progressive MS lesions<sup>21</sup>. To overcome the problem of rapid demyelination, an adaptation of this model was created, in which animals were treated with cuprizone for 12 weeks and showed chronic demyelination, coupled with reduced remyelination<sup>21,37</sup>.

##### b. Lysolecithin model of focal demyelination

Lysolecithin, also known as lysophosphatidylcholine (LPC, lysoPC), is an activator of phospholipase 2 which induces focal demyelination by damaging the myelin sheath, due to its high-lipid content. It can be applied in different animal species, from cats to rabbits and mice<sup>8,21</sup>. One characteristic of this model is that remyelination rate and efficacy depend on the age of the animal (similar to what happens with human patients), due to the inhibition of OPC recruitment or OLG differentiation and macrophage clearance, for instance<sup>21,38</sup>.

In conclusion, from the wide variety of models available it is possible to select the one that best fulfils the researchers needs: whether it is to study de– and remyelination mechanisms or the pathology behind the disease. The important thing to consider is that none of them is perfect and should not be immediately extrapolated to the human condition.

### 1.3 Cellular mechanisms behind inflammation in MS: brief considerations from the human and the mouse model

The multifactorial nature of MS unravels through an intricate process, which develops as the disease progresses involving a complex inflammatory cascade<sup>39</sup>. Chronic CNS inflammation might be in the origin of neuronal degeneration, whether it is through the resident immune cells of the CNS, or through the action of cells which enter the CNS upon external stimuli. These immune cells (CD4<sup>+</sup> and CD8<sup>+</sup> T cells, B cells and monocytes for example), along with glial cells (microglia and astrocytes) present in the brain parenchyma promote oligodendrocyte and neuronal damage, as well as demyelination<sup>39</sup>. Importantly, the mechanism of action of the EAE model (Fig. 4) is, to a certain extent, parallel to the one of humans: specific subsets of CD4<sup>+</sup> T (T<sub>H</sub>1 and T<sub>H</sub>17) cells are activated in response to the antigen administered in the periphery. The disruption of the BBB by the action of PTx allows the entrance of these cells into the CNS, where they are activated by resident antigen-presenting cells and in turn release several cytokines, such as tumour necrosis factor alpha (TNF $\alpha$ ), interferon- $\gamma$  (IFN $\gamma$ ) or interleukin-1 $\beta$  (IL-1 $\beta$ ), unleashing an inflammatory cascade and the recruitment of macrophages, ultimately contributing to myelin loss and neurodegeneration<sup>40–43</sup>.

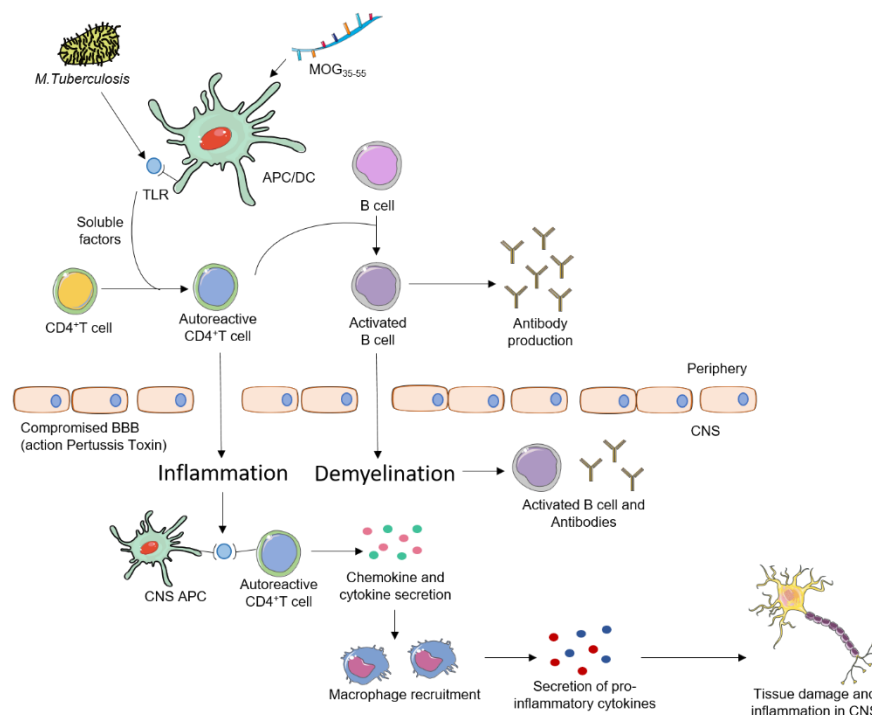


**Fig. 4 – Molecular mechanism behind the EAE model.** Subcutaneous administration of the peptide MOG<sub>35-55</sub> in emulsion with Complete Freund's Adjuvant (CFA), an adjuvant containing *M. tuberculosis*, elicits an immune response with immune cell activation and antibody production. Pertussis toxin causes the disruption of the BBB, allowing the entrance of these cells in the CNS, where they ultimately lead to inflammation and demyelination due to an inflammatory cascade with the activation of T and B cells by resident antigen-presenting cells which in turn release cytokines, chemokines and recruit macrophages, resulting in neuronal tissue damage and inflammation in the CNS.



### 1.3.1 Role for TNF $\alpha$ , IL-1 $\beta$ and the Nuclear Factor kappa B (NF- $\kappa$ B) pathway

Key players of inflammation are the soluble mediators such as cytokines, released by peripheral leukocytes which enter the CNS or CNS resident immune cells, that can control cellular function and communication<sup>44</sup>.

TNF $\alpha$  is a pro-inflammatory mediator produced by different cell types in the organism, such as the immune cells, macrophages and microglia, being an earlier intervenient in the inflammatory process<sup>44,45</sup>. TNF $\alpha$  is produced by T<sub>H</sub>1 cells, assisting in immunity against intracellular pathogens and is also involved in the initiation of CNS inflammation through chemokine induction, by binding to tumour necrosis factor receptor (TNFR)-1<sup>43,44,46</sup>. Maimone *et al.* observed that this cytokine is present in higher amounts in serum and cerebrospinal fluid (CSF) from MS patients than in healthy controls<sup>47</sup>. In EAE, this molecule can accelerate disease onset by chemokine regulation and exacerbates damage in the CNS by controlling the infiltration of inflammatory cells into the CNS<sup>48</sup>. Nevertheless, a beneficial role for TNF $\alpha$  in lymphoid organs in EAE has also been described through TNFR-2<sup>48</sup>. Moreover, TNFR-2 is responsible for the accumulation of proliferating oligodendrocyte progenitors that mature into myelinating oligodendrocytes, instrumental for the remyelination process in the cuprizone animal model<sup>49</sup> (Fig. 5A).

Activation of leukocytes leads to the release of IL-1 $\beta$ , in an inflammasome-dependent or -independent manner<sup>50</sup>. The binding of this molecule to its activating receptor complex ultimately triggers the transcription of pro-inflammatory genes due to activator protein-1 (AP-1) and nuclear factor kappa B (NF- $\kappa$ B) activation<sup>50</sup>. Lévesque *et al.* highlighted the instrumental role of IL-1 $\beta$  in EAE, since IL-1 $\beta$ -deficient mice are resistant to EAE, and the activation of interleukin-1 receptor type 1 (IL-1R1) by this cytokine promotes leukocyte infiltration into the CNS<sup>51</sup>. Similarly to TNF $\alpha$ , a beneficial role for IL-1 $\beta$  was also shown. IL-1 $\beta$  induces the production of insulin-like growth factor (IGF)-1 by microglia-macrophages and astrocytes, which in turn might contribute for OLG maturation and remyelination, as described by Mason *et al.* in a toxic demyelination model<sup>52</sup> (Fig. 5B).

NF- $\kappa$ B is a family of transcription factors regulating distinct cellular processes, from cell death and proliferation to inflammation<sup>52</sup>. In neurons, NF- $\kappa$ B modulates neuronal morphology and plasticity<sup>53,54</sup>. In resting conditions, NF- $\kappa$ B is sequestered in the cytosol by binding to I $\kappa$ B $\alpha$ , an inhibitor protein of  $\kappa$ B (I $\kappa$ B) family. This inhibition can be lost if the kinase complex IKK is activated, resulting in the phosphorylation of I $\kappa$ B $\alpha$ . Upon release, NF- $\kappa$ B translocates to the nucleus, where it acts as a transcription factor<sup>53,55</sup>. Studies performed using human brain samples have shown the activation of NF- $\kappa$ B in MS, where it localizes in oligodendrocytes, microglia, in infiltrating macrophages or close to CNS lesions<sup>56,57</sup>. Furthermore, genome wide association studies have identified several molecules associated with NF- $\kappa$ B as susceptible

candidates for MS<sup>41,58</sup>. In EAE, NF- $\kappa$ B can act through the regulation of differentiation and function of effector T cells<sup>53</sup>. Moreover Hilliard and colleagues have shown that c-Rel (member of NF- $\kappa$ B family)-deficient mice, are resistant to EAE induction, due to defective T<sub>H</sub>1 responses, being therefore unable to produce the inflammatory cytokines responsible for the EAE pathogenesis<sup>59</sup>. Activation of NF- $\kappa$ B can also result in the production and release of mediators such as TNF $\alpha$  and IL-1 $\beta$  which can also influence EAE<sup>41,53</sup>. Notwithstanding, NF- $\kappa$ B might also have a protective role for OLGs. In fact, Stone and co-workers have concluded that NF- $\kappa$ B inactivation in OLGs resulted in an increased susceptibility to develop EAE, while potentiated the remyelination failure in the cuprizone animal model<sup>60</sup> (Fig. 5C).

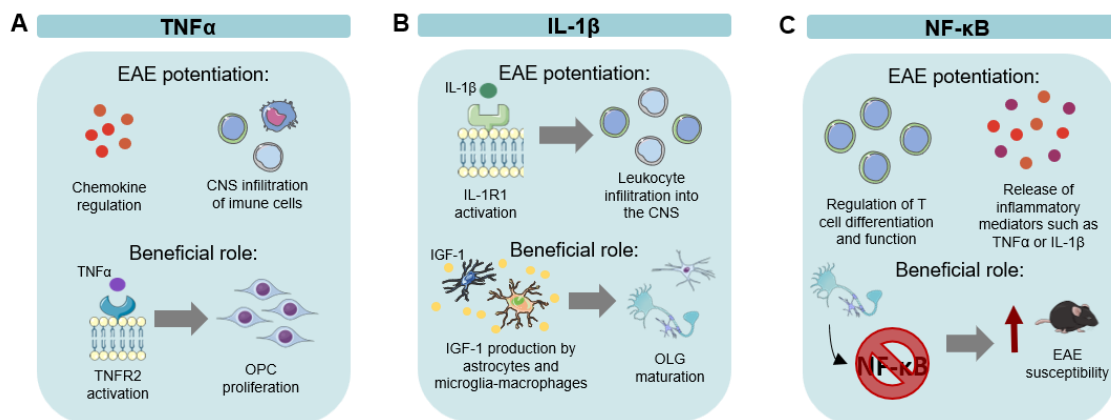


**Fig. 5 - Roles of TNF $\alpha$  (A), IL-1 $\beta$  (B) and NF- $\kappa$ B (C) in EAE pathogenesis.**

#### 1.4 Therapeutic approaches

Several therapeutic strategies have been developed to treat MS, from immunosuppression, preventing infiltration of immune cells into the brain parenchyma to depleting specific immune cells<sup>61,62</sup>. Still, these therapies are not focused on the repair of demyelinated regions, important topic when considering the progressive form of the disease which needs a more definitive resolution. At this point, there are two possible approaches: potentiating the endogenous myelination process or supplying these repair cells by transplantation.

For remyelination to occur it is necessary that progenitor cells are recruited to the target area, where they will proliferate and differentiate into mature cells, able to communicate with the demyelinated axon to ensure the repair process. To potentiate this process, the therapeutic approaches should either target endogenous myelinating cells, that could be modified to surpass the inhibitory factors preventing their migration and differentiation, or these cells should be delivered from the outside, but in this case for maximum efficacy they should have a high purity degree as well as quantity<sup>62,63</sup>. Other therapy to consider is the exogenous cell replacement, which in spite of the fact that there is the risk of tumorigenesis and cells need to

be successfully recruited to the desired area, presents several advantages such as promoting survival, differentiation and remyelination, not only of these cells but also of endogenous OLGs<sup>62,63</sup>. The fact that the migration of lineage restricted cells, such as OPCs, is limited raises the question of transplanting them directly in the injury site. Pluchino *et al.* studied the ability of multipotent neural precursors injected systemically or intracerebroventricularly to reach injured sites in the CNS. They showed that these cells might reach different areas affected by demyelination in the adult CNS, when injected both into the blood stream or directly in the brain<sup>64</sup>.

Moreover, myelin appears to respond positively to structured neuronal activity, so an alternative to potentiate endogenous remyelination and counteract the effects of aging is an active lifestyle, such as physical activity as well as mental stimulation (such as reading, learning a new language or to play a musical instrument)<sup>65–67</sup>.

## **2. Oligodendrocytes**

### **2.1 Differentiation of OPCs**

OLGs, the last brain cells to be formed during the development of the central nervous system, are responsible for producing myelin in the CNS, whereas in the peripheral nervous system (PNS) this process is secured by Schwann cells. OLGs are generated upon the differentiation of OPCs, which are glial cells that have proliferative and migrating capabilities and that are present in the CNS postnatally<sup>68–70</sup>. OPCs are identified by several specific markers, such as the proteoglycan NG2<sup>68,71</sup>, as well as the transcription factors Nkx2.2 and Olig1 and Olig2<sup>72</sup>. Since some of these markers, for instance Olig2, can also be expressed by other cells, it is common to use multiple markers to identify oligodendrocytes. Moreover, OPCs present in the adult brain have other distinctive characteristics from the OPCs present during development, namely they have longer cell cycles, they respond differently to growth factors and have distinct migrating capacities<sup>70,73</sup>.

OPCs can have two distinct fates: they can divide to form mature myelinating OLGs, or they can stay as immature cells, going through slow division processes. OPCs are widely distributed in the adult brain behaving differently accordingly to the brain region, gray matter promotes OPC proliferation whilst white matter promotes OPC differentiation<sup>70</sup>. During OLG maturation, these cells lose the ability to migrate and proliferate, and acquire an intricate morphology<sup>74</sup>. This maturation process entails four different stages (with Olig2 expression in all stages): OPCs are the precursors with proliferative and migratory abilities, which express, amongst others, platelet-derived growth factor receptor- $\alpha$  (PDGFR $\alpha$ ) and NG2, Olig1 and Nkx2.2<sup>72,74,75</sup>; preoligodendrocytes are the result of OPC differentiation and start expressing the O4 antigen (while continuing to express PDGFR $\alpha$  and NG2)<sup>74,76</sup>; premyelinating (immature)

oligodendrocytes, start expressing galactocerebroside C (GalC) and do not express NG2<sup>77</sup>; myelinating oligodendrocytes express myelin proteins such as myelin basic protein (MBP)<sup>78</sup> and are fully functional OLGs (Fig. 6).

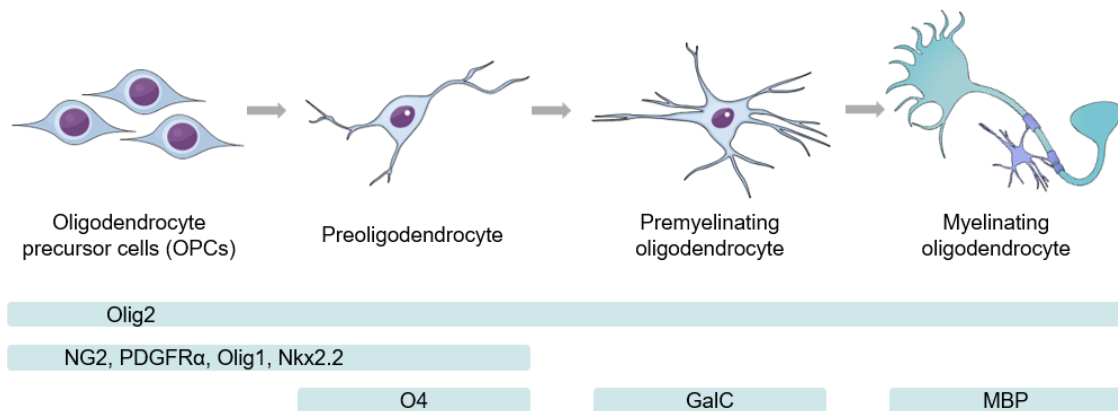


**Fig. 6 - Oligodendrocyte lineage.** Oligodendrocyte precursor cells (OPCs) which have proliferative and migratory capabilities and express proteoglycan NG2, platelet-derived growth factor receptor- $\alpha$  (PDGFR $\alpha$ ), and the transcription factors Nkx2.2 and Olig1. Pre-oligodendrocytes result from OPC differentiation and express the previous markers, as well as O4 antigen. These are followed by premyelinating oligodendrocytes, which express galactocerebroside C (GalC); and in the end these cells become functional myelinating oligodendrocytes, that express myelin proteins such as myelin basic protein (MBP).

## 2.2 Function of OLGs and synaptic communication

In the 1920s, del Río Hortega was the first to identify a new type of cells, that he named as oligodendroglia, that were distributed widely throughout the CNS and usually formed groups of cells next to neurons in the gray matter. After several experiments with a method developed by him involving silver carbonate, del Río Hortega suggested that the function of OLGs resembled the function of Schwann cells in the PNS, being responsible for myelination in the CNS<sup>79,80</sup>. Therefore, the most noticeable purpose of these cells is the formation of a myelin sheath that wraps around the axons of the CNS<sup>81</sup>. Importantly, del Río Hortega distinguished 4 different types of OLG, considering aspects as their shape, size, distribution within the CNS, and how they interacted with axons: type I cells have small and round cell body, as well as many processes which emerge in diverse directions towards axons with a small diameter, and are present both in white and gray matter; type II cells are present in white matter, have less and thicker processes than type I OLGs, and attach axons in a longitudinal direction; type III cells are less abundant and ensheath thicker white matter axons, possessing only up to four processes; and type IV cells are elongated and have a flattened cell body (similar to Schwann cells) and ensheath medium or thicker axons in white matter<sup>79,80</sup>. Nevertheless, OLGs play

other roles, namely in the gray matter, where a fraction of these cells instead of forming myelin interact with the soma of neurons and are named “perineural” satellite OLGs. Likewise, some were found to be associated with blood vessels, and are designated as “perivascular” satellite cells; or aligned in rows along the axonal tracts and are designated as interfascicular OLGs<sup>79–81</sup>.

OPCs express multiple receptors for neurotransmitters, including acetylcholine, GABA and glutamate (*N*-methyl-D-aspartate (NMDA) and  $\alpha$ -amino-3-hydroxy-5-methyl-4-isoxazolepropionic acid (AMPA)) receptors<sup>68,82</sup>. This might suggest that these neurotransmitters released by neurons in the surrounding environment can influence the activity of OPCs. Moreover, these glial cells form synapses with neurons, which occur both in white and gray matter. In addition, in the gray matter, OLGs are able to form synapses with GABAergic neurons<sup>68,83</sup>.

Furthermore, since axons are more stable structures and OPCs are very motile cells, the communications between OPCs and neurons have to be transient<sup>68,84</sup>. Furthermore, these interactions are also limited when it comes to the lineage, since the differentiation to myelinating oligodendrocytes is accompanied by a downregulation of AMPA and NMDA receptors and NaV channels, and removal of synaptic input<sup>85</sup>. These transient synapses are very useful namely to allow OPCs to assess the activity of the nearby axons. In fact, glutamatergic signals influence both proliferation and differentiation of OPCs *in vitro*<sup>86</sup>; the activity of OPCs can be affected by changes in the presynaptic neuron; and these transient synapses ensure that damaged or degenerated oligodendrocytes are efficiently replaced<sup>68,83</sup>.

### **2.3 Plasticity and homeostasis of the oligodendrocytic population**

OPCs can be derived independently from the ventral and dorsal parts of the brain and spinal cord during development. So, Bergles and Richardson questioned whether this translated into any functional differences between the OPCs produced<sup>68</sup>. The different origin of the OPCs does not appear to be significant, since they appear to be redundant. In fact, Kessaris *et al.* showed that when one of the populations was ablated, the other would replace it, showing their plasticity during development in order to achieve a normal distribution of OPCs in the developing brain<sup>68,87</sup>. These poses the hypothesis that the heterogeneity of oligodendroglial cells arises in response to distinct environmental cues, whether they are originated in the axons, the neurotransmitters released or in electrical neuronal activity<sup>67,88–90</sup>.

The homeostatic regulation of the density and differentiation of OPCs is needed to guarantee there is no uncontrolled proliferation of these cells, but also to assure that there is a replacement of damaged or insufficient OLGs in injury sites<sup>83</sup>.

OPCs are capable of migrating, during development, from their germinal zones to their final destination, likely due to the contact-interaction with molecules common to neuronal migration

(such as netrins or semaphorins)<sup>68,91,92</sup>. Several complementary studies suggest that OPCs are very dynamic in the resting brain and show processes similar to those of microglia, that are complemented by filopodia that are able to extend and retract in order to move and scan the surrounding environment. These processes assess the state of myelination of the axons in the vicinity or the viability of OLGs. Also, when these processes touch each other or neighbouring cells, they retract, in a repulsive response, showing the mechanism responsible for the OPCs discrete distribution<sup>83,93</sup>.

Additionally, platelet-derived growth factor (PDGF) is necessary for the proliferation of OPCs in culture. In fact, when the activity of PDGF signalling pathway is diminished, there is a decrease in division rate, cell cycles get longer and differentiation of OPCs is triggered<sup>68,94,95</sup>. Therefore, it was hypothesized that the population density of OPCs is established by a ratio between the amount of PDGF, provided by neurons and astrocytes, and the rate at which it is consumed by OPCs<sup>94</sup>. Nevertheless, this idea failed to clarify why there is a continuous decrease in OPC proliferation postnatally. This hints at an intrinsic timer of these cells, that controls not only the inhibition of cell cycle progression, but also the decline in the differentiation–inducing pathways<sup>68,95,96</sup>.

In conclusion, these cells are able to balance self-repulsion and active growth in order to guarantee that the proliferation process is coupled to the loss of cells, to maintain the density of these precursors in the brain to produce OLGs and assist in case of injury<sup>83</sup>.

### **3. Myelin**

#### **3.1 Myelination in development and adulthood: myelin structure and composition**

Myelin sheaths are composed of glial plasma membrane that compactly enwraps around the axons, allowing for a faster saltatory nerve conduction, and also assisting in the maintenance and integrity of the axons<sup>67,97–99</sup>. This provides insulation by increasing the electrical resistance and diminishing the capacitance, crucial for the saltatory mechanism<sup>79,98</sup>. Moreover, these myelinating cells also cluster voltage-gated sodium channels in the gaps between the myelin sheaths – known as nodes of Ranvier (NOR), to potentiate the transmission of information, since the action potential is passively transported through the myelin sheath until it reaches the NOR, where it is regenerated to modulate the activity of the ion channels<sup>79,100</sup>.

Regarding its molecular composition, myelin is a poorly hydrated structure, with 70 – 80 % lipids and few proteins, MBP and proteolipid protein (PLP) being the most abundant. The glycolipids and proteins that are found in myelin are produced in the processes of OLGs, therefore the transport of specific proteins and mRNAs to these structures is needed. Ultimately, myelin synthesis relies on several enzymes of the lipid metabolism, such as PAPS

cerebroside-sulfotransferase, which is required for the synthesis of sulfated galactosylceramide; HMG-CoA reductase for cholesterol production or peroxisomal enzymes<sup>79,81</sup>. Therefore, myelin being a particularly stable structure, owes this characteristic to the hydrophobic lipid composition, with saturated long-chain fatty-acids, glycosphingolipids, and cholesterol, that together with the hydrophobic proteins creates a repulsive force towards the cytosol and the extracellular fluid. Moreover, it also portrays intermolecular attractive forces, such as Van der Waals', that hold these lipids close together. It is also stable from the metabolic point of view, since the proteins of this sheath have half-lives of weeks to months<sup>79,101</sup>.

Myelination is an intricate process, that entails several steps, beginning with the migration of OPCs to the white matter tracts (I), followed by the recognition of the target axon and signalling between these two cells (II); differentiation of OPCs into myelinating OLGs (III); membrane outgrowth and wrapping around the axon (IV); trafficking of membrane components (V); myelin compaction (VI) and formation of NOR (VII)<sup>79,81</sup>. There are several possible paths for OPCs, some remain as precursors whilst others differentiate into myelinating OLGs<sup>79,83</sup>. At this point, to ensure that all axons are myelinated, there is an overproduction of OLGs, that are later eliminated by apoptosis, resulting in an adequate number of OLGs<sup>79,102</sup>. In summary, OPCs mature through several morphological alterations<sup>79</sup> (Fig. 7).

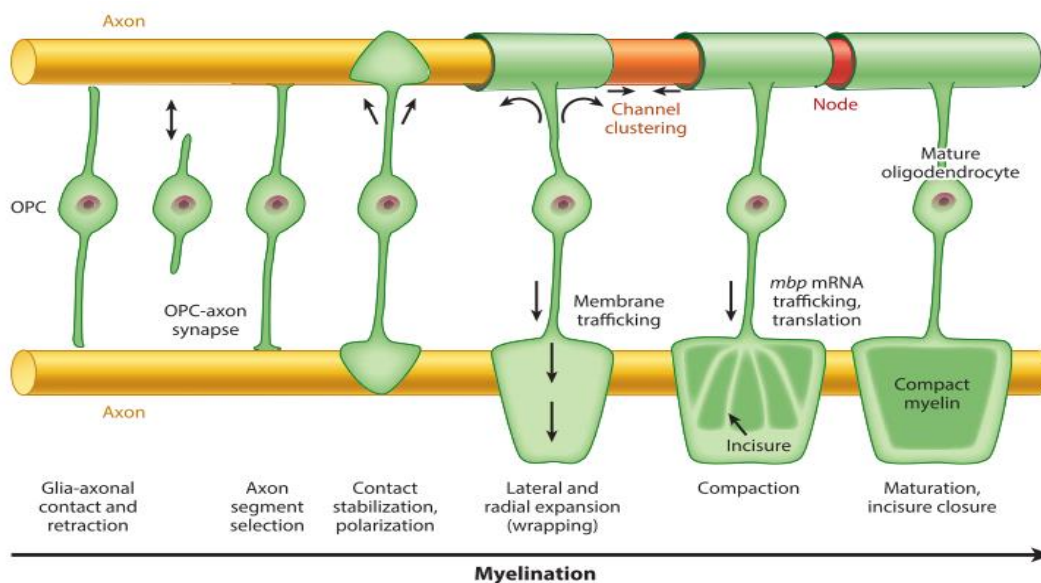


**Fig. 7 - Schematic model of the differentiation of a committed OPC into a mature myelinating oligodendrocyte.** Myelination starts with the migration of OPCs from the germinal zones or the brain parenchyma, where they are distributed under physiological conditions, to the white matter tracts (I). OPCs extend and retract cellular processes until there is recognition of the target axon and communication between the two cells is initiated (II). OPCs will then differentiate into fully myelinating OLGs (III). The myelin sheath produced will wrap around the axon, forming a compact structure and the nodes of Ranvier (NOR) (IV-VII), where voltage-gated ion channels are clustered to allow for saltatory conduction of action potentials. Adapted from *Annu Rev Cell Dev Biol.* 2014; 30:503-33.

Oligodendrocyte differentiation and maturation comprise the ability of these myelinating cells to produce membranes at a certain timepoint during development and maturation of the CNS. In addition, the time when the differentiation of OLGs is initiated is of the utmost importance, since the precursor cells can stay in an immature state for long periods of time, but once the differentiation starts it occurs rapidly<sup>79</sup>. Electrical activity of neurons is the most frequent initiator of OPC proliferation and myelination, and it will in turn regulate a multitude of transcription factors and signalling pathways that will activate (Nkx2.2, Olig1, Sox10) or repress (miRNA-219, miRNA-338 and PDGFR $\alpha$ ) the pathway<sup>79,103–105</sup>. Moreover, myelination only occurs when the oligodendrocyte is at the proper place, mature OLGs are not able to move and the process occurs very swiftly, not allowing for mistakes<sup>79</sup>. In addition, Rosenberg *et al.* showed, using fixed axons, that OLG differentiation is regulated, both in space and time, by the environment provided by the surrounding axons and not by a direct neuron, which is called OLG interaction<sup>98,106</sup>. Furthermore, studies by Lee *et al.* demonstrated that OLGs are able to myelinate “synthetic” axons with shorter diameters than the axons that were found myelinated *in vivo*, indicating that axonal diameter might be a factor controlling which axons are myelinated in the organism<sup>98,107</sup>. Together, these works highlight the role of neuronal signalling cues in the differentiation of OPCs, and the sensitivity associated with these cells for the axons that are adequate to be myelinated.

The myelination of an axon is a coordinated process: both the increase in wraps and the widening of the membrane sheet occur simultaneously with the activity of cytoplasmic channels to transport the new membrane material to the innermost layer<sup>79,98,108</sup>. The actin cytoskeleton is used by OLGs to move the myelin sheaths forward, and is depolymerized once this structure reaches its full maturation and is compacted, acting as the controller for myelin spreading and wrapping around axons<sup>98,108</sup>.

To perform its insulation function, myelin needs to be compacted around the axon, which entails removing cytoplasm and extracellular space. This can occur in one of two ways: compaction can happen between two extracellular layers or two cytoplasmic membrane layers<sup>98</sup>. The cytoplasmic protein MBP, constituent of myelin, is responsible for assisting in the process, by participating in the compaction between two cytoplasmic leaflets. The protein CNPase (2',3'-cyclic nucleotide 3'-phosphodiesterase) is the most abundant in uncompact myelin, and its function is to delay myelination, which happens when it is present in larger quantities than MBP<sup>98,108,109</sup>. The balance between these two proteins regulates the compaction rate during early development, and could possibly regulate myelin remodelling mechanisms dependent on activity<sup>79</sup>.

Myelination can control the information flow in neuronal circuits through several different mechanisms, namely regulating thickness of existing myelin sheaths, *de novo* myelination, and myelin replacement and removal, in order to functionally alter a neuronal circuit.



## 3.2 Myelin damage and remyelination

### 3.2.1 Characteristics of remyelinated axons and role of remyelination

Demyelination occurs when myelin sheaths that are wrapped around the axons are damaged. It can happen due to a primary insult, when OLGs are affected, or as a secondary process, due to the degeneration of the axon<sup>63,110,111</sup>. The process that leads to the formation of new myelin sheaths to wrap axons affected by primary demyelination insults is termed remyelination, and it is able to restore normal saltatory conduction in the designated axon, as well as the normal function of the neuron<sup>63,110,112</sup>. However, the new sheath is thinner and shorter, never achieving the original dimensions, suitable for the diameter of the axon<sup>63,110,113</sup>. Axons which have been remyelinated are usually known by the presence of thinner myelin sheaths which are identified by the G-ratio, that expresses the relationship between the diameter of the axon and the myelin sheath thickness (thinner sheaths – increased G-ratio). Nevertheless, when thin axons are remyelinated, these problems are less evident, since their original myelin sheath was already thin<sup>63,110,114</sup>.

### 3.2.2 Steps for remyelination and factors controlling the process

The first step in response to an injury consists in the activation of local OPCs – by neighbouring microglia and astrocytes activated by changes in tissue homeostasis, and that produce factors that will lead to the rapid proliferative response of OPCs. OPCs will in turn go from a quiescent to an active state, with altered shape and size, as well as with gene upregulation<sup>15,110,115,116</sup>. The following recruitment phase consists in proliferation and migration of the activated OPCs, ultimately resulting in the repopulation of the demyelinated region. At the same time myelin debris are removed by macrophages and matrix metalloproteinases (MMPs) contribute to the repair. Larsen *et al.* propose that MMP-9 processes NG2, reducing its inhibitory effect in OLG maturation, and additionally MMP-9 might facilitate cell migration to injured areas in the CNS and the elongation of OLG processes for axon remyelination<sup>117</sup>. Thereafter, cells will differentiate into fully functional OLGs, capable of performing remyelination. At this point, these cells have to communicate with the damaged axon, whilst expressing myelin genes and forming a new sheath to wrap around it<sup>110</sup> (Fig. 8).

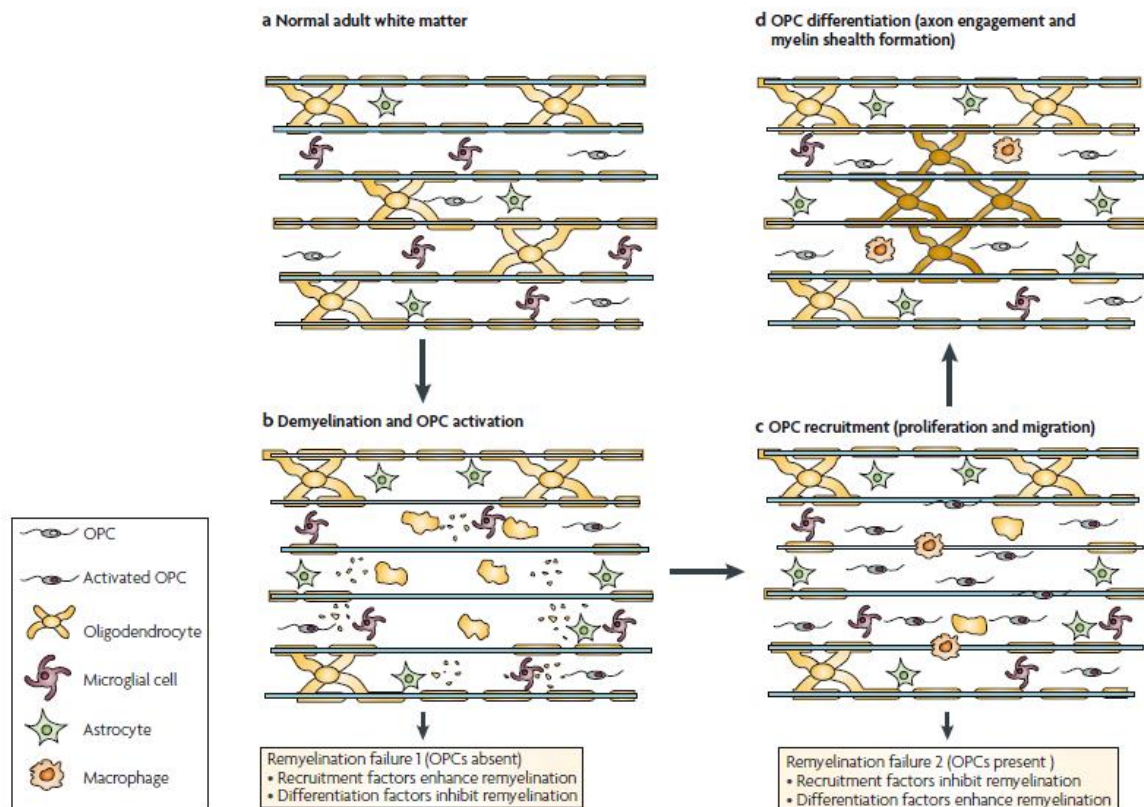


**Fig. 8 - Phases of remyelination.** (a) Normal adult white matter contains astrocytes, microglia and OPCs, as well as myelinating OLGs. (b) OPC activation: following demyelination (in which oligodendrocytes and myelin are lost) the microglia and astrocytes become activated, which in turn leads to activation of OPCs in the vicinity. (c) Recruitment phase: the activated OPCs respond to mitogens and pro-migratory factors that are generated predominantly by reactive astrocytes and inflammatory cells. The demyelinated area becomes repopulated with OPCs, due to their migration and proliferation. Macrophages start eliminating myelin debris. (d) Differentiation phase: for the recruited OPCs to differentiate into fully myelinating OLGs, they need to communicate with the damaged axon to initiate the formation of a new myelin sheath. The remyelination process can fail due to several reasons, namely a deficiency in OPCs or a failure in their recruitment, or their inability to differentiate into myelinating OLGs. Adapted from *Nat Rev Neurosc* (2008) 9, 839-855.

There are several common features between the myelinating process which occurs during development, and remyelination after a demyelinating insult<sup>118</sup>. For instance, the availability of PDGF regulates the number of OPCs in remyelination, similar to what happens during development<sup>118,119</sup>. Moreover, IGF-1 signalling within OLGs is needed during remyelination namely for the protection of the existing myelinating cells, to facilitate a rapid recovery and for the proliferation and differentiation of OPCs<sup>118,120,121</sup>. Additionally, there are some negative modulators that also participate in both myelinating situations, such as fibroblast growth factor (FGF)-2 which is upregulated in several experimental models for CNS demyelination, and its decreased activity appears to promote the repopulation of lesion sites by influencing the differentiation of this lineage<sup>118,122</sup>. Concerning the intrinsic signals, there are some examples

that are also common to both situations, namely the Notch pathway, which modulates the kinetics of repair, being a positive or negative modulator depending on the ligand<sup>118,123</sup>, or the Wnt pathway, which constitutes a negative regulator of the differentiation of OLGs both in development and remyelination<sup>63,124</sup>. Moreover, the transcription factor Olig1 has crucial roles not only during early OPC development, but also during the differentiation process in remyelination<sup>118,125</sup>. Nevertheless, it is necessary to keep in mind that both processes, myelination and remyelination, occur under different conditions with the latter being associated with inflammation.

The immune response evoked by the demyelinating injury is crucial for the remyelination process, namely because the phagocytic macrophages are responsible for eliminating the myelin debris, and different activation states of these cells are associated with different phases of remyelination, M1 phenotype (associated with antigen presentation and release of pro-inflammatory cytokines) with recruitment and M2 phenotype (responsible for secretion of anti-inflammatory cytokines and growth factors) with the beginning of differentiation<sup>63,126–128</sup>. Furthermore, there might be several causes behind the failure of this process. The most general comprise a loss in efficiency due to factors not related with the disease, such as sex and age<sup>116,118</sup>. In fact, alterations in myelin that occur during aging represent a vicious cycle, for the decline of both motor and mental capacities. In addition, it is also necessary to consider factors characteristic of the disease, and the main causes for remyelination failure in this case are a deficiency in progenitor cells, a failure in their recruitment or incapacity for these progenitors to differentiate and mature<sup>110,129</sup> (Fig. 8).

## **4. Stem cell niches in the brain**

In adulthood, OLGs can be originated from OPCs present in the brain parenchyma or from neural stem cells (NSCs) present in the SVZ, which can be recruited in case of injury.

### **4.1 From development to adulthood**

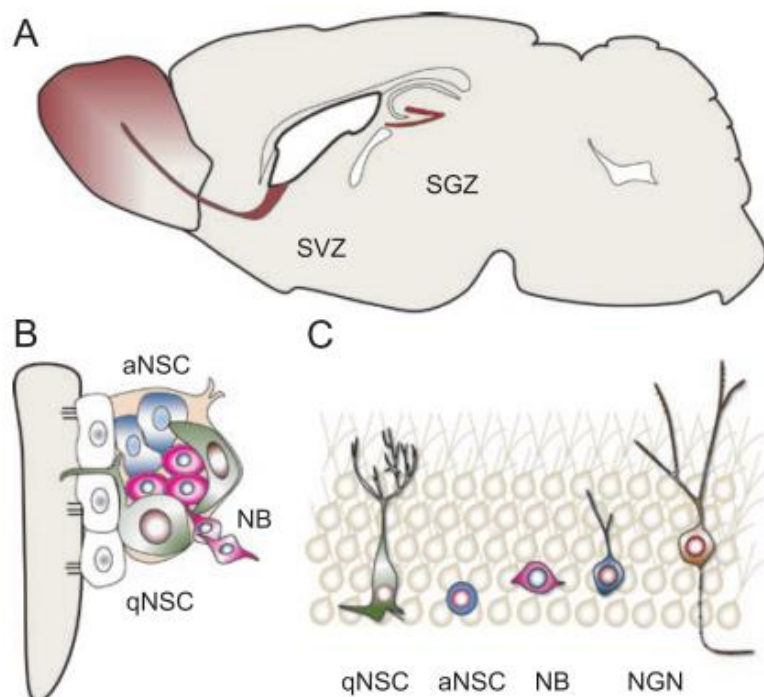
#### **4.1.1 Neurogenic niches during development**

In mammals, NSCs are originated in the early stages of development and their activity perseveres throughout life. The development of the CNS entails several processes that are tightly regulated, both in time and space. During the embryonic development, NSCs can be found in almost all the regions of the CNS, which is considered a dynamic structure that increases in size, and these cells have a specific differentiation potential and identity, according to the region where they are located<sup>130,131</sup>. Also, the precursor cells that will originate the brain are maintained essentially in two regions: the ventricular and subventricular zones (VZ and SVZ, respectively)<sup>132</sup>.

NSCs are essentially characterized by their multipotency, self-renewal and unlimited proliferation capabilities<sup>131</sup>. The initial population of these cells is homogeneous, constituted by bipolar cells that have one long process attached to the pial surface and a shorter one attached to the ventricle (denominated neuroepithelial cells, NEPs)<sup>130,133</sup>. As development proceeds, the migration of the newly formed cells from the ventricle to the pial surface will allow the formation of several layers, with different characteristics: the VZ, closest to the ventricle, will house cell bodies of radial glia (NEPs with a specific, elongated morphology, which express glial markers, having properties of astroglial cells but also residual characteristics of neuroepithelial cells<sup>134</sup>). Radial glia will assist in the migration of newly formed neurons, resulting of the division of progenitor cells with limited ability to proliferate and differentiate into more than one cell type<sup>131</sup>. The SVZ is the exterior layer, consisting of newly generated glia, neurons and basal progenitors. Finally, the mantle is the most exterior layer, closest to the pial surface, made of fully differentiated post-mitotic cells, such as neurons<sup>130,133</sup>. The environment depicted in these different layers is influenced by several signalling cues, such as neurotransmitters, cell-to-cell interactions and diffusible signals from the VZ/SVZ or other brain regions<sup>130,135</sup>.

#### 4.1.2 Neurogenic niches in the adult brain

In the adult mammalian brain, two brain regions have been characterized as neurogenic niches: the subgranular zone (SGZ) of the dentate gyrus, in the hippocampus, and the subependymal zone, also known as subventricular zone, located in the lateral ventricles (SEZ or SVZ, respectively)<sup>136</sup>(Fig. 9).



◀ **Fig. 9 - Adult NSCs in the SVZ and SGZ of the mammalian brain.** (A) Germinal niches in the adult mammalian brain in mice. Adult neural stem cells (NSCs) are primarily present in two germinal regions: the subventricular zone (SVZ) of the lateral ventricle wall and the subgranular zone (SGZ) of the hippocampal dentate gyrus. (B) Adult NSCs in the SVZ. Quiescent adult SVZ NSCs (qNSCs, type B cells) are a unique population of cells with cell bodies in the SVZ while contacting the ventricle through apical surfaces. Active self-renewing adult SVZ NSCs (aNSCs, type C cells) are located in the SVZ and give rise to neuroblasts (NB, type A cells) that migrate towards the olfactory bulb. (C) Adult NSCs in the SGZ. Quiescent adult SGZ NSCs correspond to radial-like cell, some of which might transit to active self-renewing adult SGZ NSCs and give rise to neuroblasts and newly generated neurons (NGN). Adapted from Cell Res. 19, 672–682 (2009).

In the brain of rodents, the NSCs present in the SVZ will contribute to replace and maintain the neurons of the olfactory bulb<sup>130</sup>. Moreover, as described by Morshead & van der Kooy in 1992, the proliferating cells present in the SVZ stay mitotically active throughout adult life and are still responsive to stimuli, suggesting that NSCs can be used as a reservoir to substitute damaged cells<sup>137</sup>. In 1996 Weiss *et al.*, showed that NSCs isolated from the SVZ can maintain *in vitro* the characteristics of proliferation, self-renewal and expansion when cultured with growth factors, forming neurospheres<sup>138</sup>. Upon the removal of growth factors, the neurospheres-derived cells are able to differentiate into OLGs<sup>139</sup>. Also, it was possible to conclude that stem cells are heterogeneous, possibly due to the fact that they are located in different brain regions and have different mitotic activity, which may be indicative of the presence of distinct stem cell populations in the brain with diverse functional roles *in vivo*<sup>138</sup>.

Regarding the SGZ, these proliferating cells will originate immature neurons, that migrate a short distance and ultimately differentiate into hippocampal granule neurons, integrating the pre-existing hippocampal structure during the life of the organism<sup>136</sup>. Unlike what happens in the SVZ, where there is an organized layered structure, in this region, progenitor and immature cells are mixed together, with NSCs surrounded by intermediate progenitors, mature granule cells and astroglial cells close to blood vessels<sup>130</sup>.

Concerning the SVZ, several different cells compose this layer: proliferating type B cells, with some astrocytic properties, whose processes envelop the structures formed by neuroblasts; type C cells, known as transit amplifying progenitors, which form clusters scattered throughout the neuroblasts and are characterized by their rapid divisions; and type A cells (neuroblasts) that form chain-like structures along the wall of the lateral ventricle towards the olfactory bulb forming a structure designated as the rostral migratory stream (RMS) (in rodents), where some will differentiate into periglomerular and granular neurons<sup>130,136,140</sup> (Fig. 9B). This niche is maintained due to the molecules that constitute the extracellular matrix (ECM), which are highly expressed in this region, such as specific MMPs

and chondroitin/dermatan sulfate proteoglycans. In turn, during early postnatal life the expression of these molecules is downregulated and proteoglycans such as brevican and versicans are produced for the formation of the classic ECM that constitutes the brain parenchyma<sup>130,141</sup>. Also, ependymal cells, that are neuronal support cells that constitute the epithelial lining of the ventricles, play an important role through cell-to-cell interactions and secreted molecules, that maintain stem cells quiescent and control the self-renewal process<sup>142</sup>.

#### 4.1.2.1 Oligodendrocyte production from SVZ precursor cells

The work developed by Menn *et al.* was fundamental for the understanding of the role of SVZ progenitors in oligodendrogenesis in the adult brain. In the SVZ, OPCs are the result of division and differentiation of type C cells, that will migrate out of the SVZ into the neighbouring white matter. In the adult CNS, type B cells present in the SVZ generate a large number of neurons. Still, a few of these cells will differentiate into type C (Olig2<sup>+</sup>) cells, ultimately generating OPCs<sup>69</sup>. The OPCs generated from SVZ progenitors migrate long distances, to the corpus callosum, striatum and fimbria fornix, where they differentiate into myelinating and non-myelinating OLGs<sup>69</sup>. In situations of demyelinating injuries, such as with the lysolecithin animal model, there was an increase in the number of myelinating OLGs derived from SVZ, suggesting these cells contribute to the remyelination process<sup>16,69</sup>. Also, several studies, for instance the one of Ortega *et al.*, revealed that in the SVZ there appears to exist a regionalization regarding the signalling pathways of the different regions that constitute this structure, translating into different environmental influences to assist or inhibit the production of OLGs<sup>70,143</sup>. Importantly, the number of neurons and OLGs produced by NSCs present in the SVZ tends to decrease in adulthood, until the aged brain<sup>70</sup>.

## 5. Commitment to the oligodendrocytic lineage: intrinsic and extrinsic factors

Postnatal OLG differentiation is affected by different signals that can come from the cells themselves (intrinsic), or from the exterior (extrinsic).

### 5.1.1 Intrinsic factors

There are several intrinsic signals that modulate OLG generation, and they include not only transcription factors, but also epigenetic modulators.

Regarding the transcription factors, usually the process that comprises OLG development entails regulatory signals at different fronts, both temporally and spatially, that will guide several signalling pathways such as Notch or Wnt, which can participate in multiple steps of the formation of OLGs<sup>68,144</sup>.

Olig1 and Olig2 are basic helix-loop-helix transcription factors, well studied and involved in the production of OLGs<sup>144,145</sup>. Studies show that the different cell types that constitute the

oligodendrocytic lineage express Olig2, and when it is inactivated during development the result is decreased production of OLGs, whilst inducing the overexpression of Olig2 in SVZ progenitor cells translates in an increasing number of OLGs<sup>145,146</sup>. About Olig1, if Olig2 is present, it is not required for OLG specification, acting as a backup mechanism in case Olig2 is absent<sup>68,145</sup>. However, Niu *et al.* showed that Olig1 factor appears to be necessary for remyelination in the repair of lesions of the CNS<sup>147</sup>.

There are many other transcription factors involved in these intricate processes, namely *Ascl1/Mash1*, which is involved in myelin production in the postnatal brain, as well as in OLG specification from SVZ progenitors<sup>148,149</sup>. Epidermal growth factor (EGF) also positively affects the production of OLGs when it reaches the CNS and assists in demyelination repair<sup>68,150</sup>. In conclusion, there are several transcription factors that regulate the commitment to the oligodendrocytic lineage and can also perform their role by inhibiting the differentiation of cells from the neuronal and astrocytic lineages<sup>70,144</sup>.

Concerning the epigenetic modulators, which consist of alterations in the DNA sequence, they can also regulate the production of OLGs. In fact, post-translational modifications of the histones that constitute the nucleosomes, DNA methylation, chromatin remodelling and microRNAs (miRNAs, molecules that act by repressing gene expression); have been described as regulators of oligodendrogenesis<sup>70,144,151,152</sup>. For instance, the enzymes histone deacetylases (HDAC) are important for OLG determination, since when histones are acetylated and the activity of this enzyme is inhibited, it favours gene expression of astrocytic and neuronal lineages<sup>70,144,152</sup>. As shown simultaneously by Zhao *et al.* and Dugas *et al.*, miRNAs, such as miR-219, can act in two ways: they can be overexpressed and positively influence the differentiation of mature OLGs, but they are also able to inhibit factors that are related with OPC proliferation, allowing for the differentiation of these cells<sup>103,105</sup>. In addition, signalling pathways of extracellular ligands such as the sonic hedgehog (Shh) and bone morphogenic protein-4 (BMP4) also regulate the production of OLGs by influencing the acetylation of histones, Shh promotes the differentiation of these cells, whilst BMP4 acts as an inhibitor by blocking deacetylation<sup>153</sup>.

In conclusion, the regulation of OLG differentiation through intrinsic mechanisms relies in the communication between transcription and epigenetic factors.

### 5.1.2 Extrinsic factors

Similarly to what happens with the intrinsic factors, there are many extrinsic signals that contribute to the differentiation of OLGs, namely factors present in the CSF, the ECM or the blood vessels that surround the germinal niche.

The CSF is the fluid produced by the choroid plexus that circulates in the brain and spinal cord, providing not only mechanical protection to the brain, but also participating in the

regulation of brain homeostasis. It is composed by several proteins and molecules that can act as signals for NSCs present in the SVZ<sup>154</sup>. Some of the molecules secreted by the choroid plexus that integrate the CSF and influence the SVZ in adulthood are, for instance, insulin-like growth factors such as IGF-1 and IGF-2; and basic FGF (bFGF)<sup>144,154,155</sup>. Wagner *et al.* observed an increase in cell proliferation in the SVZ when bFGF was subcutaneously injected<sup>155</sup>. Moreover, studies by Gonzalez-Perez *et al.* showed that EGF stimulation promoted proliferation, migration and differentiation into OLGs from NSCs of the SVZ<sup>156</sup>. In addition, chemorepulsive signals such as ephrins, semaphorins and slits also assist in the migration of the NSCs present in the SVZ<sup>144,154</sup>.

Importantly, in the CNS, parenchymal OPCs seem to receive signals from microglia, macrophages, astrocytes and electrical activity, with a possible less relevant local signalling mechanism by axons, to control their maturation (the axons acquire a more important role in the myelination of the PNS)<sup>67,81,157</sup>. However, there are several neuronal cues, that are responsible for the inhibition of myelination, such as LINGO-1 or Jagged, and that need to be downregulated to allow the insulation of axons. Their mechanism of action usually relies in the activation of transcription factors, which can also be regulated by epigenetic modulators (HDACs and miRNAs) and specific signalling pathways<sup>103,105,157,158</sup>.

The ECM consists of the acellular component of organs and tissues, mainly made of proteins, polysaccharides and water and which components also play a crucial role in regulating OLG production<sup>159</sup>. In fact, laminin is determinant for oligodendrocytic lineage, since laminin  $\alpha$ 2-deficient mice produce less OPCs<sup>160</sup>. Moreover, the proteoglycan heparan sulfate, which is a heterogenous ECM molecule that can bind several cytokines and growth factors, regulates the signals that are present in the ECM and controls oligodendrocyte differentiation and maturation<sup>70,151,161</sup>. In addition, the proteins fibronectin and vitronectin are also associated to maintenance and proliferation of OPCs<sup>162</sup>. Another role for the ECM is to provide mechanical support. Lourenço *et al.* described that NSCs differentiate into glial or neuronal cells according to the stiffness of the substrate, which also controls the survival and proliferation of OPCs, as well as OLG morphology. They also concluded that compliant substrates, together with the presence of laminin  $\alpha$ 2, promoted an increase in the levels of the oligodendrocytic markers MBP and PLP, and these OLGs presented a more mature morphology<sup>159</sup>.

The surrounding blood vessels also play an important function, since they are constituted by endothelial cells which secrete factors capable of regulating self-renewal and proliferation of the stem cells present in these niches. For example, they can secrete specific chemokines to regulate cells of the oligodendrocytic lineage, namely monocyte chemoattractant protein-1 (MCP1), which promotes differentiation<sup>144,163</sup>.

Taken together, the regulation of OLG production by the extrinsic factors, resembling what happens with intrinsic cues, is dependent on the communication of the stem cells in the



germinal niches with signals arising from the nearby environment, whether it is the messengers coming from the endothelial cells, the components of the ECM and its mechanical cues, or the CSF.

## Aims

Several studies have attempted, throughout the years, to unveil the mechanisms behind MS, essentially using the available *in vivo* models. However, the cause of this disease, as well as the cellular mechanisms behind neurodegeneration and oligodendrocyte loss, are yet to be elucidated.

The capacity of OPCs from the brain parenchyma or derived from NSCs of the SVZ to migrate and partially remyelinate the lesioned areas has been extensively described. Herein, the modulation of adult oligodendrogenesis can be seen as a candidate target for MS. For this hypothesis to be taken into consideration, we proposed to perform a characterization of the MS animal model, EAE, as well as of adult oligodendrogenesis, under these pathological conditions. Thus, several objectives were considered:

- i. To implement the EAE animal model in our facilities;
- ii. To characterize this model regarding behavioural and cellular features, as well as the inflammatory environment associated;
- iii. To assess adult oligodendrogenesis in the EAE model, in brain regions of interest (corpus callosum, cortex, striatum and subventricular zone).

## **CHAPTER 2 – MATERIALS & METHODS**



## 1. Ethics Statement

All experiments were conducted in accordance with the European Community guidelines (86/609/EEC; 2010/63/EU; 2012/707/EU) and Portuguese legislation (DL 113/2013) concerning the protection and use of animals for scientific purposes. In addition, all procedures were approved by the Animal Scientific Committee of *Instituto de Medicina Molecular João Lobo Antunes* (iMM – JLA) and by the portuguese authority responsible for the legislation for animal protection (*Direção Geral de Alimentação e Veterinária* - DGAV). Every effort was made to use the minimum number of animals and to reduce animal suffering.

## 2. Animals

Female C57BL/6 mice were purchased from Charles River (Barcelona, Spain). Animals were housed 5 per cage upon arrival, in a temperature (22°C) and humidity (levels between 45% - 65%) regulated room, with a 10-hour dark / 14-hour light cycle (lights on from 7 am to 9 pm), and access to food and water *ad libitum*. Animals were housed in specific-pathogen free (SPF) and virus-antibody free (VAF) facilities. Once mice started portraying the pathological phenotype, they received a gel supplement in addition to their regular diet. All animals had a minimum period of 4 days for acclimatization at the Institute's rodent facility upon arrival, before starting the experiments when mice were 8-10 weeks old. Animals were habituated to experimental manipulation and the presence of an investigator for a minimum of 2 days prior to EAE model induction and for 5 days before the beginning of behaviour experiments. Cages with animals were randomly allocated to the different experimental groups. Behaviour experiments were conducted during the light phase and around the same hour of the day. Animals were repeatedly monitored for general appearance, food and water intake, physical condition, and body weight during the protocols.

## 3. Timeline for experimental procedures

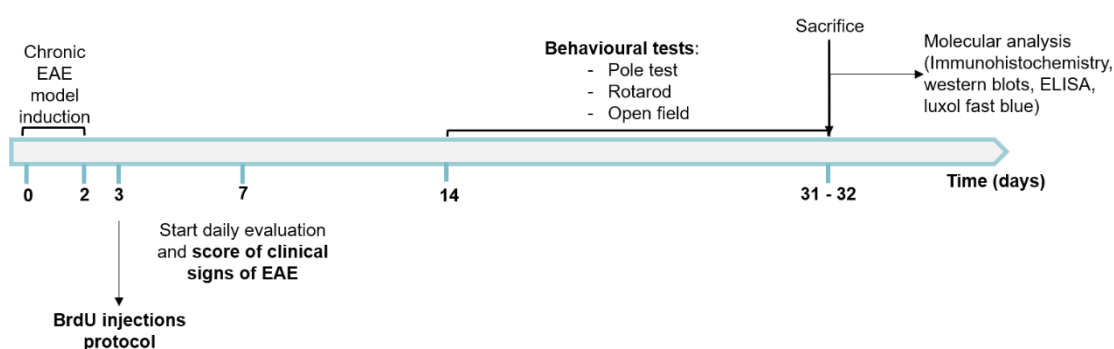


Fig. 10 – Timeline for *in vivo* experiments.

In the first 3 days the animals were induced with chronic EAE. In the following day, 5-bromo-2'-deoxyuridine (BrdU) was administered through seven intraperitoneal injections at two-hour intervals. Beginning at the seventh day post-induction, animals were daily evaluated and clinical scores for phenotype progression were registered. Analysed behaviour tests were performed between days 14-15 and 21-22 (Weeks 2 and 3, respectively, batch 1) or between days 14-16 and 21-23 (Weeks 2 and 3, respectively, batch 2) after model induction. Animals were sacrificed 28 days after BrdU injections, right brain hemispheres were collected for immunohistochemistry, ELISA and Western blot analysis. For immunohistochemistry, brain hemispheres were processed and stained while for western blot and ELISA analysis, brain cortex tissue homogenates were prepared. For representative luxol fast blue staining images, left hemisphere and spinal cord sections were used for both control and EAE mice.

## 4. EAE model induction

### 4.1 MOG emulsion preparation from scratch

To induce EAE, 2 batches of mice with 8-10 weeks were subcutaneously (s.c.) immunized with 200  $\mu$ L of a solution of MOG<sub>35-55</sub> (200  $\mu$ g/mouse) (synthetic peptide, H-Met-Glu-Val-Gly-Trp-Tyr-Arg-Ser-Pro-Phe-Ser-Arg-Val-Val-His-Leu-Tyr-Arg-Asn-Gly-Lys-OH, AnaSpec, Fremont, CA) emulsified in CFA (Incomplete Freund's Adjuvant (IFA, BD Diagnostics, Franklin Lakes, NJ) supplemented with *Mycobacterium tuberculosis* (BD Diagnostics, Franklin Lakes, NJ)) (400  $\mu$ g/mouse), followed by an intravenous (i.v.) or intraperitoneal (i.p.) injection of 100  $\mu$ l of PTx (List Biological Laboratories, Campbell, CA) (200 ng/mouse) (Table 1). The administration of PTx was repeated after 48 hours. The animals were divided into 2 subgroups: animals who received PTx via i.v. injection and animals who received the toxin through i.p. injection. These animals were housed on VAF conditions.

**Table 1 – Compounds used for emulsion preparation for EAE model induction.**

Compound	Biological activity	Supplier	Final [ ]
<b>MOG<sub>35-55</sub></b>	Induction of autoantibody production	AnaSpec, Fremont, CA	2mg/mL in PBS 1x
<b>IFA</b>	Potentiator of immune response	BD Diagnostics, Franklin Lakes, NJ	-
<b><i>M. Tuberculosis</i></b>	Development of strong delayed-type hypersensitivity against autoantigens	BD Diagnostics, Franklin Lakes, NJ	4mg/mL in IFA
<b>PTx</b>	Disruption of the BBB	List Biological Laboratories, Campbell, CA	200ng/100 $\mu$ l PBS 1x

## 4.2 EAE kit from Hooke Laboratories

Another batch of 10 mice (5 VAF and 5 SPF animals) whose samples were used for ELISA assays were induced with EAE using a kit (Cat. #EK-2110) from Hooke Laboratories (Lawrence, MA, USA) according to manufacturer's instructions. Briefly, 100µL of MOG<sub>35–55</sub> in CFA emulsion was subcutaneously injected into both flanks of each mouse (200 µL/animal). Then, each mouse received i.p. injections of PTx on the same day after 2h and 24h later (80 ng in 100 µL/animal/injection).

**Table 2 – Experimental groups of this project.**

Group ID	EAE induction method	Housing	Group size	Tests performed
CTRL IV	PBS/CFA & PBS i.v.	VAF	10	Behaviour, WB, ELISA
EAE IV	MOG/CFA & PTx i.v.	VAF	6	Behaviour, WB, ELISA
CTRL IP	PBS/CFA & PBS i.p.	VAF	10	Behaviour, WB, ELISA, LFB
EAE IP	MOG/CFA & PTx i.p.	VAF	5	Behaviour, WB, ELISA, LFB
CTRL KIT	PBS/CFA & PBS i.p.	VAF	5	ELISA
EAE VAF	Hooke lab. Kit	VAF	3	ELISA
EAE SPF	Hooke lab. Kit	SPF	5	ELISA

## 4.3 Clinical scores

The clinical signs of EAE were assessed daily with a standard scale from 0 to 5, as follows: 0, no clinical signs; 1, limp tail; 2, hind limb paralysis; 3, complete paralysis of the hind limbs; 4, hind limb paralysis and forelimb weakness; 5, moribund or deceased. Mice were considered for the following experiments when they reached a score of 2 (or higher) for at least two consecutive days<sup>164,165</sup>.

## 5. BrdU administration

BrdU is a synthetic nucleoside thymidine analogue capable of incorporating the DNA of newly formed cells, during the DNA replication process which occurs in the S phase of the cell cycle. This characteristic makes BrdU useful to study not only the formation of new neurons, but also oligodendrocytes<sup>16,166</sup>. To study oligodendroglial differentiation, BrdU (Sigma Aldrich, MO, USA) was dissolved in a sterile solution of 0,9% NaCl and administered intraperitoneally 7 times with 2-hour intervals, at a concentration of 50 mg per Kg of body weight, to specifically follow the differentiation of precursor cells originated in the SVZ<sup>16</sup>.

## 6. Behaviour tests

Behaviour tests aimed at depicting the progression of the EAE phenotype and thus perform a complete characterization of the animal model. Since this model is characterized by motor impairments, i.e, progressive paralysis starting at the tail and evolving to the forelimbs, the tests performed allowed the assessment of the physical condition of the animals<sup>167</sup>. For this, the pole test, rotarod and open field were used. In all tests, lighting and noise conditions, as well as animal manipulation were kept as similar as possible between the animals. For each test, animals were habituated to the room and lighting (red light for the pole test and dim yellow light for the rotarod and open field) for a minimum of 30 min before the beginning of the experiments. To remove olfactory clues, the apparatuses and the arena were carefully cleaned with a 30 % ethanol solution between each animal for all tests. For the rotarod and pole test, the experimenter remained in the room while the animals were being tested whereas for the open field, the experimenter moved outside of the room immediately after placing the animal in the arena. Parameters assessed in the open field were recorded using the ANY-maze V4.99 behavioural tracking software (Dublin, Ireland). The reference point used by the software to determine the animal's position was the centre of the body. The rotarod test results were registered by the apparatus. Conversely, pole test trials were video recorded, and blind analysed *a posteriori*, as described ahead in this section.

### 6.1 Open field

The open field (OF) is well established as a reference test to assess animal locomotor activity, as well as the animal's exploratory drive specific reactions which may happen in a novel environment<sup>168-170</sup>. Hence, this test was used to characterize locomotor activity of the animals throughout disease progression. This test was conducted in a square wood arena (40 x 40 x 40 cm). The animals were released in the centre of the arena and allowed to freely explore the environment for 10 min. The arena was virtually divided into three square zones: peripheral zone (PZ), intermediate zone (IZ), and central zone (CZ) (Fig. 11). The parameters average velocity (m/s), distance (m) and number of transitions between zones were used to quantify locomotor activity.



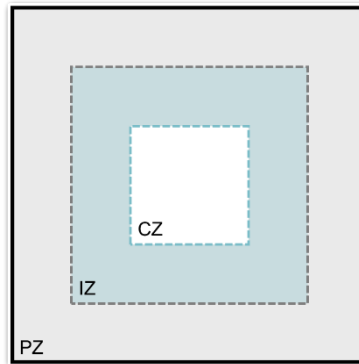


**Fig. 11 -Schematic representation of the open field arena.** The arena was divided into three distinct zones: the peripheral zone (PZ), the intermediate zone (IZ) and the central zone (CZ).

## 6.2 Rotarod

The Rotarod (RR) test is generally performed to study motor balance and coordination in animal models of neurodegenerative diseases, indicating the progression of motor dysfunction<sup>171,172</sup>. Impairments in rotarod performance can arise in situations of neuronal degeneration in brain areas such as the cerebellum, substantia nigra or striatum<sup>170,173</sup>, as well as when there is demyelination in the spinal cord<sup>174</sup>. This test was preceded by a training phase in the first day, in which the animals were habituated to stay on the rod (Panlab, Harvard Apparatus, Barcelona, Spain), at a constant speed of 7 rpm. Every time the mouse fell it was placed back on the rotating rod. The habituation period was considered to be over when animals were able to stay on the rod without falling for a minimum of 2 minutes. Immediately after the habituation phase, the experiment changed to the accelerating protocol (first trial of test phase), in which the velocity increased from 4 to 40 rpm in 5 min. Until 8 rpm were reached, if the mouse fell it was placed back on the rod (and the time was registered and added to the final time of fall). Two more trials were performed, with a minimum interval of 30 min between trials. Time of fall (sec) and the velocity (rpm) were registered and the average of the three trials was used. If the animal was physically impaired and immediately fell of the rod, the minimum values for time of fall and velocity were attributed (1 sec and 4 rpm, respectively). The trials were excluded if the animal rotated around the rod.

## 6.3 Pole test

The pole test (PT) was originally developed to study bradykinesia in Parkinson's disease models and nowadays is commonly used to assess motor dysfunction in mice<sup>175,176</sup>. Integrity of striatal neurons has been previously described as being relevant for pole test performance<sup>176,177</sup>. Hence, since the striatum is one of the brain regions known to be affected by demyelination in the EAE model, the pole test was used to assess motor function in these mice. The test was performed as previously described, with slight alterations<sup>178-180</sup>. The

apparatus consisted of a square wood base (15 x 15 x 1,5 cm) in which a pole covered in black felt (to increase the adhesion of the animals' paws to the surface of the pole) with 50 cm of height and 2 cm diameter was attached. In the table where the apparatus was placed, several rolls and bedding material were placed in order to stimulate the mice to descend the pole. Immediately before the start of the test, mice were left to freely explore the table and the existent material for 1 min, to habituate to the surrounding environment. Then, the pole was placed horizontally, and the mouse was placed in the top, with its head facing upwards, and the pole was immediately turned to a vertical position. The trial was concluded when the mouse touched with its four paws in the base of the pole and the animal was returned to its home cage. Three more trials were performed, with a minimum interval of 15 min between trials. All trials were video recorded and blindly identified for posterior analysis, in which the time it took for the animal to orient downwards ( $t_{\text{orient}}$ , in sec), i.e, when the animal completed a full turn and was facing the base of the pole was manually registered, as was the time it took for the mouse to reach the base of the pole ( $t_{\text{descend}}$ , in sec), i.e, when the mouse had its four paws on the base of the pole, and the total time of the trial ( $t_{\text{total}}$ , in sec). The trials were excluded if the animal went up the pole. Time started counting when the animal had its four paws on the pole. If the animal was unable to make a complete turn and instead descended the pole with a lateral body position,  $t_{\text{total}}$  was attributed to  $t_{\text{orient}}$ . If the animal was unable to stay on the pole and immediately fell, the longest  $t_{\text{total}}$  for that group in that trial was assigned to both  $t_{\text{total}}$  and  $t_{\text{orient}}$ , as previously described<sup>176</sup>.

## **7. Animal sacrifice**

At the end of the protocol, animals were sacrificed by cardiac perfusion for further molecular characterization of the model and of adult oligodendrogenesis. Mice were deeply anaesthetized with isoflurane and transcidentally perfused with phosphate-buffered saline (PBS) (NaCl 137mM, KCl 2.1mM,  $\text{KH}_2\text{PO}_4$  1.8mM and  $\text{Na}_2\text{HPO}_4 \cdot 2\text{H}_2\text{O}$  10mM, pH 7.4). Afterwards, brain and spinal cord intended for histological analysis were removed and placed in PBS containing 4% paraformaldehyde (PFA) for tissue post-fixation (4°C). At the end of 72 hours, both brain and spinal cord were stored at 4°C in an increased sucrose gradient (PBS containing 15% or 30% sucrose) for tissue preservation. For ELISA and Western blots, brain hemispheres were collected after perfusion and cryopreserved at -80°C.

## **8. Tissue processing**

For immunohistochemistry, brains were embedded in gelatine and coronally sectioned in 40  $\mu\text{m}$ -thick slices using a cryostat Leica CM3050 S (Leica Biosystems, Wetzlar, Germany). Only the right hemisphere was sectioned between the coordinates +1.5 mm and -1.5 mm,

having Bregma as reference. Sections were collected in ten series, each one being an anterior-posterior reconstruction of the SVZ and corpus callosum regions, where sections are separated by 400  $\mu\text{m}$ . Sections were kept at  $-20^{\circ}\text{C}$  in 24-well plates in anti-freezing medium (30% glycerol, 30% ethylene glycol, phosphate buffer 0.1 M (8.9%  $\text{Na}_2\text{HPO}_4 \cdot 2\text{H}_2\text{O}$ , 7.8%  $\text{NaH}_2\text{PO}_4 \cdot 2\text{H}_2\text{O}$ , pH 7.3-7.4).

For luxol fast blue staining, brains were gelatine-embedded whilst spinal cords were embedded in Optimal Cutting Temperature (OCT) compound. Left brain hemispheres were sectioned at a thickness of 20  $\mu\text{m}$  using a microtome Leica RM2245 (Leica Biosystems) between -0.34 mm and -1.58 mm in reference to Bregma. 5 sets of twin blades were created, each one representing an anterior-posterior reconstruction of the desired region, where sections are separated by 100  $\mu\text{m}$ . Regarding spinal cord samples, a maximum of 5 slides per animal was obtained, each slide containing the maximum number of 10  $\mu\text{m}$  sections. Sections were collected to microscope slides (Superfrost™ Plus, ThermoFisher Scientific, MA, USA) and stored at  $-20^{\circ}\text{C}$ .

## **9. Cellular and Molecular Analysis**

### **9.1 Histological protocol**

#### **9.1.1 Luxol Fast Blue staining**

To study the area of demyelinated white matter, both in brain and spinal cord, slices were stained using a luxol fast blue protocol, as previously described<sup>181</sup>. Slices were stained with 0.1% Luxol Fast Blue solution in 70% ethyl alcohol at  $56^{\circ}\text{C}$  overnight, the excess stain was rinsed off with 70% ethyl alcohol and washed with distilled water for 5 min. Slides were differentiated in 0.5% lithium carbonate solution for 5 min and rinsed in distilled water for 5 min. Then, slides were counterstained with hematoxylin for 10 min and washed with tap water for 5 min, 1% hydrochloric acid was then used for 5 sec to differentiate and slides were rinsed with tap water one last time for 5 min. Finally, slides were mounted using Fluoromount-G (Southern Biotech, Birmingham, AL) for optical microscope. Representative images were acquired using Nanozoomer SQ (Hamamatsu, Japan) with a 20x resolution.

### **9.2 Free-floating immunohistochemistry (IHC)**

To assess oligodendroglial differentiation, free-floating IHC was performed on brain slices of mice that were injected with BrdU. For each antibody combination tested, a complete series of slices from each animal was considered  $n=1$ . Information regarding the primary antibodies used for this technique is present in the table below (Table 3).

First, slices were degelatinized in PBS (3 x 10 min, 37°C), followed by a treatment with HCL 1M (10 min, 4°C) and HCL 2M (30 min, 37°C) resulting in the exposure of BrdU epitopes. Slices were then incubated with borate buffer 0.1M (pH 8.5) (2 x 5 min, RT) and washed with PBS (3 x 10 min). Next, a blocking solution (3% bovine serum albumin (BSA) and 0.2% Triton™ X-100 in PBS) was applied (1h, RT). Slices were then incubated with primary antibodies rat anti-BrdU (1:500) and rabbit anti-NG2, anti-MBP or anti-Doublecortin (DCX) (1:200) in blocking solution (20-24h, 4°C). In the following day, slices were washed in PBS (3 x 10 min) and incubated with secondary antibodies anti-rat Alexa Fluor® 488 (1:500) and anti-rabbit Alexa Fluor® 568 (1:500) (Life Technologies, Thermo Fisher Scientific, MA, USA) (2h, RT). Slices were washed in PBS (3 x 10 min) and mounted with Mowiol on microscope slides (Superfrost™ Plus, ThermoFisher Scientific) and covered with glass coverslips.

**Table 3 – Primary antibodies used to assess adult oligodendrogenesis.**

Antibody	Host	Supplier	Reference	Dilution
Anti-BrdU	Rat	BioRad Laboratories, CA, USA	OBT0030CX	1:500
Anti-NG2	Rabbit	Merk, Darmstadt, Germany	AB5320	1:200
Anti-MBP	Rabbit	Cell Signalling Technology, MA, USA	78896	1:200
Anti-DCX	Rabbit	Abcam, Cambridge, UK	Ab18723	1:200

### 9.2.1 Image acquisition and analysis

The corpus callosum (CC), cortex (CT) and striatum (ST) are three of the brain regions frequently studied, due to the demyelination observed in the EAE model<sup>16,182</sup>. Moreover, the SVZ is the germinal niche which has NSCs responsible for originating oligodendrocytes in EAE<sup>16</sup>. Hence, all these regions (Fig. 12) were analysed.

Images of the entire brain slice were captured using the Zeiss Axio Scan Z.1 (Carl Zeiss, Oberkochen, Germany) slide scanner, throughout the entire thickness of the slice (40 µm) with a 40x objective. Manual cell counting was performed to quantify BrdU-, NG2- and DCX-positive cells, using the ZEN 2.5 lite software (Carl Zeiss, Oberkochen, Germany). The area (mm<sup>2</sup>) of each brain region was measured by drawing a line around the whole region, using the same software. The total volume (mm<sup>3</sup>) of each region for each mouse was extrapolated by multiplying the mean of the areas per slice by the distance between slices (400 µm). Results are presented as the number of immune-positive cells per volume (mm<sup>-3</sup>) in each section, normalized for the percentage of control (100%). For MBP staining, images were captured using the slide scanner with a 20x objective, in the maximum intensity projection calculated using the same software (Carl Zeiss, Oberkochen, Germany). The corpus callosum was manually delimited and area and mean fluorescence intensity were quantified with ZEN 2.5 lite

software (Carl Zeiss, Oberkochen, Germany). Results are presented as the ratio mean intensity/area, normalized for the percentage of control (100%).

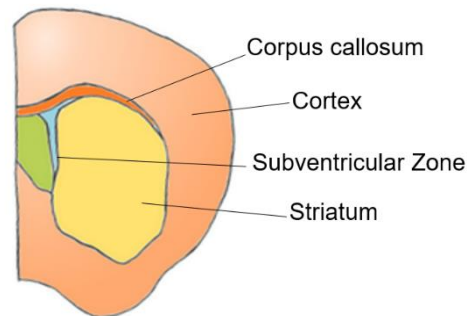


**Fig. 12 – Brain regions evaluated in IHC experiments.**

### **9.3 Western Blot (WB)**

To quantify the levels of NF- $\kappa$ B and its inhibitor I $\kappa$ B $\alpha$ , as well as of the myelin proteins MBP and PLP, western blots were performed. Samples from brain cortex tissue were collected from the frozen hemispheres of Control and EAE IP and IV animals and homogenized under sonication with Radio Immuno Precipitation Assay (RIPA) lysis buffer (4% Nonidet<sup>®</sup> P40 Substitute (NP40), 10% sodium dodecyl sulphate (SDS), 1mM ethylenediamine tetraacetic acid (EDTA), 150mM NaCl, 50mM Tris base), containing a cOmplete<sup>™</sup> Mini, EDTA-free, protease inhibitor cocktail tablet (Roche, Penzberg, Germany) for each 10 mL. For protein quantification, DC<sup>™</sup> Protein Assay kit (Bio-Rad Laboratories, CA, USA) and the Bradford method were used, having BSA as standard. Then, 6x sample buffer (36% glycerol, 12% SDS, 0.015% bromophenol blue, 720mM dithiothreitol, 420mM Tris, pH 6.8) was added and the samples were denatured (10 min, 95°C).

Proteins were separated by SDS-polyacrylamide gel electrophoresis (SDS-PAGE), in running buffer (0.1% SDS, 192mM glycine, 25mM Tris pH 8.3), at constant voltage (80-120 V), using 12% acrylamide/bis-acrylamide resolving gels (0.1% SDS, 0.1% ammonium persulfate (APS), 0.04% N,N,N',N'-tetramethylethane-1,2-diamine (TEMED), 375mM Tris pH 8.8), and 5% acrylamide/bis-acrylamide stacking gels (0.1% SDS, 0.1% APS, 0.1% TEMED, 125mM Tris pH 6.8), with 1.5 mm thickness. The protein molecular weight marker NZYColour Protein Marker II (NZYTech, Lisbon, Portugal) was used. After, proteins were transferred to polyvinylidene difluoride (PVDF) membranes, previously activated in methanol, in transfer buffer (10% methanol, 192mM glycine, 25mM Tris pH 8.3), at constant amperage (350 mA, 1h15). Membranes were blocked with 3% BSA in Tris buffered saline with Tween<sup>®</sup> 20 (TBS-T) (200nM Tris, 1.5M NaCl, 0.1% Tween<sup>®</sup> 20, pH 7.6) (1h, RT). Then membranes were washed in TBS-T (3 x 5 min) followed by incubation with primary antibodies rabbit anti-phosphoNF- $\kappa$ B

(pNF- $\kappa$ B) (1:500), as well as mouse anti-phosphoI $\kappa$ B $\alpha$  (pI $\kappa$ B $\alpha$ ) (1:500) (overnight, 4°C). To determine myelin protein levels (MBP and PLP), the following primary antibodies were used: rabbit anti-MBP (1:1000) and anti-myelin PLP (1:1000). Information regarding the primary antibodies used is depicted in Table 4. After, membranes were washed (3 x 5 min) and incubated with secondary antibodies conjugated with horseradish peroxidase (HRP), IgG anti-rabbit (1:10 000) and IgG anti-mouse (1:10 000) (Santa Cruz Biotechnology, TX, USA) (1h, RT). All antibodies used were prepared in blocking solution. Finally, after washing, proteins were revealed with Clarity™ Western ECL Substrate (Bio-Rad Laboratories, CA, USA), using ChemiDoc™ XRS+ imaging system with Image Lab™ software (Bio-Rad Laboratories, CA, USA). An additional stripping step was performed between the incubations previously described and the incubations with rabbit anti-totalNF- $\kappa$ B (tNF- $\kappa$ B) (1:1000) and mouse anti-totalI $\kappa$ B $\alpha$  (tI $\kappa$ B $\alpha$ ) (1:200).  $\beta$ -actin was used as a loading control (1:1000). For this, membranes were washed (3 x 5 min) and incubated with stripping buffer (200mM glycine, 3mM SDS, 1% Tween-20, 50% acetic acid glacial, pH 2.2) (30 min, RT). After, membranes were washed with distilled water to increase the pH and then washed again with TBS-T (2 x 15 min). Resulting images were processed and analysed using ImageJ 1.51s (Fiji) software (MD, USA)<sup>183</sup>. Results are expressed as protein levels, normalized to the percentage of control (100%).

**Table 4 – Primary antibodies used for western blotting.**

Antibody	Host	Supplier	Reference	Dilution
Anti- tNF- $\kappa$ B	Rabbit	Santa Cruz Biotechnology TX, USA	Sc-372	1:1000
Anti- pNF- $\kappa$ B	Rabbit	Abcam, Cambridge,UK	ab131109	1:500
Anti- tI $\kappa$ B $\alpha$	Mouse	Abcam, Cambridge,UK	ab12135	1:200
Anti- pI $\kappa$ B $\alpha$	Mouse	Cell Signalling Technology, MA, USA	9246	1:500
Anti - MBP	Rabbit	Cell Signalling Technology, MA, USA	78896	1:1000
Anti-myelin PLP	Rabbit	Abcam, Cambridge,UK	ab105784	1:1000
$\beta$ -actin	Mouse	Santa Cruz Biotechnology, TX, USA	sc-47778	1:1000

#### 9.4 Enzyme-Linked Immunosorbent Assay (ELISA)

ELISA was done to assess the levels of TNF $\alpha$  and IL-1 $\beta$  in frozen brain cortex samples from Control, EAE IP, IV, VAF and SPF animals. Samples were prepared and quantified as described above for western blot with the exception of the RIPA buffer, which did not contain SDS (RIPA lysis buffer (4% Nonidet® P40 Substitute (NP40), 1mM ethylenediamine tetraacetic acid (EDTA), 150mM NaCl, 50mM Tris base), containing a cOmplete™ Mini, EDTA-free, protease inhibitor cocktail tablet (Roche, Penzberg, Germany) for each 10 mL). For both assays commercially available kits were used (DuoSet ELISA Rat IL1 $\beta$ /IL-1F2 Cat. #DY201

and DuoSet ELISA Rat TNF $\alpha$  Cat. #DY510, both from R&D Systems (Abingdon, UK)). After diluting the capture antibody (CA) in PBS to the working concentration, a 96-well microplate was coated with 100  $\mu$ l per well (overnight, RT). Then, each well was aspirated and washed three times with 400  $\mu$ l of wash buffer (WB). In the last wash, any remaining WB was removed by inverting the plate and blotting it against clean paper towels. To block the plate, 300  $\mu$ l of reagent diluent (RD) were added (1h, RT). Meanwhile, the standard curve solutions were prepared following a sequential dilution from the reconstituted standard, in the following concentrations: 4000, 2000, 1000, 500, 250, 125, 62.5, 31.25, 15.625 pg/mL. The washing step (3 x 400  $\mu$ l) was repeated and 50  $\mu$ l of sample and standards in RD were added to each well (2h, RT). The wells were again washed (3 x 400  $\mu$ l) and 100  $\mu$ l of detection antibody (DA) diluted in RD were added to each well (2h, RT). After washing the plate (3 x 400  $\mu$ l), 100  $\mu$ l of the Streptavidin-HRP solution was added (20 min, RT) and from this point on, the plate was protected from direct light. The plate was washed (3 x 400  $\mu$ l) and 100  $\mu$ l of the substrate solution were added per well (20 min, RT), triggering an enzymatic solution with a coloured end product. To stop this reaction, 50  $\mu$ l of stop solution were added to each well. Absorbance was read at 450 nm and 540 nm using an Infinite M200 multimode microplate reader (Tecan, Männedorf, Switzerland).

Protein levels were extrapolated from the difference in absorbance by performing a four-parameter logistic (4PL) curve, using the MyAssays<sup>®</sup> online data analysis tool (Brighton, UK)<sup>184</sup>. Results are depicted as protein levels (pg/mL) normalized to the percentage of control (100%).

## **10. Statistical analysis**

Data is presented as mean  $\pm$  standard error of the mean (SEM). Unpaired two-tailed Student's *t*-test and one-way analyses of variance (ANOVA) followed by Bonferroni's multiple comparisons test were used to evaluate the significance of differences between means of two or more conditions, considering  $p < 0.05$  to represent statistically significant differences. All statistical analyses and graphs were performed using the software Graphpad Prism 6 (CA, USA).





## **CHAPTER 3 - RESULTS**



## 1. Clinical scores

To characterize the progression of the EAE phenotype, EAE clinical scores were evaluated daily in all groups of animals (Fig. 13). Four different experimental groups were tested: IV and IP animals (Fig. 13A), and VAF and SPF (Fig. 13B). EAE was induced in IV and IP animals by immunization with MOG-CFA emulsion prepared in the lab and received PTx through i.v. or i.p. injection (IV and IP groups, respectively) (Fig. 13A). PTx was administered i.v. and i.p. to choose the best protocol<sup>28,185</sup>. In fact, the disruption of the BBB caused by the PTx is crucial for MOG antigen arrival at the CNS and the successful induction of the model<sup>40</sup>, however i.p. injections are easier to perform than i.v. injections. Despite a high success rate (80% for both IP and IV groups) in one batch of animals used, the outcome for the following group of animals was less consistent (efficacy of about 10-20%). Therefore, a commercially available kit, with prepared MOG-CFA emulsion and PTx solution was used. In this case, the best animal housing for EAE induction was tested, since the environment and microbiome may influence it<sup>186</sup> (Fig. 13B).

EAE IV animals took longer than IP mice to display the disease phenotype (EAE peak at around day 21 p.i. for IV and at day 17 p.i. for IP) and returned to a score of 1 – 2 around two days after reaching the peak (Fig. 13A). Regarding the animals that were induced with EAE using the kit (Fig. 13B), it was possible to observe that SPF animals reached their maximum score around day 16 p.i., whereas VAF animals only reached the peak of EAE onset around day 35 p.i.. SPF animals showed an EAE profile gradually recovering to a score of 1, whilst VAF animals appear to have two distinct stages of EAE progression, depicting a lower clinical score between two periods of higher scores when they were sicker, and then recovering again to a lower score. Moreover, it was possible to observe a high heterogeneity for each group of animals, as seen by the error bars in both graphs, because not all animals got sick and reached their maximum score on the same day.

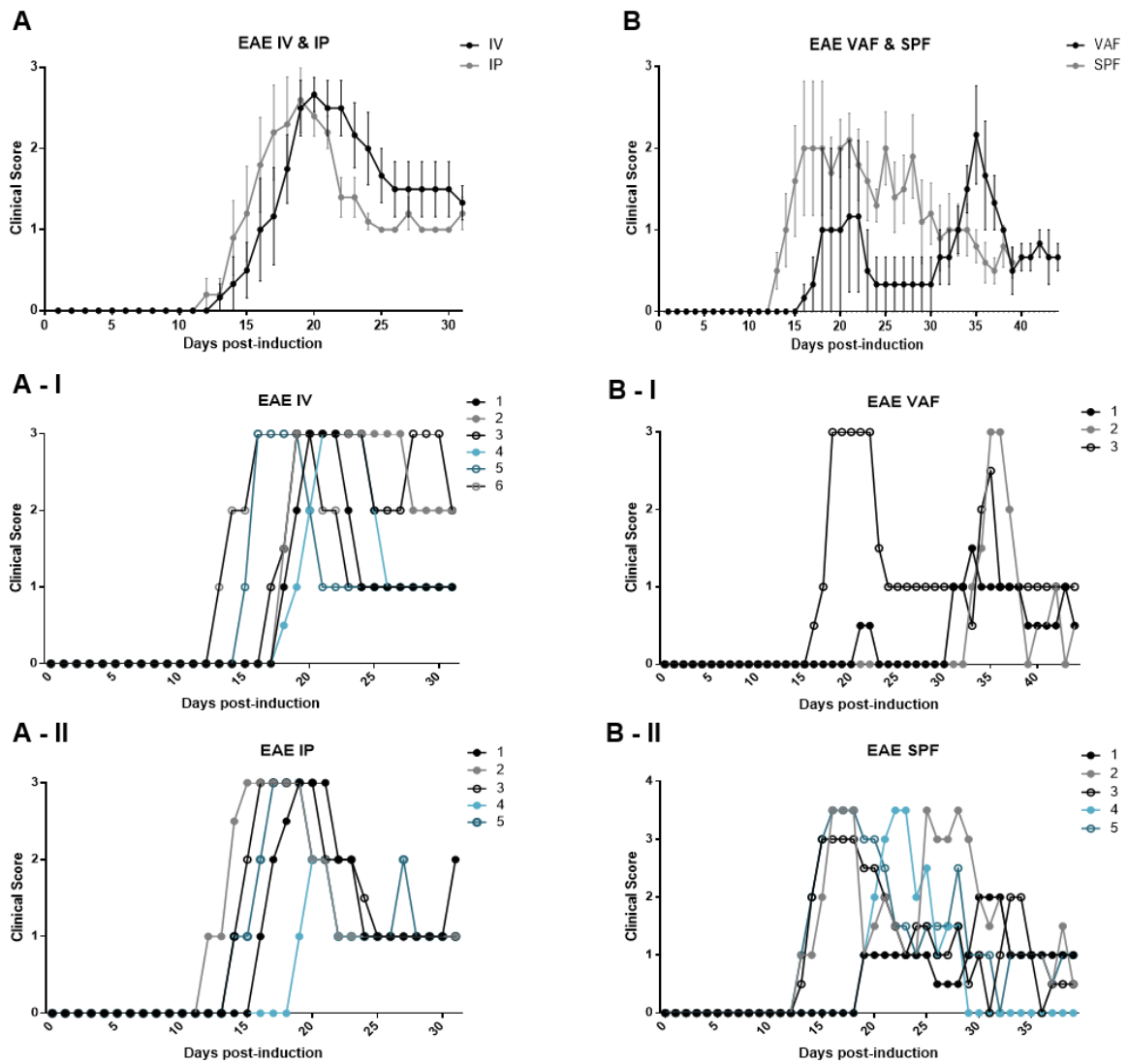


**Fig. 13 - Clinical scores registered as a measure of EAE phenotype progression for the different experimental groups. (A)** Clinical score representation for IV (—) and IP (—) animals. IV animals took longer than IP mice to display the phenotype. **(B)** Scores registered for VAF (—) and SPF (—) animals. VAF animals showed a more inconsistent pattern of EAE severity, reaching the peak of EAE around day 35 post-induction(p.i.). In turn, SPF animals, reached the peak of EAE phenotype around day 16 p.i. **(A, B-I and II)** Individual scores registered for all animal groups. Data are expressed as mean  $\pm$  SEM (n=3-6).

## 2. Locomotor activity characterization of the EAE animal model

As it has been previously described, EAE animals portray motor impairments<sup>167</sup>. Thus, aiming at characterizing the animal model, several behaviour tests assessing motor function were performed.

### 2.1 EAE IV animals show impaired OF performance on weeks 2 and 3 post-induction

The OF test was used to evaluate the locomotor and exploratory activity of the animals, by allowing them to explore a square arena for 10 min. EAE IV animals showed a decrease in average velocity (week 2 p.i. – CTRL IV:  $0.0600 \pm 0.0044$  m/s; EAE IV:  $0.0343 \pm 0.0073$  m/s; week 3 p.i. – CTRL IV:  $0.0446 \pm 0.0025$  m/s; EAE IV:  $0.0223 \pm 0.0068$  m/s, \* $p < 0.05$  and \*\* $p < 0.01$ , respectively,  $n=6-10$ ; Fig. 14A) and in distance travelled (week 2 p.i. – CTRL IV:  $40.82 \pm 1.218$  m; EAE IV:  $20.56 \pm 4.349$  m; week 3 p.i. – CTRL IV:  $26.67 \pm 1.463$  m; EAE IV:  $13.44 \pm 4.066$  m, \*\*\* $p < 0.001$  and \*\* $p < 0.01$ , respectively,  $n=6-10$ ; Fig. 14B) on weeks 2 and 3 of model induction when compared to the correspondent controls. Control animals from IV and IP groups showed a decrease in average velocity (week 2 p.i. – CTRL IV:  $0.0600 \pm 0.0044$  m/s; CTRL IP:  $0.0583 \pm 0.0030$  m/s; week 3 p.i. – CTRL IV:  $0.0446 \pm 0.0025$  m/s; CTRL IP:  $0.0431 \pm 0.0031$  m/s; # $p < 0.05$ ,  $n=10$ ; Fig. 14A) and in distance travelled (week 2 – CTRL IV:  $40.82 \pm 1.218$  m; CTRL IP:  $34.78 \pm 2.110$  m; week 3 p.i. – CTRL IV:  $26.67 \pm 1.463$  m; CTRL IP:  $25.85 \pm 1.846$  m; # $p < 0.05$ ; ### $p < 0.001$ ,  $n=10$ , Fig. 14B), when comparing week 2 with week 3. Moreover, the number of crossings entails the number of times the mouse entered one of the three virtually designed areas (central, intermediate and peripheral) during the testing period. For this parameter, only on week 3 was observed a significant difference between CTRL IV and EAE IV animals (CTRL IV:  $147.9 \pm 7.161$ ; EAE IV:  $59.83 \pm 16.24$ ; \*\*\* $p < 0.001$ ,  $n=6-10$ ; Fig. 14C). However, regarding EAE IP animals no significant differences were observed regarding the average velocity (average velocity: week 2 p.i. – CTRL IP:  $0.0583 \pm 0.0030$  m/s; EAE IP:  $0.0558 \pm 0.0098$  m/s; week 3 p.i. – CTRL IP:  $0.0431 \pm 0.0031$  m/s; EAE IP:  $0.0388 \pm 0.0025$  m/s), distance travelled (week 2 p.i. – CTRL IP:  $34.78 \pm 2.110$  m; EAE IP:  $33.31 \pm 5.888$  m; week 3 p.i. – CTRL IP:  $25.85 \pm 1.846$  m; EAE IP:  $23.38 \pm 1.485$  m) and number of crossings (week 2 p.i. – CTRL IP:  $162.7 \pm 17.23$ ; EAE IP:  $187.6 \pm 38.02$ ; week 3 p.i. – CTRL IP:  $128.6 \pm 13.81$ ; EAE IP:  $126.0 \pm 12.93$ ) when comparing with correspondent CTRL IP mice in both weeks ( $p > 0.05$ ,  $n=5-10$ ; Fig. 14A, B, C). Hence, results obtained show that locomotor activity and exploratory drive for EAE IV mice were impaired on both test dates, whilst no alterations were observed for EAE IP animals.

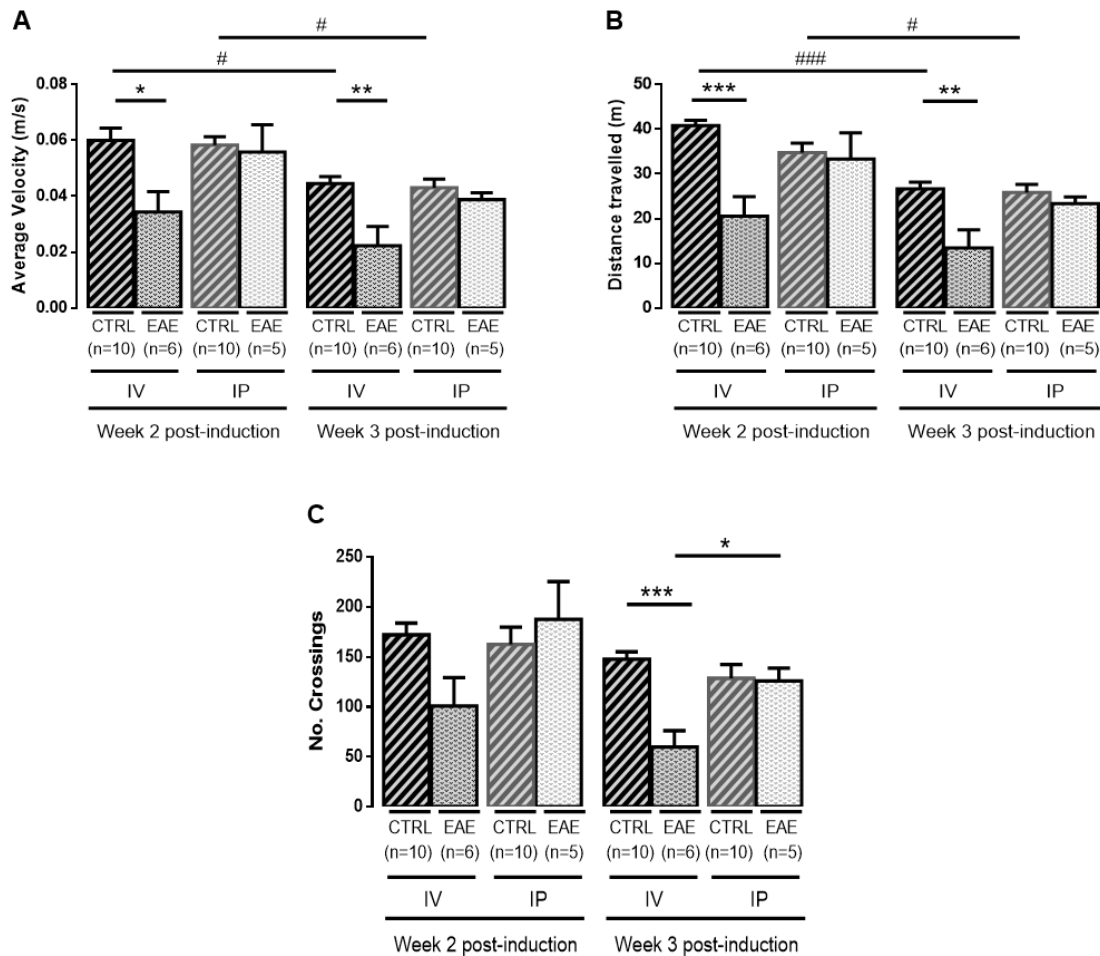


**Fig. 14 - Locomotor activity is impaired on EAE IV animals on weeks 2 and 3 after model induction, as assessed by the OF test.** In the OF test animals were left to freely explore a square arena for 10 min. The parameters average velocity (**A**), distance travelled (**B**) and number of crossings (**C**) between three virtual concentric squares, delimiting the central, intermediate and periphery areas were quantified. (**A, B**) Significant differences were observed between CTRL and EAE IV animals on weeks 2 and 3 p.i. (\* $p < 0.05$ , \*\* $p < 0.01$  and \*\*\* $p < 0.001$ ; ordinary one-way ANOVA followed by Bonferroni's multiple comparison test). A decrease in average velocity and distance travelled between test weeks is also shown for CTRL IV and CTRL IP groups (# $p < 0.05$ , ### $p < 0.001$ ; ordinary one-way ANOVA followed by Bonferroni's multiple comparison test). (**C**) Significant differences in the number of crossings were only registered in week 3 after model induction, between CTRL and EAE IV animals (\*\*\* $p < 0.001$ ; ordinary one-way ANOVA followed by Bonferroni's multiple comparison test). Data are expressed as mean  $\pm$  SEM (n=5-10). ▨ : CTRL IV; ▩ : EAE IV; ▧ : CTRL IP; ▦ : EAE IP.

## 2.2 EAE IV and IP animals show impaired rotarod performance on week 3 post – induction

The RR test was used to evaluate the motor coordination and balance of the animals through their ability to stay on a rotating rod for 5 min. Consequently, animals presenting higher clinical scores lose their ability to stay on the rod, resulting in shorter  $t_{fall}$ , and showing a decrease in velocity (Fig. 15). No differences were observed between the EAE groups and the correspondent controls, in week 2, regarding  $t_{fall}$  (CTRL IV: 79.33±8.349 s; EAE IV: 77.67±19.29 s; CTRL IP: 77.07±8.827 s; EAE IP: 47.67±13.09 s;  $p>0.05$ ,  $n=5-10$ , Fig. 15A) and velocity (CTRL IV: 13.70±1.012 rpm; EAE IV: 13.22±2.358 rpm; CTRL IP: 13.17±1.084 rpm; EAE IP: 10.60±1.077 rpm;  $p>0.05$ ,  $n=5-10$ , Fig. 15B). Notwithstanding, EAE IV and IP mice showed impaired performances at week 3 for both  $t_{fall}$  (CTRL IV: 79.97±6.875 s; EAE IV: 10.44±5.044 s; CTRL IP: 72.25±6.615 s; EAE IP: 20.67±5.090 s;  $***p<0.001$ ,  $n=5-10$ ; Fig. 15A) and velocity (CTRL IV: 13.58±0.8063 rpm; EAE IV: 5.444±0.9135 rpm; CTRL IP: 12.57±0.7873 rpm; EAE IP: 6.600±0.6864 rpm;  $***p<0.001$ ,  $n=5-10$ , Fig. 15B). Furthermore, between week 2 and week 3 p.i., there was a significant decrease in both parameters, for EAE IV animals ( $t_{fall}$  – week 2 p.i.: 77.67±19.29 s; week 3 p.i.: 10.44±5.044 s; velocity – week 2 p.i.: 13.22±2.358 rpm; week 3 p.i.: 5.444±0.9135 rpm,  $###p<0.001$ ;  $n=6$ , Fig. 15). Overall results show a worsening of motor coordination and balance for EAE mice performance on the RR test on week 3, when scores were higher.

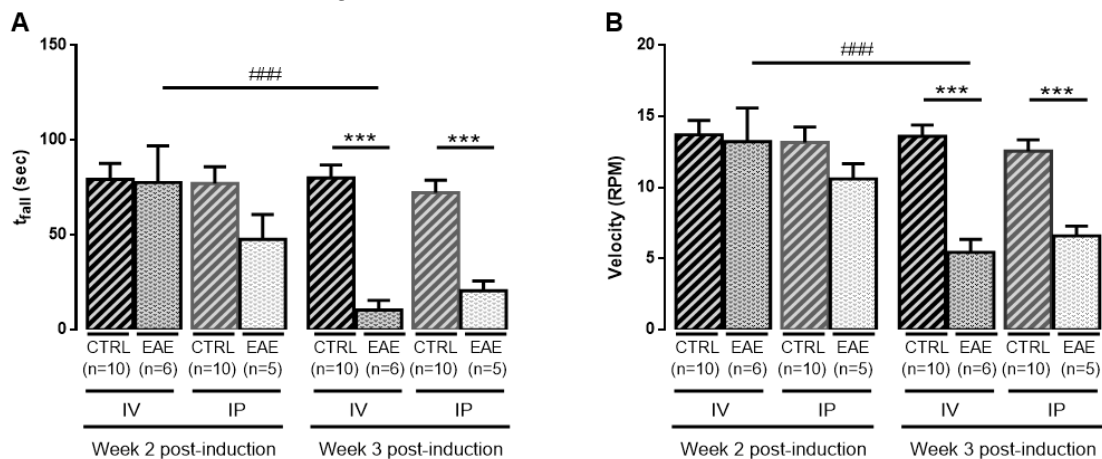


**Fig. 15 - Rotarod test results expose impairments for EAE IV and IP animals on week 3 after model induction.** In the RR test, mice had to maintain their balance on a rotating rod, from 4-40 rpm in 5 minutes. Time of fall (A) and velocity (B) were registered. (A, B) For all experimental groups, no significant differences can be observed on week 2 after model induction. Significant decreases both in  $t_{fall}$  and velocity occurred on week 3 p.i. between IV and IP animals and the correspondent controls ( $***p<0.001$ ; ordinary one-way ANOVA followed by Bonferroni's multiple comparison test). A significant decrease for both parameters can be observed between weeks 2 and 3 p.i. for EAE IV animals ( $###p<0.001$ ; ordinary one-way ANOVA followed by Bonferroni's multiple comparison test). Data are expressed as mean ± SEM ( $n=5-10$ ). ▨ : CTRL IV; ▩ : EAE IV; ▧ : CTRL IP; ▦ : EAE IP.

### 2.3 EAE IV animals show impaired pole test performance in week 3 post-induction

Aiming at assessing the agility and balance of the animals, the PT was performed. In this test, mice have to orient downwards and descend a vertical pole, and time to orient ( $t_{\text{orient}}$ ) and descend ( $t_{\text{descend}}$ ) the pole, as the total time ( $t_{\text{total}}$ ) of the trial were registered. On week 3 p.i. EAE IP animals showed an increased latency to orient downwards (CTRL IP:  $3.028 \pm 0.2870$  s; EAE IP:  $11.50 \pm 2.072$  s;  $*p < 0.05$ ,  $n=5-10$ ; Fig. 16A), whereas  $t_{\text{descend}}$  and  $t_{\text{total}}$  were already augmented in week 2 p.i. (CTRL IP:  $7.972 \pm 1.713$  s; EAE IP:  $14.30 \pm 2.103$  s and CTRL IP:  $12.31 \pm 1.776$  s; EAE IP:  $19.80 \pm 3.271$  s;  $*p < 0.05$ ,  $n=5-10$ ; Fig. 16B, C). For EAE IV animals,  $t_{\text{orient}}$ ,  $t_{\text{descend}}$  and  $t_{\text{total}}$  were increased when compared to control, on week 3 after model induction ( $t_{\text{orient}}$  – CTRL IV:  $3.167 \pm 0.5187$  s; EAE IV:  $24.92 \pm 3.652$  s;  $t_{\text{descend}}$  – CTRL IV:  $8.167 \pm 1.880$  s; EAE IV:  $24.92 \pm 3.652$  s;  $t_{\text{total}}$  – CTRL IV:  $11.33 \pm 2.327$  s; EAE IV:  $49.83 \pm 7.305$  s;  $***p < 0.001$ ,  $n=5-10$ ; Fig. 16A, B, C). Moreover, comparing week 2 and week 3 from EAE IV animals a significant increase was observed for the three parameters addressed ( $t_{\text{orient}}$  – week 2 p.i.:  $4.500 \pm 0.9332$  s; week 3 p.i.:  $24.92 \pm 3.652$  s;  $t_{\text{descend}}$  – week 2 p.i.:  $8.250 \pm 0.9399$  s; week 3 p.i.:  $24.92 \pm 3.652$  s;  $t_{\text{total}}$  – week 2 p.i.:  $12.75 \pm 1.216$  s; week 3 p.i.:  $49.83 \pm 7.305$  s;  $##p < 0.01$ ;  $###p < 0.001$ ,  $n=6$ ; Fig. 16A, B, C). Finally, an increase was always observed when comparing EAE IV with EAE IP groups on week 3 p.i., for  $t_{\text{orient}}$  (EAE IV:  $24.92 \pm 3.652$  s; EAE IP:  $11.50 \pm 2.072$  s;  $***p < 0.001$ ,  $n=5-6$ ; Fig. 16A),  $t_{\text{descend}}$  (EAE IV:  $24.92 \pm 3.652$  s; EAE IP:  $11.20 \pm 2.199$  s;  $**p < 0.01$ ,  $n=5-6$ ; Fig. 16B) and  $t_{\text{total}}$  (EAE IV:  $49.83 \pm 7.305$  s; EAE IP:  $22.70 \pm 4.262$  s;  $***p < 0.001$ ,  $n=5-6$ ; Fig. 16C). Thus, these results show that EAE IV animals present deficits in all parameters on week 3 after model induction. However, EAE IP animals present impairments in their time to orient downwards on week 3 p.i., but the remaining aspects of this test were affected on week 2 after model induction. We can conclude that animals portraying more severe EAE phenotype show higher values for all parameters tested.



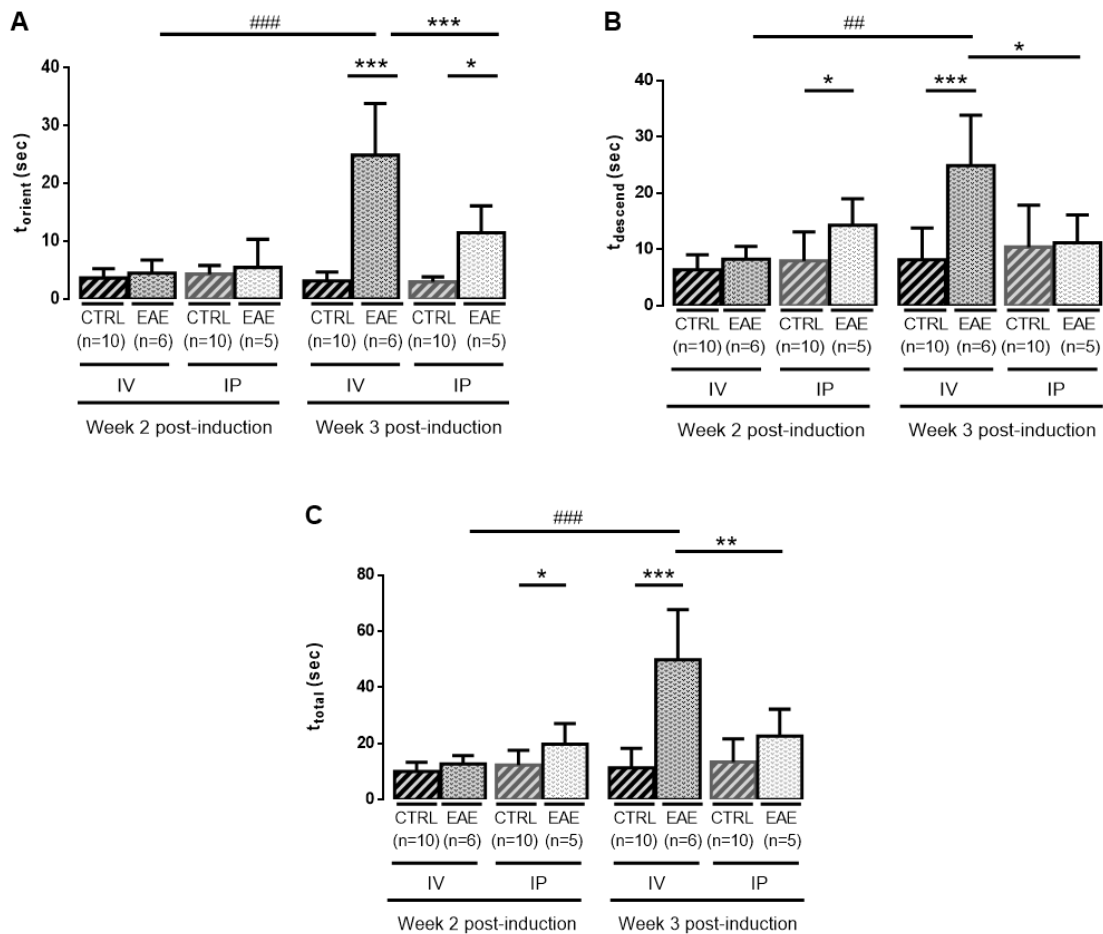


**Fig. 16 - Pole test performance on week 3 post-induction shows deficits for EAE IV mice in all criteria.** Motor dysfunction in EAE mice was assessed with the pole test. The time it took for the animal to orient downwards (**A**), the time to descend the pole (**B**) and the total duration of the trial (**C**) were quantified. (**A, B, C**) EAE IV animals show differences from week 2 to week 3 p.i. and EAE IV mice show significant increases in all parameters on week 3 p.i., when compared to the correspondent controls and to EAE IP mice (### $p < 0.01$ ; ### $p < 0.001$ ; \* $p < 0.05$ ; \*\* $p < 0.01$ ; \*\*\* $p < 0.001$ ; ordinary one-way ANOVA followed by Bonferroni's multiple comparison test). (**A**) Results show an increase when comparing EAE IP with its control on week 3 p.i. (\* $p < 0.05$ ; ordinary one-way ANOVA followed by Bonferroni's multiple comparison test). (**B, C**) Significant differences in  $t_{descend}$  and  $t_{total}$  are shown in week 2 p.i. for EAE IP animals (\* $p < 0.05$ ; ordinary one-way ANOVA followed by Bonferroni's multiple comparison test). Data are expressed as mean  $\pm$  SEM (n=5-10). ▨ : CTRL IV; ▩ : EAE IV; ▧ : CTRL IP; ▦ : EAE IP.

### 3. Cellular and molecular analysis

After characterizing the phenotype of mice portraying EAE, where overall results highlighted that motor impairment was most robust on week 3 after EAE model induction, when animals presented highest clinical scores, cellular and molecular characterization of this model, as well as of adult oligodendrogenesis, was performed.

#### 3.1 Demyelination in brain and spinal cord of EAE animals was not observed

To evaluate demyelination in white matter, both in spinal cord and brain, luxol fast blue staining was performed, with myelin staining in blue, in CTRL, EAE IP and naïve (male C57BL/6 mice with 10 weeks of age) mice sacrificed in the end of experimental protocol (31 days p.i. with average score of 1-2). Representative images (Fig. 17) depicted below show a similar blue tone (myelin is stained in blue by luxol) for all groups, hinting at identical myelin levels.

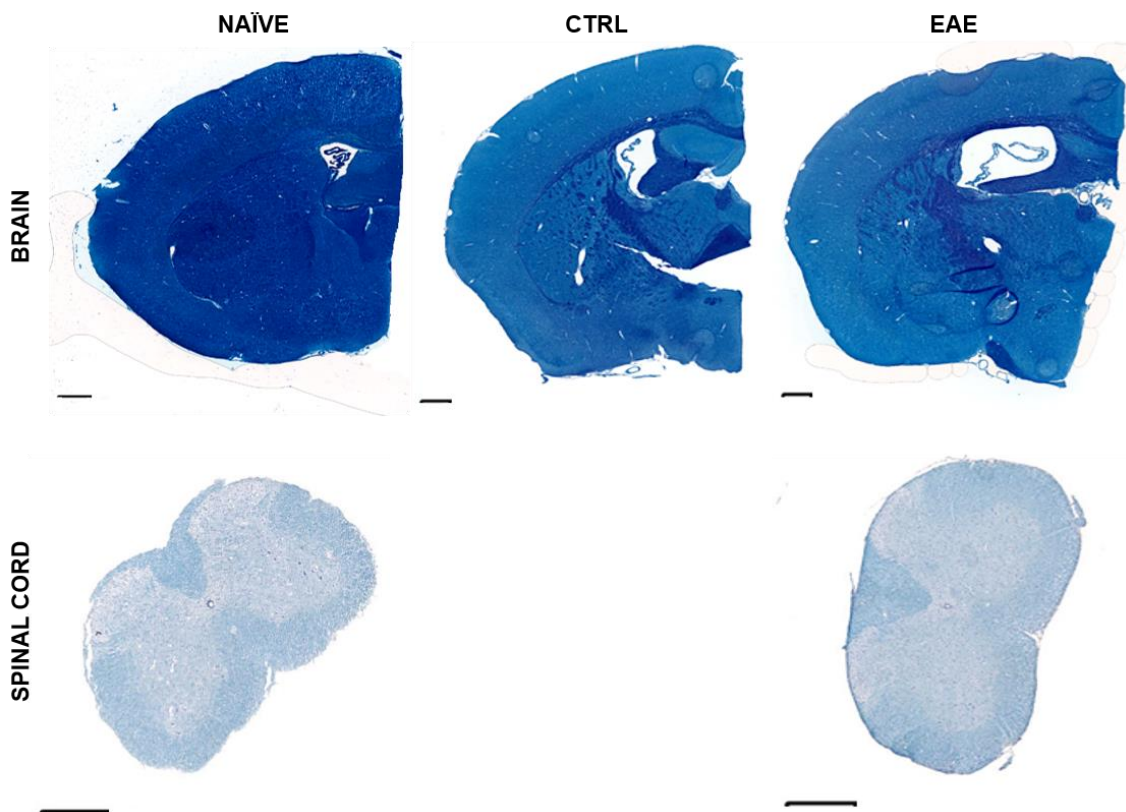
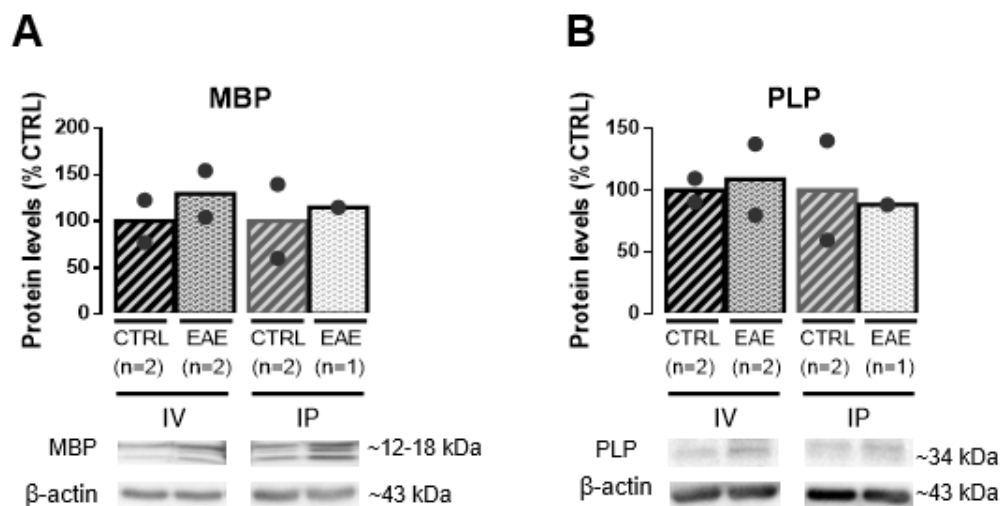


**Fig. 17 - Myelin in EAE brain and spinal cord appears similar to controls.** Representative images for luxol fast blue staining of brain and spinal cord for Naïve, CTRL IP and EAE IP animals. Scale bar = 0.5 mm.

### 3.2 Myelin proteins MBP and PLP seem to remain unaltered in EAE mice

Upon EAE onset, demyelination occurs, meaning that myelin sheaths and constituting proteins are degraded<sup>63</sup>. Therefore, in an attempt to quantify the degree of demyelination in the brain of those animals, levels of MBP and PLP were assessed by western blot in brain cortex samples from EAE IV and IP animals sacrificed in the end of experimental protocol (day 31 p.i. with average score of 1-2) (Fig. 18).

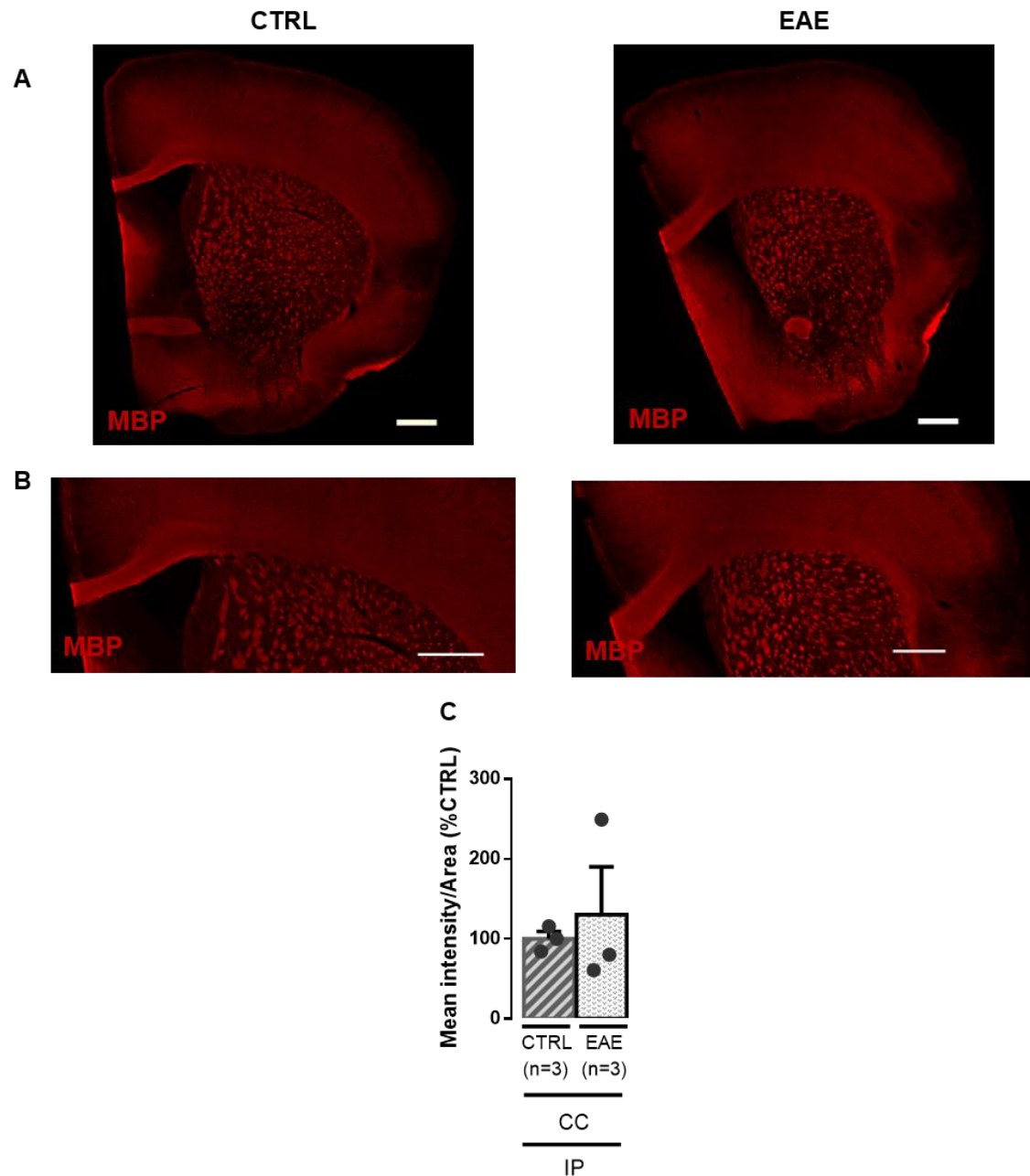
Once again, the sample size is insufficient to take any solid conclusions, however no apparent differences in MBP and PLP levels between EAE IV and EAE IP and its controls seem to be present (MBP – CTRL IV: 99.98 %; EAE IV: 129.6 %; CTRL IP: 100.0 %; EAE IP: 115.1 %; PLP – CTRL IV: 99.98 %; EAE IV: 108.8 %; CTRL IP: 100.0 %; EAE IP: 88.31 %; n=1-2; Fig. 18).





**Fig. 18 - Levels of myelin proteins MBP (A) and PLP (B) did not seem to change in EAE animals at 31 days p.i..** (A, B, top) Protein levels were quantified and normalized to the percentage of control (%CTRL). (A, B, bottom) Representative western blots depict immunoreactive bands for MBP (~12-18 kDa); PLP (~34 kDa) and β – actin (loading control, ~43 kDa) obtained from brain cortex samples for EAE IV and IP animals and correspondent controls. Data are expressed as mean (n=1-2). ▨ : CTRL IV; ▩ : EAE IV; ▧ : CTRL IP; ▦ : EAE IP.

### 3.3 MBP fluorescence levels in the corpus callosum do not change in EAE

MBP fluorescence in the CC was assessed in an attempt to quantify the level of demyelination in the brain of EAE animals. Results obtained show no significant differences between the groups studied (CTRL IP:  $100.0 \pm 9.137$  %; EAE IP:  $130.1 \pm 59.86$  %;  $p > 0.05$ ,  $n = 3$ ; Fig. 19).



**Fig. 19 - MBP fluorescence in the CC is not altered by EAE.** (A) Representative images for MBP staining for CTRL IP and EAE IP mice, and corresponding amplification (B) of the CC. (C) Results are depicted as a ratio between mean intensity and the area of the CC, normalized to the percentage of control (%CTRL). No differences were observed between control and EAE groups. ( $p > 0.05$ ; unpaired Student's t-test). Data are expressed as mean  $\pm$  SEM ( $n = 3$ ).  : CTRL IP;  : EAE IP; CC – corpus callosum. Scale bar = 500  $\mu$ m.

### 3.4 SPF animals show significantly increased levels of TNF $\alpha$ inflammatory responses, combined with a tendency for increased levels of IL-1 $\beta$

Several cytokines are involved in the inflammatory cascade of EAE<sup>44</sup>. Amongst those, IL-1 $\beta$  and TNF $\alpha$  levels were studied by ELISA in samples of brain cortex of IV, IP, VAF and SPF animals sacrificed in the end of the experimental protocol (Fig. 20). Regarding the EAE IV and IP mice, although the number of samples is insufficient for statistical analysis and further conclusions, EAE IV animals do not seem to show differences relative to CTRL IV, both for IL-1 $\beta$  and TNF $\alpha$  (IL-1 $\beta$  - CTRL IV: 100.0 %; EAE IV: 95.57 %, TNF $\alpha$  - CTRL IV: 100 %; EAE IV: 101.6 %; n=2; Fig. 20A, B), while for EAE IP mice, a tendency for increased levels of cytokines was observed when comparing with CTRL IP (IL-1 $\beta$  - CTRL IP: 100.0 %; EAE IP: 188 %, TNF $\alpha$  - CTRL IP: 99.99 %; EAE IP: 159.3 %; n=1-2; Fig. 20A, B). Furthermore, for EAE VAF mice no differences in IL-1 $\beta$  levels were observed when comparing with control mice (CTRL: 100.0 $\pm$ 6.915 %; EAE VAF: 118.3 $\pm$ 32.36 %; n=3-5; Fig. 20A), whilst a tendency for increased levels of IL-1 $\beta$  was observed when comparing EAE SPF mice with the CTRL mice (CTRL: 100.0 $\pm$ 6.915 %; SPF: 142.5 $\pm$ 8.576 %; n=5; Fig. 20A). Nevertheless, EAE SPF animals displayed a significant increase in TNF $\alpha$  levels when compared to CTRL and EAE VAF groups (CTRL: 100.0 $\pm$ 9.435 %; EAE VAF: 112.4 $\pm$ 23.07 %; EAE SPF: 299.3 $\pm$ 53.36 %; \*p<0.05; \*\*p<0.01, n=3-5; Fig. 20B).

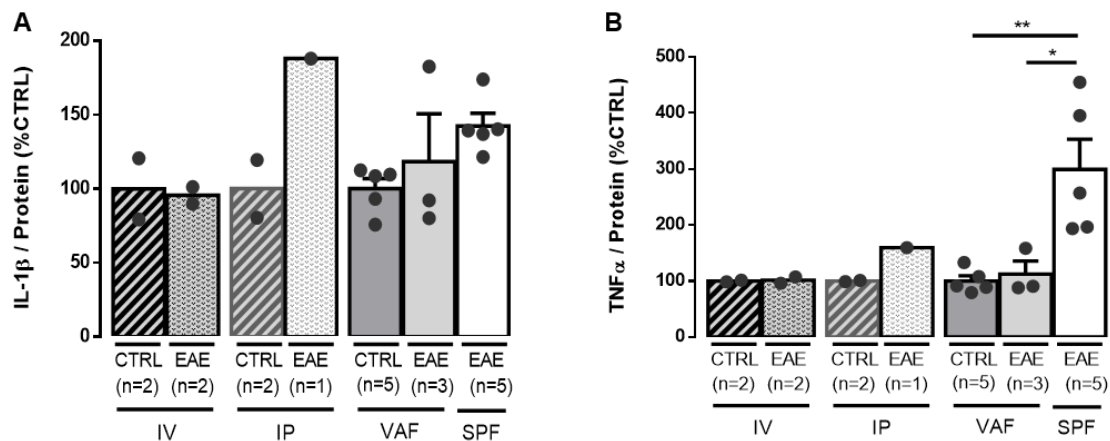


**Fig. 20 - Inflammatory cytokines IL-1 $\beta$  (A) and TNF $\alpha$  (B) levels in EAE animals.** IL-1 $\beta$  and TNF $\alpha$  levels from samples of brain cortex were quantified by ELISA assays and are expressed as a ratio of cytokine levels over total protein, normalized to the percentage of control (%CTRL). (A) No significant differences were observed between EAE VAF and the correspondent control, but a tendency for increased IL-1 $\beta$  levels was observed between CTRL and SPF groups (p>0.05 for all comparisons, ordinary one-way ANOVA followed by Bonferroni's multiple comparison test). (B) A significant increase in TNF $\alpha$  is shown in EAE SPF animals, when compared to the control or VAF groups (\*p<0.05; \*\*p<0.01; ordinary one-way ANOVA followed by Bonferroni's multiple comparison test). Data are expressed as mean (n=1-2) or mean  $\pm$  SEM (n=3-5). ▨ : CTRL IV; ▩ : EAE IV; ▧ : CTRL IP; ▦ : EAE IP; ▥ : CTRL VAF+SPF; ▤ : EAE VAF; ▣ : EAE SPF.

### 3.5 NF- $\kappa$ B pathway does not seem to be activated in the EAE mice

Attempting at assessing the activation of NF- $\kappa$ B pathway, the ratio between the phosphorylated and the total forms of both NF- $\kappa$ B and I $\kappa$ B $\alpha$  were quantified by western blot in samples of brain cortex from control and EAE IV and IP animals sacrificed in the end of the experimental protocol (day 31 p.i., with average score of 1-2) (Fig. 21). Preliminary data do not seem to show alterations between control and experimental groups for the pNF- $\kappa$ B/tNF- $\kappa$ B ratio (CTRL IV: 100.0 %; EAE IV: 107.4 %; CTRL IP: 99.99 %; EAE IP: 100.1 %, n=1-2, Fig. 21A). Similarly, no changes appear to be present for the pI $\kappa$ B $\alpha$ /tI $\kappa$ B $\alpha$  ratio for the groups tested (CTRL IV: 100.0 %; EAE IV: 131.4 %; CTRL IP: 100.0 %; EAE IP: 82.76 %, n=1-2, Fig. 21B).

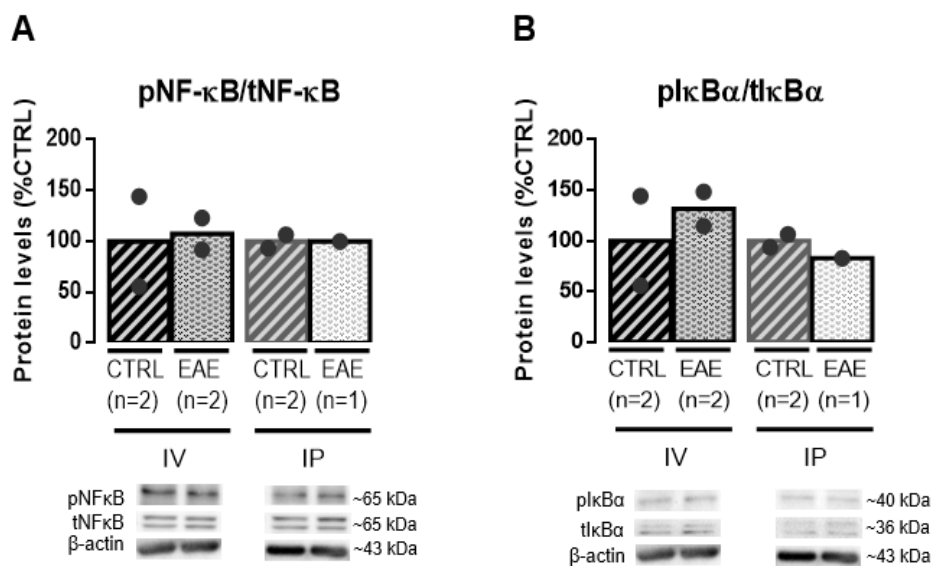


**Fig. 21 - Levels of pNF $\kappa$ B (A) and pI $\kappa$ B $\alpha$  (B) seem to remain unaltered in EAE mice 31 days p.i..** (A, B, top) Protein levels were quantified, presented as a ratio between the phosphorylated and the total protein, and normalized to the percentage of control (%CTRL). (A, B, bottom) Representative western blots depict immunoreactive bands for pNF $\kappa$ B (~65 kDa); tNF $\kappa$ B (~65 kDa); pI $\kappa$ B $\alpha$  (~40 kDa); tI $\kappa$ B $\alpha$  (~36 kDa) and  $\beta$  – actin (loading control, ~43 kDa) obtained from brain samples for EAE IV and IP animals and correspondent controls. Data are expressed as mean (n=1-2). ▨ : CTRL IV; ▩ : EAE IV; ▧ : CTRL IP; ▦ : EAE IP.

### 3.6 Oligodendroglial differentiation in the EAE brain from adult progenitors of the SVZ

#### 3.6.1 Volume of the brain regions studied

To assess if alterations in cell differentiation might be due to variations in volume between CTRL IP and EAE IP animals, the volume of SVZ, CC, CT and ST, was quantified. The volume was similar between CTRL and EAE in all studied regions (SVZ – CTRL:  $0.01067 \pm 0.001453$  mm<sup>3</sup>; EAE:  $0.01556 \pm 0.002576$  mm<sup>3</sup>; CC – CTRL:  $0.2591 \pm 0.02724$  mm<sup>3</sup>; EAE:  $0.2352 \pm 0.008893$  mm<sup>3</sup>; CT – CTRL:  $3.163 \pm 0.1608$  mm<sup>3</sup>; EAE:  $2.825 \pm 0.1069$  mm<sup>3</sup>; ST – CTRL:  $1.114 \pm 0.03761$  mm<sup>3</sup>; EAE:  $1.075 \pm 0.01559$  mm<sup>3</sup>; n=3; Fig. 22).

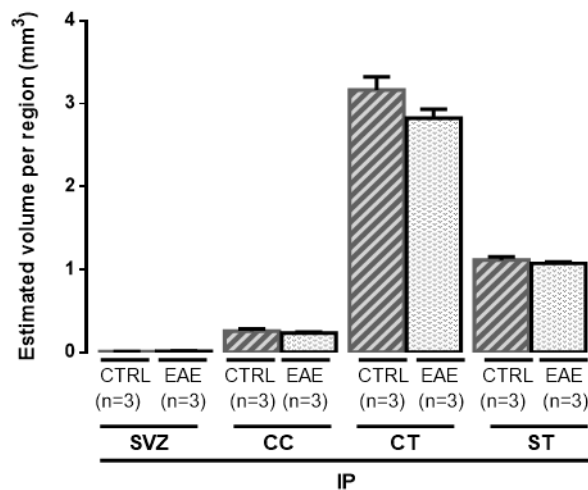


**Fig. 22 - Volume does not change in EAE animals in the different brain regions studied.** Volume (mm<sup>3</sup>) of each region (CC, SVZ; CT, ST) for CTRL IP and EAE IP mice. No significant differences were found for each region, between CTRL and EAE groups ( $p > 0.05$  for all comparisons; unpaired Student's t-test). Data are expressed as mean  $\pm$  SEM (n=3). ▨ : CTRL IP; ▩ : EAE IP; SVZ – subventricular zone, CC – corpus callosum; CT – cortex; ST – striatum.

### 3.6.2 Cellular survival

Since BrdU has the ability to incorporate the DNA of dividing cells, BrdU<sup>+</sup> cells observed correspond to cells that incorporated BrdU during proliferation in the beginning of the protocol (day 3) and survived the four weeks of protocol. In particular, the protocol used (7 i.p. injections with two-hour intervals) specifically marked cells originated in the SVZ<sup>16</sup>. Results show no variations between CTRL IP and EAE IP groups, for SVZ, CT, and ST (SVZ – CTRL: 100.0±6.393 %; EAE: 124.3±15.35 %; CT – CTRL: 100.0±12.37 %; EAE: 124.5±24.63 %; ST – CTRL: 99.99±7.131 %; EAE: 94.19±15.31 %; p>0.05, n=3; Fig. 23), while there is a clear tendency for an increase in cell survival in the CC (CC – CTRL: 100.0±11.70 %; EAE: 143.4±11.86 %; p=0.0598, n=3; Fig. 23).

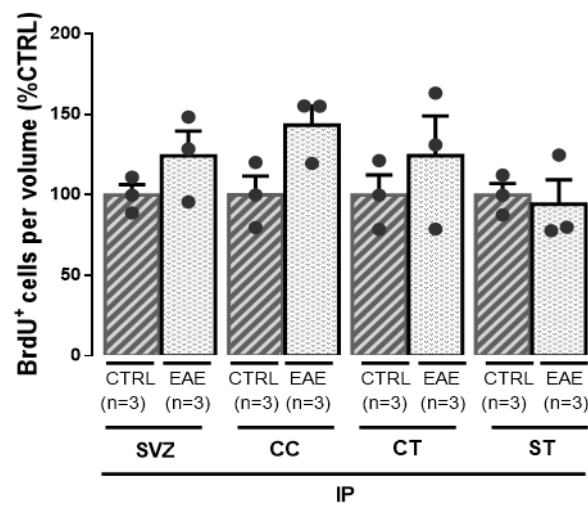


**Fig. 23 - Cell survival is not altered between CTRL and EAE groups.** BrdU<sup>+</sup> cells per volume were normalized to the percentage of control (%CTRL). No significant differences were observed between CTRL IP and EAE IP groups for the regions analysed. (p>0.05 for all comparisons; unpaired Student's t-test). Data are expressed as mean ± SEM (n=3). ▨ : CTRL IP; ▩ : EAE IP; SVZ – subventricular zone, CC – corpus callosum; CT – cortex; ST – striatum.

### 3.6.3 Oligodendroglial differentiation

The proteoglycan NG2 is a marker of OPCs<sup>68</sup>. Thus, cells that incorporated BrdU (BrdU<sup>+</sup>) and are also positive for NG2 (NG2<sup>+</sup>BrdU<sup>+</sup>) are cells that differentiated into OPCs since the beginning of the protocol. Data shows an increase in the number of NG2<sup>+</sup>BrdU<sup>+</sup> cells in the CC (CC – CTRL: 100.0±8.506 %; EAE: 178.5±23.71 %; \*p<0.05, n=3; Fig. 24C), whereas no changes were observed in the remaining three regions (SVZ – CTRL: 100.0±100.0 %; EAE: 0.0±0.0 %; CT – CTRL: 100.0±24.46 %; EAE: 88.54±18.25 %; ST – CTRL: 100.0±26.51 %; EAE: 94.73±27.90 %; n=3; Fig. 24C).



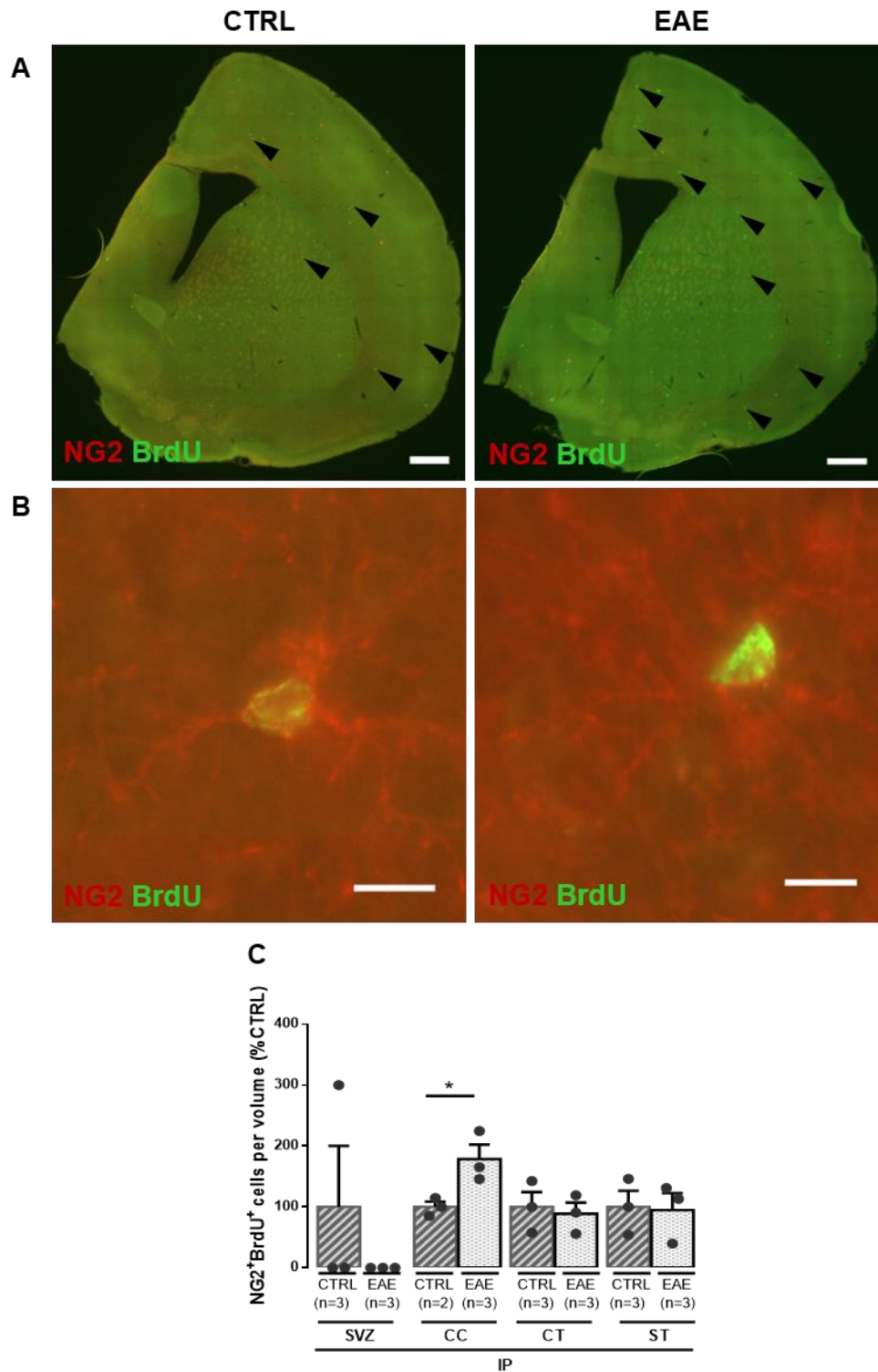


**Fig. 24 - NG2<sup>+</sup>BrdU<sup>+</sup> cells are increased in the corpus callosum of EAE animals.** (A) Representative images for NG2 staining for CTRL IP and EAE IP mice, and corresponding amplification (B) of a NG2<sup>+</sup>BrdU<sup>+</sup> cell. (C) NG2<sup>+</sup>BrdU<sup>+</sup> cells per volume were normalized to the percentage of control (%CTRL). An increase in double positive cells was observed in the CC for EAE animals, when compared to control. (\*p<0.05; unpaired Student's t-test). Data are expressed as mean ± SEM (n=3). ▨: CTRL IP; ▩: EAE IP; SVZ – subventricular zone, CC – corpus callosum; CT – cortex; ST – striatum. Scale bar = 500 μm (A) and 10 μm (B). Arrows = BrdU<sup>+</sup> cells.

### 3.6.4 Neuronal differentiation

Since NSCs of the SVZ in physiological conditions mainly produce new neurons, doublecortin (DCX), protein involved in microtubule polymerization, was used as a marker of neuroblasts and immature neurons<sup>187,188</sup>. Therefore, DCX staining was used as a control to assess if EAE was changing neuronal differentiation. In Fig. 25 are displayed representative images for DCX<sup>+</sup>BrdU<sup>+</sup> immunostaining. An apparent decrease in DCX staining (red) was observed in the SVZ of EAE animals (Fig. 25), hinting at a possible decrease in neuronal differentiation under pathological conditions (EAE).

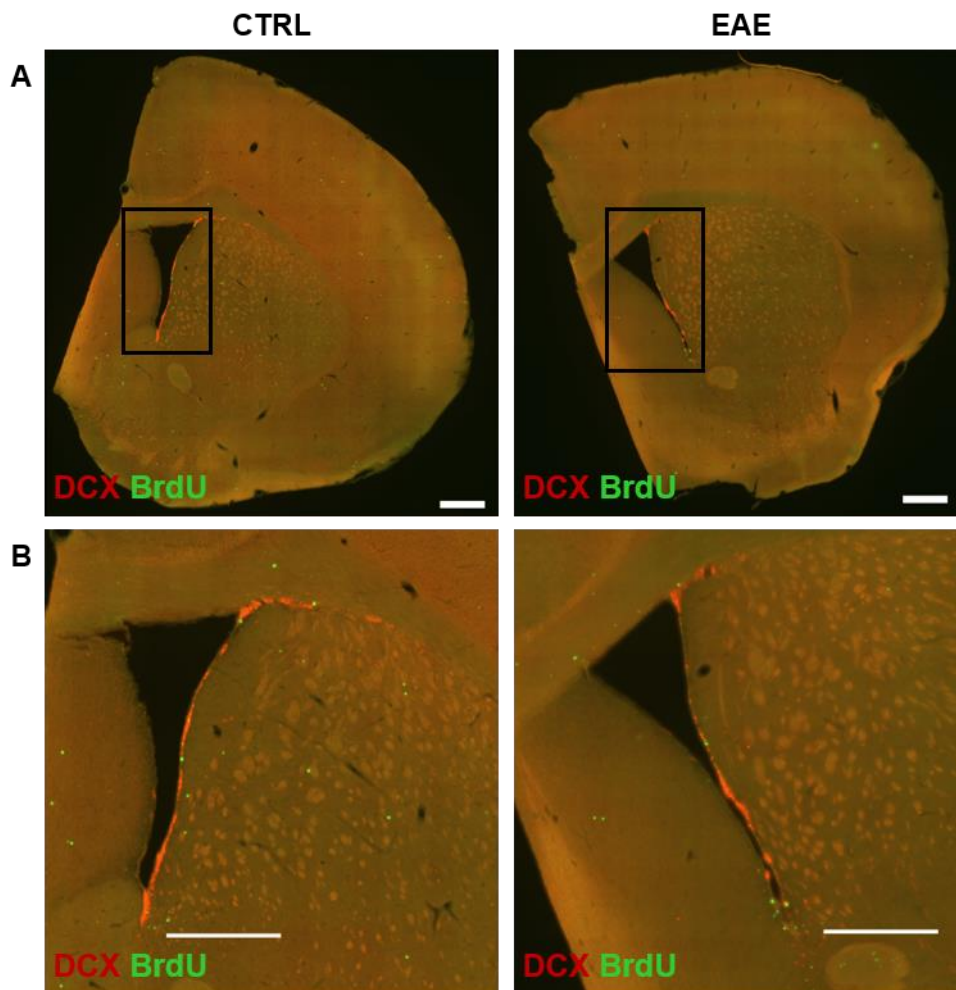


**Fig. 25 - Neuronal differentiation in the SVZ of control and EAE animals.** Representative images of brain slices (A) of CTRL IP and EAE IP animals with staining for DCX (red) and BrdU (green) and corresponding amplifications for the SVZ (B). Scale bar = 500  $\mu$ m.

## **CHAPTER 4 – DISCUSSION**



MS is an inflammatory demyelinating disease with a worldwide distribution, affecting young individuals, more commonly women. It is characterized by the progressive impairment of motor capacities and cognitive abilities. To this day, the basis for MS development remains unclear, despite extensive studies which have already highlighted several putative players, such as genetic susceptibility or environmental factors. Moreover, the available therapeutic options are mainly focused on controlling the immune component of the disease, disregarding the crucial role of myelin repair. The NSCs present in the SVZ, one of the two germinal niches present in the adult mammalian brain, are responsible for the generation of both neuronal and glial progenitors. In MS, not only axons and myelin are affected, but there is also extensive loss of OLGs. Research has shown that not only SVZ neural precursors can give rise to OLGs, but also that this same process is upregulated under pathological conditions. Hence, the aim of this work was to characterize the most commonly used animal model of MS, the EAE model, as well as the process of adult oligodendrogenesis which occurs in these animals.

The EAE animal model is the most widely used model for *in vivo* MS research. Original studies go back to early XX century, with experiments evolving from rabbits to guinea pigs, rats and mice, amongst others. EAE is mediated by complex interactions between different immune cells, ultimately resulting in an extreme inflammatory response responsible for the pathological characteristics portrayed by the mice. According to published protocols for this model, clinical signs of the disease commonly appear between days 9 and 14 p.i.<sup>28,167,185,189</sup>. Moreover, Miller and colleagues, when studying different EAE induction protocols, observed that EAE onset could be faster on animals who received PTX through i.v. (1 to 2 days) than on mice that received an i.p. injection<sup>28</sup>. In our studies, EAE IV animals had the first symptoms between days 13 and 19 p.i., EAE IP animals took between 12 and 19 days to reach the minimum clinical score, EAE VAF animals started displaying clinical score of 1 between days 17 and 33 p.i, and finally SPF animals started displaying the EAE phenotype between days 13 and 19 p.i.. For all experimental groups tested, EAE phenotype was displayed heterogeneously amongst the members of the groups, and for some mice, later than what is described. Nevertheless, onset of EAE is affected by several factors such as housing, diet and age<sup>190</sup>. The decreased success rate when inducing EAE IV or IP groups might have several explanations. As stated previously, a possible (and most likely) loss of function of one of the compounds used might have rendered them ineffective. Moreover, the preparation of the MOG emulsion at the adequate consistency is critical requiring an experienced experimenter to understand the optimal emulsion state. Furthermore, the subcutaneous injections of MOG emulsion also require practice. Additionally, stress, such as acclimatization timing, handling or noise is also described as an influential factor for EAE induction, whether by decreasing EAE severity or by hampering EAE development<sup>190</sup>. Thus, we hypothesized that the intense protocol of BrdU injections administered the day after model induction could influence the course of

disease. However, in one batch we tested this by only giving BrdU injections to some of the animals, and contrary to what was expected, some BrdU-injected animals got sick, while some non-injected BrdU animals did not get sick. Moreover, differences between VAF and SPF animals, encompass not only EAE onset, but also its progression. EAE SPF animals show a different profile when comparing with the EAE VAF animals and it can be related to the distinct pathogens present in their environment in the rodent facility. SPF animals are housed in a specific-pathogen free facility, whereas VAF animals are housed in a virus-antibody free facility, which has a 'dirtier' environment than the first. Lee *et al.* concluded that animals housed in axenic (germ-free) conditions were resistant to EAE, whereas animals housed in SPF facilities, which have a lower health status, still developed the phenotype<sup>186</sup>. Concordantly, Arndt and colleagues studied the difference in EAE severity on animals housed in SPF and conventional housings. Mice were induced with EAE using the fusion protein MP4/Apogen emulsified in CFA, together with two doses of PTx. Results show that animals conventionally housed portray less severe phenotypes than those housed in SPF facilities<sup>191</sup>.

Regarding behavioural characterization, the absence of significant results for EAE IP animals on the OF and PT is related with the days the tests were performed, and with the different motor skills evaluated in the three different tests. Since both groups (IV and IP) did not develop EAE in the same timeframe, only EAE IV animals were significantly impaired on the days the tests were performed, and thus the results corroborated the impairment. EAE IV animals showed significant impairments in locomotor activity, coordination and balance when at the highest EAE scores. Still, the phenotype at maximum EAE onset was similar for EAE IV and IP, hinting that EAE IP animals would also present significant differences if the tests had been performed at a different timepoint. Accordingly, Sands and colleagues observed a negative correlation between the clinical scores and the latency to fall from the rotarod during the active phase of the disease, but that was not observed during the preclinical or early EAE stages<sup>192</sup>.

Despite being solely representative, our luxol fast blue histopathological analysis showed no apparent differences between control and EAE mice for brain and spinal cord samples. Again, this evaluation was done at the end of the protocol, with a clinical score of 1. Most probably, assessing the degree of demyelination at the disease peak may have revealed a different outcome, likely in accordance to what is commonly described in the literature for this model<sup>21,24,42</sup>. In fact, EAE model relies in myelin loss and consequent axonal dysfunction<sup>24</sup>. Contrary to our data, several groups have stated in their studies a significant increase in demyelination for EAE animals. For instance, Wang and colleagues observed in their EAE group, spinal cord demyelination at peak of disease onset (day 15), when compared to controls<sup>193</sup>.

Since MBP and PLP are the most abundant proteins that constitute compacted myelin, they are highly susceptible targets of degradation in the inflammatory environment of EAE and might act as neuroantigens for disease development<sup>79,194</sup>. Our results, however, denoted no alterations for MBP and PLP evaluated by immunofluorescence or western blot. Once again, the sample size is not sufficient for definitive conclusions. Nevertheless, these results go accordingly with the hypothesis that endogenous remyelination occurs after EAE induction re-establishing neuronal and oligodendroglial functions, since our samples are from 31 days p.i. EAE mice with a clinical score of 1-2. On the contrary, Mangiardi and colleagues clearly show in the corpus callosum, as in the spinal cord, a significant decrease in MBP intensity in early and late EAE. However, late EAE animals still have a score of around 3<sup>195</sup>, further elucidating that clinical scores are in accordance with myelination. Moreover, Garay and colleagues demonstrated significant decreases in mRNA levels for MBP and PLP in the spinal cord of EAE mice induced with MOG<sub>40-54</sub> or MOG<sub>40-45</sub>. Interestingly, administration of progesterone before EAE induction attenuated these results, combined with a decrease in EAE severity<sup>196,197</sup>. Concomitantly, Yao and co-workers observed, using a rat model of EAE, a decrease in both MBP and PLP levels upon EAE induction, recovered if IGF-1 was administered<sup>198</sup>.

The cellular mechanisms behind EAE have been extensively studied. IL-1 $\beta$  is one of the inflammatory cytokines released by T cells upon EAE induction. Reale and colleagues observed an increase in the levels of this mediator in both serum and CSF of patients with relapsing-remitting MS<sup>199</sup>. Furthermore, the relevance of IL-1 $\beta$  for EAE onset was studied by Matsuki and co-workers, who demonstrated that the presence of IL-1 $\alpha$  or IL-1 $\beta$  alone is sufficient to initiate EAE development<sup>200</sup>. Moreover, Murphy and colleagues showed that concentration of IL-1 $\beta$  was significantly increased starting 7 days p.i., reaching a maximum value on day 10 p.i. and remaining higher than the control until the end of the experiments, 21 days after induction<sup>201</sup>. Concomitantly, our results show a tendency for increased concentration of IL-1 $\beta$  in brain cortex homogenates in EAE SPF animals. Importantly, a higher sample size would be necessary for further conclusions. Also, at time of sample collection, four weeks after model induction, animals already showed decreased clinical scores, which possibly means that at the time of the sacrifice, inflammation and consequently the levels of cytokines present in the brain, were more reduced, and the endogenous remyelination process had already occurred.

TNF $\alpha$  also has a role in MS and EAE pathology. Rieckmann and colleagues described a relationship between the transcription of mRNA for this cytokine and MS relapse, by assessing mRNA levels of blood mononuclear cells in patients with relapsing-remitting MS<sup>202</sup>. Besides, Baker and co-workers also observed that TNF $\alpha$  is present both in brain and spinal cord of MBP-induced relapsing-remitting EAE mice. Moreover, authors have shown that binding of

TNF $\alpha$  with its receptor, whether by addition of soluble receptor constructs or by blocking this cytokine with monoclonal antibodies could prevent or even treat EAE<sup>203</sup>. Furthermore, Valentin-Torres and colleagues studied how TNF regulated disability in EAE, through immunization with MOG of GFAP $\gamma$ R1 $\Delta$  transgenic mice (astrocytes of these animals are unable to respond to IFN $\gamma$ ) and treated with anti-TNF antibody. They observed an increase in the levels of TNF in EAE GFAP $\gamma$ R1 $\Delta$  mice, while TNF neutralization led to a rescue of BBB integrity, as well as an improvement in inflammatory responses of the CNS<sup>204</sup>. Our results demonstrated a significant increase in TNF $\alpha$  concentration for EAE SPF animals which, when compared to VAF animals, can be explained by the differences in housing environment. If a 'cleaner' environment is associated with an increase in EAE severity, it can also be related with increased levels of pro-inflammatory cytokines such as TNF $\alpha$ .

NF- $\kappa$ B signalling pathway is behind multiple responses, such as immune, cell survival and infectious<sup>205</sup>. Hilliard and co-workers have shown that NF- $\kappa$ B<sup>-/-</sup> mice are resistant to MOG-induced EAE<sup>206</sup>. Furthermore, Chen and colleagues observed in B cells from RRMS and SPMS patients stimulated with CD40, a member of the TNFR superfamily, that they exhibited increased levels of pNF- $\kappa$ B, when compared to healthy donor controls<sup>207</sup>. Jia and colleagues studied the effect of Plumbagin, an herbal compound known for its immunosuppressive properties on EAE. Results showed an amelioration of EAE, accomplished through the regulation of Jak-STAT and NF- $\kappa$ B signalling pathways, where an inhibition of I $\kappa$ B degradation and NF- $\kappa$ B phosphorylation was observed<sup>208</sup>. pNF- $\kappa$ B and pI $\kappa$ B levels did not appear to be significantly altered in our studies. Albeit the reduced number of samples assessed, the putative reason for our discordant results might be explained by the late sample collection timepoint.

Thus, the apparent disparity observed in our results should not be attributed to incoherent data, but instead to the ill-timed assessment of pro – inflammatory cytokines and myelination. Most likely, the 'golden window' to study these parameters was missed.

The ability of SVZ neural stem cells to remain in the brain into adulthood highlights their likely role in healthy and diseased brain throughout life. A plethora of studies has shown the role of these precursors in demyelinating conditions, where these cells were capable of differentiating and migrating to affected regions contributing to remyelination<sup>16,69</sup>. To assess the behaviour of these cells in our EAE animals, cell survival and differentiation of these precursors was evaluated by immunohistochemistry. Our results regarding the volume of SVZ, CC, CT and ST denoted no significant differences between control and EAE animals, however, an apparent tendency for a decrease in CT volume was observed in EAE mice. Concomitantly, a progressive atrophy of the cerebral cortex during EAE was observed by MacKenzie-Graham's group<sup>209</sup>. With respect to cell survival, our data show no significant distinctions between EAE and control animals, for all regions evaluated. However, once again a tendency



for increased survival appears to be present in the SVZ, CC and CT of EAE animals. Importantly, our results portray a significant increase in NG2<sup>+</sup>BrdU<sup>+</sup> cells in the CC, a brain region prone to EAE lesions, meaning that differentiation of BrdU<sup>+</sup> cells from the SVZ into OPCs, had occurred with migration of cells to the CC. Data for CT and ST showed no significant differences between CTRL and EAE groups, while for the SVZ, a big variability was observed in the controls, unabling a conclusion regarding NG2<sup>+</sup>BrdU<sup>+</sup> cells in SVZ. Therefore, further samples have to be analysed, in an attempt at understanding if there is indeed a decrease in NG2<sup>+</sup>BrdU<sup>+</sup> cells in the SVZ, or if there are no alterations in NG2<sup>+</sup>BrdU<sup>+</sup> cells in this region. Since the NSCs present in the SVZ are mainly responsible for generating neuroblasts and immature neurons, an immunohistochemistry for DCX was performed. Our preliminary data, of an apparent decrease in DCX staining in EAE brain slice, seem to be in accordance to what has been described in literature, that these precursors tend to generate oligodendrocytes instead of neuronal cells in the EAE model<sup>16,69</sup>. Interestingly, Soundarapandian and colleagues showed that the oligodendrocyte-specific zinc finger transcription repressor Zfp488 would promote the differentiation of SVZ NSCs into OLGs, when overexpressed in the cuprizone animal model<sup>210</sup>. Moreover, *in vitro* assays using anti-sera from EAE mice and neural precursor cells performed by Kesidou and co-workers demonstrated that EAE anti-sera triggers the apoptotic pathway of the neural precursors, rendering them unable to perform remyelination due to the immune response associated with EAE<sup>211</sup>.

Together, these results highlight the urgency of finding a mechanism to potentiate the proliferation, differentiation and survival of OPCs derived from SVZ NSCs in MS.



## **CHAPTER 5 – CONCLUSIONS AND FUTURE PERSPECTIVES**





This work aimed at characterizing the EAE mouse model as well as adult oligodendrogenesis in this model. Clinical scores and behavioural characterization of the EAE model, suggested that motor impairment is proportional to the score of the disease. Notwithstanding, only tests evaluating motor function were performed, and it would be interesting to study, in the future cognitive performance in this animal model, since cognitive deficits have been described<sup>212</sup>. Also, it is fundamental to optimize model induction as soon as possible, not only regarding the expertise of the experimenter or the drugs used, but also the animal housing. Behavioural test dates must be predefined based on the clinical scores, to allow for comparison between batches studied.

Cellular and molecular data showed an increase in the levels of the pro-inflammatory cytokine TNF $\alpha$ , together with a tendency for increased IL-1 $\beta$ . Furthermore, a tendency for increased cell survival in the SVZ, CC and CT was observed, accompanied by a significant increase in NG2<sup>+</sup>BrdU<sup>+</sup> cells in the CC. Using flow cytometry for the characterization of immune cells in the CNS in EAE mice would also be an adequate approach, since it would allow for the measure of different immune cells types and also of cytokines produced by them. Myelin protein parameters did not denote any alteration and the likely reason for this was the late date for animal sacrifice, that allowed endogenous remyelination. One of the goals of this work was to fully characterize the clinical progression of the model through registering the clinical scores along the experimental protocol. Notwithstanding, for successful characterization of the inflammatory and myelin cellular components, animals need to be sacrificed at the peak of EAE onset, for an adequate characterization of the changes created by the EAE model. Also, increasing the sample size not only for the tests regarding inflammation and myelination but also for the oligodendrogenesis studies would be of an added value. This would allow to observe the relationship between the changes in oligodendrocyte cell populations and the remyelination process. In fact, it would be important to ascertain whether the tendencies we observed in this work are indeed confirmed or, contrarily to what has been previously described, rendered insignificant. Furthermore, cell proliferation should be assessed using different proliferation markers, such as Ki67, or alternatively a specific protocol of BrdU administration in the last day of the experiments.

Altogether, this work allowed the characterization of the oligodendrogenesis process and of the EAE model throughout time, together with its behaviour traits and some of the cellular components. Performing the optimizations here described will allow further conclusions, thus granting future studies in our group using this model and the modulation of adult oligodendrogenesis as a candidate for MS.

In Fig. 26 are depicted the main conclusions of this work.

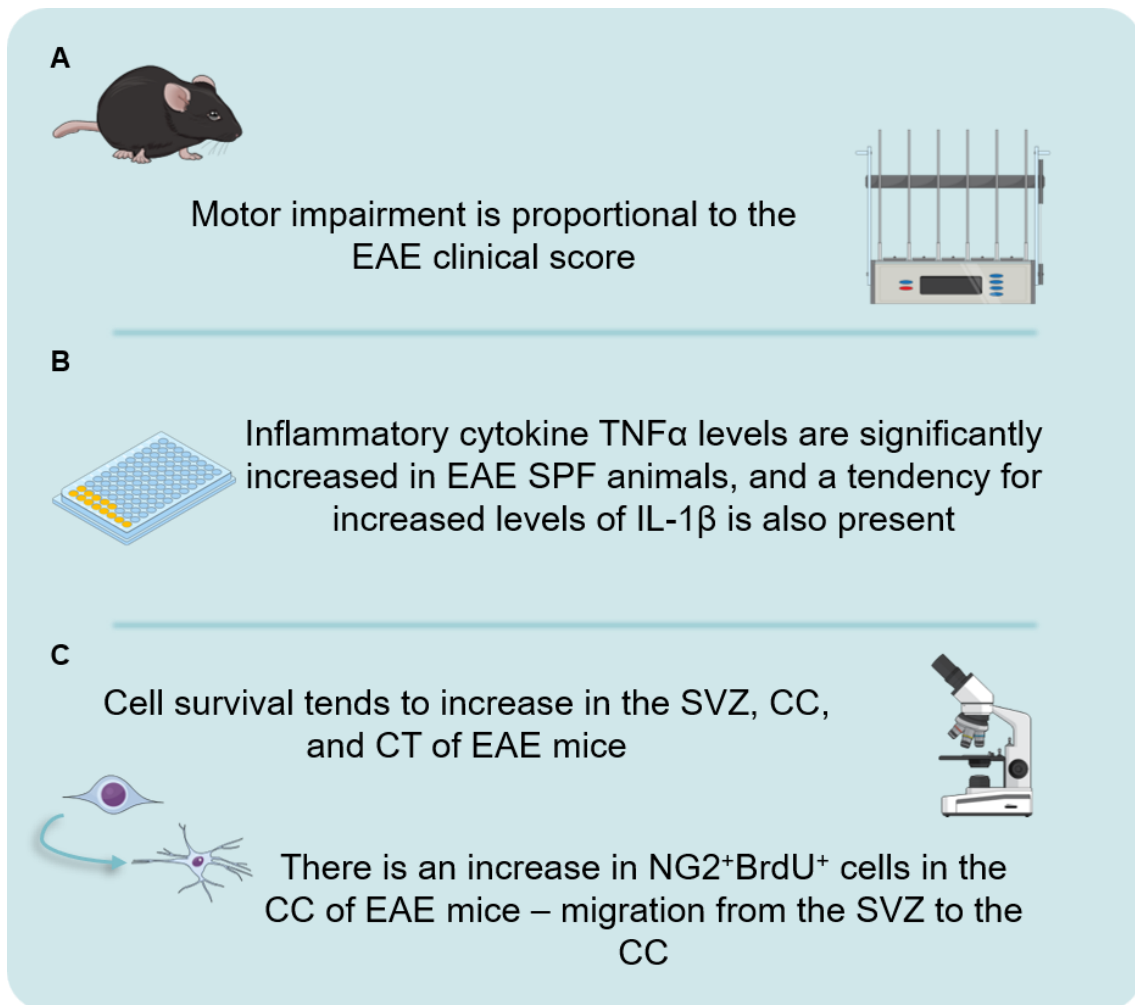


**Fig. 26 - Schematic summary of the main findings of this work.** (A) Motor impairment evaluated through the OF, RR and PT is proportional to the EAE clinical score of the animal. (B) Pro-inflammatory cytokine levels were assessed by ELISA: TNF $\alpha$  showed a significant increase in EAE SPF animals. Concomitantly, IL-1 $\beta$  levels tend to increase for EAE SPF mice. (C) When evaluating adult oligodendrogenesis in EAE mice, cell survival tended to increase in the SVZ, CC and CT of EAE mice. Moreover, an increase in NG2<sup>+</sup>BrdU<sup>+</sup> cells in the CC was also observed, which translates in cell migration from the SVZ to the CC.

## **CHAPTER 6 – BIBLIOGRAPHY**







1. Nait-Oumesmar, B. *et al.* Activation of the subventricular zone in multiple sclerosis: evidence for early glial progenitors. *Proc. Natl. Acad. Sci.* **104**, 4694–4699 (2007).
2. Compston, A. & Coles, A. Multiple sclerosis. *Lancet* **372**, 1502–1517 (2008).
3. Atlas of MS 2013 - Multiple Sclerosis International Federation. Available at: <https://www.msif.org/about-us/who-we-are-and-what-we-do/advocacy/atlas/>. (Accessed: 9th June 2018)
4. Ransohoff, R. M., Hafler, D. A. & Lucchinetti, C. F. Multiple sclerosis—a quiet revolution. *Nat. Publ. Gr.* **11**, 134–142 (2015).
5. Trapp, B. D. & Nave, K.-A. Multiple Sclerosis: An Immune or Neurodegenerative Disorder? *Annu. Rev. Neurosci.* **31**, 247–269 (2008).
6. Ascherio, A. & Munger, K. L. Environmental risk factors for multiple sclerosis. Part II: Noninfectious factors. *Ann. Neurol.* **61**, 504–513 (2007).
7. Ascherio, A. & Munger, K. L. Environmental risk factors for multiple sclerosis. Part I: The role of infection. *Ann. Neurol.* **61**, 288–299 (2007).
8. Procaccini, C. *et al.* Animal models of Multiple Sclerosis. *Eur. J. Pharmacol.* **759**, 182–191 (2015).
9. Simon, K. C., Munger, K. L. & Rioux, J. D. Integrating risk factors HLA-DRB1 \* 1501 and Epstein – Barr virus in multiple sclerosis. *Neurology* **70**, 1113–1118 (2008).
10. Stys, P. K. *et al.* Will the real multiple sclerosis please stand up? *Nat Rev Neurosci* **13**, 507–514 (2012).
11. Pérez-Cerdá, F., Sánchez-Gómez, M. V. & Matute, C. The link of inflammation and neurodegeneration in progressive multiple sclerosis. *Mult. Scler. Demyelinating Disord.* **1**, 1–8 (2016).
12. Lassmann, H. What drives disease in multiple sclerosis: Inflammation or neurodegeneration? *Clin. Exp. Neuroimmunol.* **1**, 2–11 (2010).
13. Hohlfeld, R. Biotechnological agents for the immunotherapy of multiple sclerosis Principles , problems and perspectives. *Brain* **120**, 865–916 (1997).
14. Lassmann, H. Hypoxia-like tissue injury as a component of multiple sclerosis lesions. *J. Neurol. Sci.* **206**, 187–191 (2003).
15. Levine, J. M. & Reynolds, R. Activation and Proliferation of Endogenous Oligodendrocyte Precursor Cells during Ethidium Bromide-Induced Demyelination. *Exp.*

- Neurol.* **160**, 333–347 (1999).
16. Picard-Riera, N. *et al.* Experimental autoimmune encephalomyelitis mobilizes neural progenitors from the subventricular zone to undergo oligodendrogenesis in adult mice. *Proc. Natl. Acad. Sci. U. S. A.* **99**, 13211–6 (2002).
  17. Nait-Oumesmar, B. *et al.* The role of SVZ-derived neural precursors in demyelinating diseases: From animal models to multiple sclerosis. *J. Neurol. Sci.* **265**, 26–31 (2008).
  18. Vogel, D. Y., Kipp, M. & Baker, D. In Vitro and In Vivo Models of Multiple Sclerosis. *CNS Neurol. Disord. - Drug Targets* **11**, 570–588 (2012).
  19. Abbott, N. J. *et al.* Neurobiology of Disease Structure and function of the blood – brain barrier. *Neurobiol. Dis.* **37**, 13–25 (2010).
  20. Correale, J. The blood – brain-barrier in multiple sclerosis: Functional roles and therapeutic targeting. *Autoimmunity* **40**, 148–160 (2007).
  21. Lassmann, H. & Bradl, M. Multiple sclerosis: experimental models and reality. *Acta Neuropathol.* **133**, 223–244 (2017).
  22. Pachner, A. R. Experimental models of multiple sclerosis. *Curr. Opin. Neurol.* **24**, 291–299 (2011).
  23. Kabat, E., Wolf, A. & Bezer, E. The rapid production of acute disseminated encephalomyelitis in Rhesus monkey by injection of heterologous and homologous brain tissue with adjuvants. *J. Exp. Med.* **85**, 117–130 (1946).
  24. Glatigny, S. & Bettelli, E. Experimental Autoimmune Encephalomyelitis (EAE) as Animal Models of Multiple Sclerosis (MS). *Cold Spring Harb. Perspect. Med.* 1–19 (2018).
  25. Bittner, S. *et al.* Myelin Oligodendrocyte Glycoprotein (MOG35-55) Induced Experimental Autoimmune Encephalomyelitis (EAE) in C57BL/6 Mice. *J. Vis. Exp.* **86**, 1–5 (2014).
  26. Stromnes, I. M. & Goverman, J. M. Passive induction of experimental allergic encephalomyelitis. *Nat. Protoc.* **1**, 1952–1960 (2006).
  27. Terry, R. L., Ifergan, I. & Miller, S. D. Experimental Autoimmune Encephalomyelitis in Mice. in *Multiple Sclerosis. Methods in Molecular Biology.* (ed. Robert Weissert) (Humana Press, New York, NY, 2014).
  28. Miller, S. D., Karpus, W. J. & Davidson, T. S. Experimental Autoimmune Encephalomyelitis in the Mouse. in *Current Protocols in Immunology* 15.1.1-15.1.20

(John Wiley & Sons, Inc., 2007).

29. Stromnes, I. M. & Goverman, J. M. Active induction of experimental allergic encephalomyelitis. *Nat. Protoc.* **1**, 1810–1819 (2006).
30. Tsunoda, I. *et al.* Antibody association with a novel model for primary progressive multiple sclerosis: induction of relapsing-remitting and progressive forms of EAE in H2s mouse strains. *Brain Pathol.* **10**, 402–418 (2000).
31. Lennon, V. A. *et al.* A serum autoantibody marker of neuromyelitis optica: distinction from multiple sclerosis. *Lancet* **364**, 2106–2112 (2004).
32. Poser, C. M. Pathogenesis of Multiple Sclerosis - a critical reappraisal. *Acta Neuropathol.* **71**, 1–10 (1986).
33. McGavern, D. B. *et al.* Axonal loss results in spinal cord atrophy, electrophysiological abnormalities and neurological deficits following demyelination in a chronic inflammatory model of multiple sclerosis. *Brain* **123**, 519–531 (2000).
34. Denic, A. *et al.* The relevance of animal models in multiple sclerosis research. *Pathophysiology* **18**, 21–29 (2011).
35. Praet, J., Guglielmetti, C. & Berneman, Z. Neuroscience and Biobehavioral Reviews Cellular and molecular neuropathology of the cuprizone mouse model: Clinical relevance for multiple sclerosis. *Neurosci. Biobehav. Rev.* **47**, 485–505 (2014).
36. Matsushima, G. K. *et al.* The relevance of animal models in multiple sclerosis research. *Brain Pathol.* **11**, 107–116 (2001).
37. Matsushima, G. K. & Morell, P. The neurotoxicant, cuprizone, as a model to study demyelination and remyelination in the central nervous system. *Brain Pathol.* **11**, 107–116 (2001).
38. Franklin, R. J. M., Zhao, C. A. C. & Sim, F. J. Ageing and CNS remyelination. *Neuroreport* **13**, 923–928 (2002).
39. Dendrou, C. A., Fugger, L. & Friese, M. A. Immunopathology of multiple sclerosis. *Nat. Rev. Immunol.* **15**, 545–558 (2015).
40. Ransohoff, R. M. & Engelhardt, B. The anatomical and cellular basis of immune surveillance in the central nervous system. *Nat. Rev. Immunol.* **12**, 623–635 (2012).
41. Liu, T. *et al.* NF- $\kappa$ B signaling in inflammation. *Signal Transduct. Target. Ther.* **2**, 1–9 (2017).

42. 't Hart, B. A., Gran, B. & Weissert, R. EAE: Imperfect but useful models of multiple sclerosis. *Trends Mol. Med.* **17**, 119–125 (2011).
43. Abbas, A. K., Lichtmann, A. H. & Pillai, S. *Cellular and Molecular Immunology*. (Saunders, 2015).
44. Codarri, L., Fontana, A. & Becher, B. Cytokine networks in multiple sclerosis: Lost in translation. *Curr. Opin. Neurol.* **23**, 205–211 (2010).
45. Locksley, R. M., Killeen, N. & Lenardo, M. J. The TNF and TNF receptor superfamilies: Integrating mammalian biology. *Cell* **104**, 487–501 (2001).
46. Murphy, C. A. *et al.* Interactions Between Hemopoietically Derived TNF and Central Nervous System-Resident Glial Chemokines Underlie Initiation of Autoimmune Inflammation in the Brain. *J. Immunol.* **169**, 7054–7062 (2002).
47. Maimone, D. *et al.* Cytokine levels in the cerebrospinal fluid and serum of patients with multiple sclerosis. *J. Neuroimmunol.* **32**, 67–74 (1991).
48. Kruglov, A. A. *et al.* Pathogenic and Protective Functions of TNF in Neuroinflammation Are Defined by Its Expression in T Lymphocytes and Myeloid Cells. *J. Immunol.* **187**, 5660–5670 (2011).
49. Arnett, H. A. *et al.* TNF $\alpha$  promotes proliferation of oligodendrocyte progenitors and remyelination. *Nat. Neurosci.* **4**, 1116–1122 (2001).
50. Lin, C.-C. & Edelson, B. T. New Insights into the Role of IL-1 $\beta$  in Experimental Autoimmune Encephalomyelitis and Multiple Sclerosis. *J. Immunol.* **198**, 4553–4560 (2017).
51. Lévesque, S. A. *et al.* Myeloid cell transmigration across the CNS vasculature triggers IL-1 $\beta$ -driven neuroinflammation during autoimmune encephalomyelitis in mice. *J. Exp. Med.* **213**, 929–949 (2016).
52. Mason, J. L. *et al.* Interleukin-1beta promotes repair of the CNS. *J. Neurosci.* **21**, 7046–7052 (2001).
53. Mc Guire, C. *et al.* Nuclear factor kappa B (NF- $\kappa$ B) in multiple sclerosis pathology. *Trends Mol. Med.* **19**, 604–613 (2013).
54. Kaltschmidt, B. & Kaltschmidt, C. NF- B in the Nervous System. *Cold Spring Harb. Perspect. Biol.* 1–13 (2009).
55. Oeckinghaus, A., Hayden, M. S. & Ghosh, S. Crosstalk in NF- $\kappa$ B signaling pathways.

- Nat. Immunol.* **12**, 695–708 (2011).
56. Gveric, D. *et al.* Transcription factor NF-kappaB and inhibitor I kappaBalpha are localized in macrophages in active multiple sclerosis lesions. *J. Neuropathol. Exp. Neurol.* **57**, 168–178 (1998).
  57. Bonetti, B. *et al.* Activation of NF-kappaB and c-jun transcription factors in multiple sclerosis lesions. Implications for oligodendrocyte pathology. *Am. J. Pathol.* **155**, 1433–8 (1999).
  58. Hussman, J. P. *et al.* GWAS analysis implicates NF-kB-mediated induction of inflammatory T cells in multiple sclerosis. *Genes Immun.* **17**, 305–312 (2016).
  59. Hilliard, B. A. *et al.* Critical roles of c-Rel in autoimmune inflammation and helper T cell differentiation. *J. Clin. Invest.* **110**, 843–850 (2002).
  60. Stone, S. *et al.* NF-kB Activation Protects Oligodendrocytes against Inflammation. *J. Neurosci.* **37**, 9332–9344 (2017).
  61. Aktas, O., Kieseier, B. & Hartung, H. Neuroprotection , regeneration and immunomodulation : broadening the therapeutic repertoire in multiple sclerosis. *Trends Neurosci.* **33**, 140–152 (2010).
  62. Jadasz, J. J. *et al.* Recent achievements in stem cell-mediated myelin repair. *Curr. Opin. Neurol.* **29**, 205–212 (2016).
  63. Franklin, R. J. M. & Goldman, S. A. Glia disease and repair—Remyelination. *Cold Spring Harb. Perspect. Biol.* **7**, 1–28 (2015).
  64. Pluchino, S. *et al.* Injection of adult neurospheres induces recovery in a chronic model of multiple sclerosis. *Nature* **422**, 688–694 (2003).
  65. Jensen, S. K. & Yong, V. W. Activity-Dependent and Experience-Driven Myelination Provide New Directions for the Management of Multiple Sclerosis. *Trends Neurosci.* **39**, 356–365 (2016).
  66. Keller, T. A. & Just, M. A. Altering Cortical Connectivity: Remediation-Induced Changes in the White Matter of Poor Readers. *Neuron* **64**, 624–631 (2009).
  67. Nave, K.-A. & Werner, H. B. Myelination of the Nervous System: Mechanisms and Functions. *Annu. Rev. Cell Dev. Biol.* **30**, 503–533 (2014).
  68. Bergles, D. E. & Richardson, W. D. Oligodendrocyte development and plasticity. *Cold Spring Harb. Perspect. Biol.* 1–28 (2015).

69. Menn, B. *et al.* Origin of oligodendrocytes in the subventricular zone of the adult brain. *J Neurosci* **26**, 7907–7918 (2006).
70. Waly, B. El *et al.* Oligodendrogenesis in the normal and pathological central nervous system. *Front. Neurosci.* **8**, 1–22 (2014).
71. Nishiyama, A., Chang, A. & Trapp, B. D. NG2+ glial cells: a novel glial cell population in the adult brain. *J. Neuropathol. Exp. Neurol.* **58**, 1113–1124 (1999).
72. Fancy, S. P. J., Zhao, C. & Franklin, R. J. M. Increased expression of Nkx2.2 and Olig2 identifies reactive oligodendrocyte progenitor cells responding to demyelination in the adult CNS. *Mol. Cell. Neurosci.* **27**, 247–254 (2004).
73. Wren, D., Wolswijk, G. & Noble, M. In vitro analysis of the origin and maintenance of O-2Aadult progenitor cells. *J Cell Biol* **116**, 167–176 (1992).
74. Barateiro, A. & Fernandes, A. Temporal oligodendrocyte lineage progression: In vitro models of proliferation, differentiation and myelination. *Biochim. Biophys. Acta - Mol. Cell Res.* **1843**, 1917–1929 (2014).
75. Nishiyama, A. *et al.* Co-Localization of NG2 Proteoglycan and PDGF  $\alpha$ -Receptor on O2A Progenitor Cells in the Developing Rat Brain. *J. Neurosci. Res.* **43**, 299–314 (1996).
76. Schachner, M. & Sommer, I. Monoclonal Antibodies ( 01 to 04 ) to Oligodendrocyte Cell Surfaces : An Immunocytological Study in the Central Nervous System. *Dev. Biol.* **83**, 311–327 (1981).
77. Yu, W. *et al.* Embryonic Expression of Myelin Genes : Evidence for a Focal Source of Oligodendrocyte Precursors in the Ventricular Zone of the Neuro Tube. *Neuron* **12**, 1353–1362 (1994).
78. Reynolds, R. & Wilkin, G. P. Development of macroglial cells in rat cerebellum. II. An in situ immunohistochemical study of oligodendroglial lineage from precursor to mature myelinating cell. *Development* **102**, 409–425 (1988).
79. Simons, M. & Nave, K.-A. Oligodendrocytes: Myelination and Axonal Support. *Cold Spring Harb. Perspect. Biol.* 1–16 (2015).
80. Pérez-Cerdá, F., Sánchez-Gómez, M. V. & Matute, C. Pío del Río Hortega and the discovery of the oligodendrocytes. *Front. Neuroanat.* **9**, 1–6 (2015).
81. Baumann, N. & Pham-Dinh, D. Biology of oligodendrocyte and myelin in the mammalian central nervous system. *Physiol. Rev.* **81**, 871–927 (2001).

82. Wyllie, D. J. A. *et al.* Activation of glutamate receptors and glutamate uptake in identified macroglial cells in rat cerebellar cultures. *J. Physiol.* **432**, 235–258 (1991).
83. Hughes, E. G. *et al.* Oligodendrocyte progenitors balance growth with self-repulsion to achieve homeostasis in the adult brain. *Nat. Neurosci.* **16**, 668–76 (2013).
84. Jabs, R. *et al.* Synaptic transmission onto hippocampal glial cells with hGFAP promoter activity. *J. Cell Sci.* **118**, 3791–3803 (2005).
85. De Biase, L. M., Nishiyama, A. & Bergles, D. E. Excitability and Synaptic Communication within the Oligodendrocyte Lineage. *J. Neurosci.* **30**, 3600–3611 (2010).
86. Gallo, V. *et al.* Oligodendrocyte Progenitor Cell Proliferation and Lineage Progression Are Regulated by Glutamate Receptor-Mediated K<sup>+</sup> Channel Block. *J. Neurosci.* **76**, 2659–2670 (1996).
87. Kessaris, N. *et al.* Competing waves of oligodendrocytes in the forebrain and postnatal elimination of an embryonic lineage. *Nat. Neurosci.* **9**, 173–179 (2006).
88. Wake, H., Lee, P. R. & Fields, R. D. Control of Local Protein Synthesis and Initial Events in Myelination by Action Potentials. *Science (80-. )*. **333**, 1647–1651 (2011).
89. Attwell, D. *et al.* Why do oligodendrocyte lineage cells express glutamate receptors? *F1000 Biol. Rep.* **2**, 4–7 (2010).
90. Almeida, R. G. *et al.* Individual axons regulate the myelinating potential of single oligodendrocytes in vivo. *Development* **138**, 4443–4450 (2011).
91. Spassky, N. *et al.* Directional Guidance of Oligodendroglial Migration by Class 3 Semaphorins and Netrin-1. *J. Neurosci.* **22**, 5992–6004 (2002).
92. De Castro, F. & Bribián, A. The molecular orchestra of the migration of oligodendrocyte precursors during development. *Brain Res. Rev.* **49**, 227–241 (2005).
93. Nimmerjahn, A., Kirchhoff, F. & Helmchen, F. Resting microglial cells are highly dynamic surveillants of brain parenchyma in vivo. *Neuroforum* **11**, 95–96 (2005).
94. Van Heyningen, P., Calver, A. R. & Richardson, W. D. Control of progenitor cell number by mitogen supply and demand. *Curr. Biol.* **11**, 232–241 (2001).
95. Durand, B. & Raff, M. A cell-intrinsic timer that operates during oligodendrocyte development. *BioEssays* **22**, 64–71 (2000).
96. Billon, N. *et al.* Roles for p53 and p73 during oligodendrocyte development.

- Development* **131**, 1211–20 (2004).
97. Domingues, H. S. *et al.* Oligodendrocyte, Astrocyte, and Microglia Crosstalk in Myelin Development, Damage, and Repair. *Front. Cell Dev. Biol.* **4**, 1–16 (2016).
  98. Chang, K.-J., Redmond, S. A. & Chan, J. R. Remodeling myelination: implications for mechanisms of neural plasticity. *Nat. Neurosci.* **19**, 190–197 (2016).
  99. Hartline, D. K. & Colman, D. R. Rapid Conduction and the Evolution of Giant Axons and Myelinated Fibers. *Curr. Biol.* **17**, 29–35 (2007).
  100. Eshed-eisenbach, Y. & Peles, E. The making of a node: a co-production of neurons and glia. *Curr. Opin. Neurobiol.* **23**, 1049–1056 (2013).
  101. Aggarwal, S., Yurlova, L. & Simons, M. Central nervous system myelin: Structure, synthesis and assembly. *Trends Cell Biol.* **21**, 585–593 (2011).
  102. Trapp, B. D. *et al.* Differentiation and death of premyelinating oligodendrocytes in developing rodent brain. *J. Cell Biol.* **137**, 459–468 (1997).
  103. Zhao, X. *et al.* MicroRNA-Mediated Control of Oligodendrocyte Differentiation. *Neuron* **65**, 612–626 (2010).
  104. Gibson, E. M. *et al.* Neuronal Activity Promotes Oligodendrogenesis and Adaptive Myelination in the Mammalian Brain. *Science (80-. ).* **344**, 1252304 1-12 (2014).
  105. Dugas, J. C. *et al.* Dicer1 and miR-219 Are Required for Normal Oligodendrocyte Differentiation and Myelination. *Neuron* **65**, 597–611 (2010).
  106. Rosenberg, S. S. *et al.* The geometric and spatial constraints of the microenvironment induce oligodendrocyte differentiation. *Proc. Natl. Acad. Sci.* **105**, 14662–14667 (2008).
  107. Lee, S. *et al.* A culture system to study oligodendrocyte myelination processes using engineered nanofibers. *Nat. Methods* **9**, 917–922 (2012).
  108. Snaidero, N. *et al.* Myelin membrane wrapping of CNS axons by PI(3,4,5)P3-dependent polarized growth at the inner tongue. *Cell* **156**, 277–290 (2014).
  109. Yin, X. *et al.* CNP overexpression induces aberrant oligodendrocyte membranes and inhibits MBP accumulation and myelin compaction. *J. Neurosci. Res.* **50**, 238–247 (1997).
  110. Franklin, R. J. M. & ffrench-Constant, C. Remyelination in the CNS: from biology to therapy. *Nat. Rev. Neurosci.* **9**, 839–855 (2008).



111. Gallo, V. & Armstrong, R. C. Myelin repair strategies: a cellular view. *Curr. Opin. Neurol.* **21**, 278–283 (2008).
112. Liebetanz, D. & Merkler, D. Effects of commissural de- and remyelination on motor skill behaviour in the cuprizone mouse model of multiple sclerosis. *Exp. Neurol.* **202**, 217–224 (2006).
113. Blakemore, W. F. Pattern of remyelination in the CNS. *Nature* **249**, 577–578 (1974).
114. Stidworthy, M. F. *et al.* Quantifying the early stages of remyelination following cuprizone-induced demyelination. *Brain Pathol.* **13**, 329–339 (2003).
115. Rhodes, K. E., Raivich, G. & Fawcett, J. W. The injury response of oligodendrocyte precursor cells is induced by platelets, macrophages and inflammation-associated cytokines. *Neuroscience* **140**, 87–100 (2006).
116. Sim, F. J. *et al.* The age-related decrease in CNS remyelination efficiency is attributable to an impairment of both oligodendrocyte progenitor recruitment and differentiation. *J. Neurosci.* **22**, 2451–9 (2002).
117. Larsen, P. H. *et al.* Matrix metalloproteinase-9 facilitates remyelination in part by processing the inhibitory NG2 proteoglycan. *J. Neurosci.* **23**, 11127–35 (2003).
118. Fancy, S. P. J. *et al.* Myelin Regeneration : A Recapitulation of Development ? *Annu. Rev. Neurosci.* **34**, 21–43 (2011).
119. Woodruff, R. H. *et al.* Platelet-derived growth factor regulates oligodendrocyte progenitor numbers in adult CNS and their response following CNS demyelination. *Mol. Cell. Neurosci.* **25**, 252–262 (2004).
120. Mason, J. L. *et al.* Insulin-Like Growth Factor-1 Inhibits Mature Oligodendrocyte Apoptosis during Primary Demyelination. *J. Neurosci.* **20**, 5703–5708 (2000).
121. Mason, J. L. *et al.* Insulin-Like Growth Factor ( IGF ) Signaling through Type 1 IGF Receptor Plays an Important Role in Remyelination. *J. Neurosci.* **23**, 7710–7718 (2003).
122. Armstrong, R. C. *et al.* Absence of Fibroblast Growth Factor 2 Promotes Oligodendroglial Repopulation of Demyelinated White Matter. *J. Neurosci.* **22**, 8574–8585 (2002).
123. Seifert, T. *et al.* Notch1 and its ligand Jagged1 are present in remyelination in a T-cell- and antibody-mediated model of inflammatory demyelination. *Acta Neuropathol.* **113**, 195–203 (2007).

124. Fancy, S. P. J. *et al.* Dysregulation of the Wnt pathway inhibits timely myelination and remyelination in the mammalian CNS. *Genes Dev.* **23**, 1571–1585 (2009).
125. Xin, M. *et al.* Myelinogenesis and Axonal Recognition by Oligodendrocytes in Brain Are Uncoupled in Olig1 -Null Mice. *J. Neurosci.* **25**, 1354–1365 (2005).
126. Edwards, J. P. *et al.* Biochemical and functional characterization of three activated macrophage populations. *J. Leukoc. Biol.* **80**, 1298–1307 (2006).
127. Kotter, M. R. *et al.* Myelin Impairs CNS Remyelination by Inhibiting Oligodendrocyte Precursor Cell Differentiation. *J. Neurosci.* **26**, 328–332 (2006).
128. Miron, V. E. *et al.* M2 microglia and macrophages drive oligodendrocyte differentiation during CNS remyelination. *Nat. Neurosci.* **16**, 1211–1218 (2013).
129. Franklin, R. J. M. Why does remyelination fail in multiple sclerosis? *Nat. Rev. Neurosci.* **3**, 705–714 (2002).
130. Kazanis, I., Lathia, J. & Moss, L. The neural stem cell microenvironment. in *StemBook* (The Stem cell Research Community, 2008).
131. Lee, V. M. *et al.* Mini-review - Neural Stem cells. *Mini-Review from Stem Cell Technol.* (2015).
132. Martínez-Cerdeño, V., Noctor, S. C. & Kriegstein, A. R. The role of intermediate progenitor cells in the evolutionary expansion of the cerebral cortex. *Cereb. Cortex* **16**, (2006).
133. Götz, M. & Huttner, W. B. The cell biology of neurogenesis. *Nat Rev Mol Cell Biol* **6**, 777–788 (2005).
134. Kriegstein, A. & Alvarez-buylla, A. The Glial Nature of Embryonic and Adult Neural Stem Cells. *Annu. Rev. Neurosci.* **32**, 149–184 (2009).
135. Shimogori, T. *et al.* Embryonic signaling centers expressing BMP, WNT and FGF proteins interact to pattern the cerebral cortex. *Development* **131**, 5639–5647 (2004).
136. Alvarez-Buylla, a, García-Verdugo, J. M. & Tramontin, a D. A unified hypothesis on the lineage of neural stem cells. *Nat. Rev. Neurosci.* **2**, 287–93 (2001).
137. Morshead, C. M. & van der Kooy, D. Postmitotic death is the fate of constitutively proliferating cells in the subependymal layer of the adult mouse brain. *J Neurosci* **12**, 249–256 (1992).
138. Weiss, S. *et al.* Multipotent CNS stem cells are present in the adult mammalian spinal

- cord and ventricular neuroaxis. *J. Neurosci.* **16**, 7599–609 (1996).
139. McKay, R. Stem cells in the central nervous system. *Science* (80-. ). **276**, 66–71 (1997).
  140. Doetsch, F. *et al.* Subventricular zone astrocytes are neural stem cells in the adult mammalian brain. *Cell* **97**, 703–716 (1999).
  141. Rauch, U. Modeling an extracellular environment for axonal pathfinding and fasciculation in the central nervous system. *Cell Tissue Res.* **290**, 349–356 (1997).
  142. Ma, D. K. *et al.* Adult neural stem cells in the mammalian central nervous system. *Cell Res.* **19**, 672–82 (2009).
  143. Ortega, F. *et al.* Oligodendroglial and neurogenic adult subependymal zone neural stem cells constitute distinct lineages and exhibit differential responsiveness to Wnt signalling. *Nat. Cell Biol.* **15**, 602–613 (2013).
  144. Maki, T. *et al.* Mechanisms of oligodendrocyte regeneration from ventricular-subventricular zone-derived progenitor cells in white matter diseases. *Front. Cell. Neurosci.* **7**, 275 (2013).
  145. Lu, Q. R. *et al.* Common developmental requirement for Olig function indicates a motor neuron/oligodendrocyte connection. *Cell* **109**, 75–86 (2002).
  146. Maire, C. L. *et al.* Gain-of-function of olig transcription factors enhances oligodendrogenesis and myelination. *Stem Cells* **28**, 1611–1622 (2010).
  147. Niu, J. *et al.* Phosphorylated Olig1 localizes to the cytosol of oligodendrocytes and promotes membrane expansion and maturation. *Glia* **60**, 1427–1436 (2012).
  148. Sugimori, M. *et al.* Ascl1 is required for oligodendrocyte development in the spinal cord. *Development* **135**, 1271–1281 (2008).
  149. Nakatani, H. *et al.* Ascl1/Mash1 Promotes Brain Oligodendrogenesis during Myelination and Remyelination. *J. Neurosci.* **33**, 9752–9768 (2013).
  150. Scafidi, J. *et al.* Intranasal epidermal growth factor treatment rescues neonatal brain injury. *Nature* **506**, 230–234 (2013).
  151. Liu, J. & Casaccia, P. Epigenetic regulation of oligodendrocyte identity. *Trends Neurosci.* **33**, 193–201 (2010).
  152. Liu, A. *et al.* The Glial or Neuronal Fate Choice of Oligodendrocyte Progenitors Is Modulated by Their Ability to Acquire an Epigenetic Memory. *J. Neurosci.* **27**, 7339–7343 (2007).

153. Wu, M. *et al.* Differential Modulation of the Oligodendrocyte Transcriptome by Sonic Hedgehog and Bone Morphogenetic Protein 4 via Opposing Effects on Histone Acetylation. *J. Neurosci.* **32**, 6651–6664 (2012).
154. Falcão, A. M. *et al.* The path from the choroid plexus to the subventricular zone: go with the flow! *Front. Cell. Neurosci.* **6**, 1–8 (2012).
155. Wagner, J. P., Black, I. B. & DiCicco-Bloom, E. Stimulation of neonatal and adult brain neurogenesis by subcutaneous injection of basic fibroblast growth factor. *J. Neurosci.* **19**, 6006–16 (1999).
156. Gonzalez-Perez, O. *et al.* Epidermal growth factor induces the progeny of subventricular zone type B cells to migrate and differentiate into oligodendrocytes. *Stem Cells* **27**, 2032–2043 (2009).
157. Simons, M. & Nave, K. Oligodendrocytes : Myelination and Axonal Support. *Cold Spring Harb. Perspect. Biol.* 1–16 (2015).
158. Simons, M. & Trajkovic, K. Neuron-glia communication in the control of oligodendrocyte function and myelin biogenesis. *J. Cell Sci.* **119**, 4381–4389 (2006).
159. Lourenço, T. *et al.* Modulation of oligodendrocyte differentiation and maturation by combined biochemical and mechanical cues. *Sci. Rep.* **6**, 21563 (2016).
160. Relucio, J. *et al.* Laminin regulates postnatal oligodendrocyte production by promoting oligodendrocyte progenitor survival in the subventricular zone. *Glia* **60**, 1451–1467 (2012).
161. Mercier, F. & Arikawa-Hirasawa, E. Heparan sulfate niche for cell proliferation in the adult brain. *Neurosci. Lett.* **510**, 67–72 (2012).
162. Buttery, P. C. & French-Constant, C. Laminin-2/Integrin Interactions Enhance Myelin Membrane Formation by Oligodendrocytes. *Mol. Cell. Neurosci.* **14**, 199–212 (1999).
163. Chintawar, S. *et al.* Blood-brain barrier promotes differentiation of human fetal neural precursor cells. *Stem Cells* **27**, 838–846 (2009).
164. Chora, Â. A. *et al.* Heme oxygenase–1 and carbon monoxide suppress autoimmune neuroinflammation. *J. Clin. Invest.* **117**, 438–447 (2007).
165. Brambilla, R. *et al.* Astrocytes play a key role in EAE pathophysiology by orchestrating in the CNS the inflammatory response of resident and peripheral immune cells and by suppressing remyelination. *Glia* **62**, 452–467 (2014).

166. Gratzner, H. G. Monoclonal Antibody to 5-Bromo- and 5-Iododeoxyuridine : A New Reagent for Detection of DNA Replication Placental Mononuclear Phagocytes as a Source of Interleukin-1. *Science* (80-. ). **218**, 474–475 (1982).
167. Barthelmes, J. *et al.* Induction of Experimental Autoimmune Encephalomyelitis in Mice and Evaluation of the Disease-dependent Distribution of Immune Cells in Various Tissues. *J. Vis. Exp.* 1–10 (2016).
168. Mouro, F. M. *et al.* Chronic and acute adenosine A2A receptor blockade prevents long-term episodic memory disruption caused by acute cannabinoid CB1 receptor activation. *Neuropharmacology* **117**, 316–327 (2017).
169. Wilson, R. C. *et al.* Open-field behavior in muroid rodents. *Behav. Biol.* **17**, 495–506 (1976).
170. Brooks, S. P. & Dunnett, S. B. Tests to assess motor phenotype in mice: a user's guide. *Nat. Rev. Neurosci.* **10**, 519–29 (2009).
171. Mandillo, S. *et al.* Reliability, robustness, and reproducibility in mouse behavioral phenotyping: a cross-laboratory study. *Physiol. Genomics* **34**, 243–255 (2008).
172. Dunham, N. W. & Miya, T. S. A note on a simple apparatus for detecting neurological deficit in rats and mice. *J. Am. Pharm. Assoc.* **46**, 208–209 (1957).
173. Guerreiro, P. S. *et al.* Mutant A53T  $\alpha$ -Synuclein Improves Rotarod Performance Before Motor Deficits and Affects Metabolic Pathways. *NeuroMolecular Med.* **19**, 113–121 (2017).
174. van den Berg, R. *et al.* Rotarod motor performance and advanced spinal cord lesion image analysis refine assessment of neurodegeneration in experimental autoimmune encephalomyelitis. *J. Neurosci. Methods* **262**, 66–76 (2016).
175. Ogawa, N. *et al.* A simple quantitative bradykinesia test in MPTP-treated mice. *Res. Commun. Chem. Pathol. Pharmacol.* **50**, 435–441 (1985).
176. Balkaya, M. *et al.* Assessing Post-Stroke Behavior in Mouse Models of Focal Ischemia. *J. Cereb. Blood Flow Metab.* **33**, 330–338 (2013).
177. Winter, B. *et al.* Anxious and hyperactive phenotype following brief ischemic episodes in mice. *Biol. Psychiatry* **57**, 1166–1175 (2005).
178. Matsuura, K. *et al.* Pole test is a useful method for evaluating the mouse movement disorder caused by striatal dopamine depletion. *J. Neurosci. Methods* **73**, 45–48 (1997).

179. Fleming, S. M. *et al.* Early and Progressive Sensorimotor Anomalies in Mice Overexpressing Wild-Type Human  $\alpha$ -Synuclein. *J. Neurosci.* **24**, 9434–9440 (2004).
180. Rial, D. *et al.* Behavioral phenotyping of Parkin-deficient mice: Looking for early preclinical features of Parkinson's disease. *PLoS One* **9**, 1–21 (2014).
181. Santos, G. F. A. Deciphering the involvement of S100B-Rage axis in inflammation-associated myelin damage. (2018).
182. Heneka, M. T. *et al.* The heat shock response reduces myelin oligodendrocyte glycoprotein-induced experimental autoimmune encephalomyelitis in mice. *J. Neurochem.* **77**, 568–579 (2001).
183. Schindelin, J. *et al.* Fiji: An open-source platform for biological-image analysis. *Nat. Methods* **9**, 676–682 (2012).
184. Four Parameter Logistic Curve - data analysis at MyAssays. Available at: <https://www.myassays.com/four-parameter-logistic-curve.assay>. (Accessed: 23rd June 2018)
185. Stromnes, I. M. & Goverman, J. M. Active induction of experimental allergic encephalomyelitis. *Nat. Protoc.* **1**, 1810–1819 (2006).
186. Lee, Y. K. *et al.* Proinflammatory T-cell responses to gut microbiota promote experimental autoimmune encephalomyelitis. *Proc. Natl. Acad. Sci.* **108**, 4615–4622 (2011).
187. Saaltink, D. J. *et al.* Doublecortin and doublecortin-like are expressed in overlapping and non-overlapping neuronal cell population: Implications for neurogenesis. *J. Comp. Neurol.* **520**, 2805–2823 (2012).
188. Fu, S. *et al.* Aberrant adult neurogenesis in the subventricular zone-rostral migratory stream-olfactory bulb system following subchronic manganese exposure. *Toxicol. Sci.* **150**, 347–368 (2016).
189. Birkner, K. *et al.* The role of ERK signaling in experimental autoimmune encephalomyelitis. *Int. J. Mol. Sci.* **18**, 1–14 (2017).
190. Laboratories, H. EAE Induction by Active Immunization in C57BL/6 Mice - Hooke kits EK-2110, EK-2160. 1–20
191. Arndt, A. *et al.* Conventional housing conditions attenuate the development of experimental autoimmune encephalomyelitis. *PLoS One* **9**, 1–9 (2014).

192. Sands, S. A. *et al.* The effect of omeprazole on the development of experimental autoimmune encephalomyelitis in C57BL/6J and SJL/J mice. *BMC Res. Notes* **7**, 1–11 (2014).
193. Wang, I.-C. *et al.* Peripheral sensory neuron injury contributes to neuropathic pain in experimental autoimmune encephalomyelitis. *Sci. Rep.* **7**, 1–14 (2017).
194. Belogurov, A. *et al.* Ubiquitin-independent proteosomal degradation of myelin basic protein contributes to development of neurodegenerative autoimmunity. *FASEB J.* **29**, 1901–1913 (2015).
195. Mangiardi, M. *et al.* An animal model of cortical and callosal pathology in multiple sclerosis. *Brain Pathol.* **21**, 263–278 (2011).
196. Garay, L. *et al.* Steroid protection in the experimental autoimmune encephalomyelitis model of multiple sclerosis. *Neuroimmunomodulation* **15**, 76–83 (2008).
197. Garay, L. I. *et al.* Progesterone down-regulates spinal cord inflammatory mediators and increases myelination in experimental autoimmune encephalomyelitis. *Neuroscience* **226**, 40–50 (2012).
198. Yao, D. L. *et al.* Insulin-like growth factor I treatment reduces demyelination and up-regulates gene expression of myelin-related proteins in experimental autoimmune encephalomyelitis. *Proc. Natl. Acad. Sci. U. S. A.* **92**, 6190–6194 (1995).
199. Reale, M. *et al.* Relation between pro-inflammatory cytokines and acetylcholine levels in relapsing-remitting multiple sclerosis patients. *Int. J. Mol. Sci.* **13**, 12656–12664 (2012).
200. Matsuki, T. *et al.* Abnormal T cell activation caused by the imbalance of the IL-1/IL-1R antagonist system is responsible for the development of experimental autoimmune encephalomyelitis. *Int. Immunol.* **18**, 399–407 (2006).
201. Murphy, Á. C. *et al.* Infiltration of Th1 and Th17 cells and activation of microglia in the CNS during the course of experimental autoimmune encephalomyelitis. *Brain. Behav. Immun.* **24**, 641–651 (2010).
202. Rieckmann, P. *et al.* Tumor necrosis factor-alpha messenger RNA expression in patients with relapsing-remitting multiple sclerosis is associated with disease activity. *Ann. Neurol.* **37**, 82–88 (1995).
203. Baker, D. *et al.* Control of established experimental allergic encephalomyelitis by inhibition of tumor necrosis factor ( TNF ) activity within the central nervous system using

- monoclonal antibodies and TNF receptor-immunoglobulin fusion proteins. *Eur. J. Immunol.* **24**, 2040–2048 (1994).
204. Valentin-Torres, A. *et al.* Sustained TNF production by central nervous system infiltrating macrophages promotes progressive autoimmune encephalomyelitis. *J. Neuroinflammation* **13**, 1–14 (2016).
205. Leibowitz, S. M. & Yan, J. NF- $\kappa$ B Pathways in the Pathogenesis of Multiple Sclerosis and the Therapeutic Implications. *Front. Mol. Neurosci.* **9**, 1–23 (2016).
206. Hilliard, B. *et al.* Experimental Autoimmune Encephalomyelitis in NF- $\kappa$ B- Deficient Mice: Roles of NF- $\kappa$ B in the Activation and Differentiation of Autoreactive T Cells. *J. Immunol.* **163**, 2937–2943 (1999).
207. Chen, D. *et al.* CD40-Mediated NF- $\kappa$ B Activation in B Cells Is Increased in Multiple Sclerosis and Modulated by Therapeutics. *J. Immunol.* **197**, 4257–4265 (2016).
208. Jia, Y. *et al.* Amelioration of experimental autoimmune encephalomyelitis by plumbagin through down-regulation of JAK-STAT and NF- $\kappa$ B signaling pathways. *PLoS One* **6**, 1–7 (2011).
209. MacKenzie-Graham, A. *et al.* Cortical atrophy in experimental autoimmune encephalomyelitis: In vivo imaging. *Neuroimage* **60**, 95–104 (2012).
210. Soundarapandian, M. M. *et al.* Zfp488 promotes oligodendrocyte differentiation of neural progenitor cells in adult mice after demyelination. *Sci. Rep.* **1**, 1–9 (2011).
211. Kesidou, E. *et al.* Humoral response in experimental autoimmune encephalomyelitis targets neural precursor cells in the central nervous system of naive rodents. *J. Neuroinflammation* **14**, 1–14 (2017).
212. Dutra, R. C. *et al.* Spatial reference memory deficits precede motor dysfunction in an experimental autoimmune encephalomyelitis model: The role of kallikrein-kinin system. *Brain. Behav. Immun.* **33**, 90–101 (2013).



